Study on Finned Tube Type Adsorber Employing Activated Carbon-Ethanol Pair for Cooling Applications

マージア, カナン

Study on Finned Tube Type Adsorber Employing Activated Carbon-Ethanol Pair for Cooling Applications

MARZIA KHANAM

July 2018

Department of Energy and Environmental Engineering
Interdisciplinary Graduate School of
Engineering Sciences

Kyushu University
Japan

Study on Finned Tube Type Adsorber Employing Activated Carbon-Ethanol Pair for Cooling Applications

A THESIS SUBMITTED IN PARTIAL FULFILLMENT OF THE REQUIREMENT FOR THE AWARD OF THE DEGREE OF

DOCTOR OF PHILOSOPHY (Ph.D.)

By

MARZIA KHANAM

Supervisor

Prof. Takahiko Miyazaki

Department of Energy and Environmental Engineering
Interdisciplinary Graduate School of Engineering Sciences

Kyushu University, Japan

Acknowledgement

I would like to express my deepest sense of gratitude and indebtedness to my honorable supervisors, **Professor Takahiko Miyazaki (Supervisor), Professor Shigeru Koyama,** for their invaluable guidance and inspiration throughout my entire research work. I consider myself fortunate to have the opportunity of working in this laboratory. Besides, I am thankful to **Professor Bidyut Baran Saha** for his valuable guidance and inspiration throughout my entire research work.

I am also indebted to **Dr. Skander Jribi** for his valuable assistance and providing me the opportunity to discuss technical results of this work at any time. Besides, I wish to express my heartiest gratitude and thanks to all of the laboratory members for their warm relationship and kind cooperation every time.

For this dissertation, I would like to thank **Professor Takahiko Miyazaki, Professor Bidyut Baran Saha, Professor Aya Hagishima, Associate Professor Jin Miyawaki**, in taking time to examine the thesis in spite of their busy schedule.

I wish to express my sincere appreciation to the **Green Asia Program** for the funding. It is an amazing program with helpful and friendly staff and I feel honored to be a part of this program.

Finally I wish to thank my parents, siblings and friends for the understanding, quiet patience and encouragement during my study. Last but not the least, I am very much grateful to my elder brother **Md. Mezbah Uddin** for his inspiration and support throughout my whole study. I also wish to thank all of my family members for keeping faith on me.

Marzia Khanam

Table of Contents

List of Figures

List of Tables

Summary

Cooling system has great importance for a growing and sustainable global economy. It contributes significantly to food and drug conservation, thermal comfort, etc. However, greenhouse gases (GHG) emissions from this sector represent 7.8% of total emissions. Conventional vapor compression system employs refrigerants with high global warming potential (GWP) such as CFCs, HCFCs and HFCs gases produced 37% of the emissions and the remaining 63% is caused indirectly by the energy consumption of conventional cooling systems.

In this context, to consider energy and environmental conservation, adsorption cooling systems (ACS) can be a feasible alternative to vapor compression cooling systems. ACS can be driven by low-grade waste heat (below 100^{o}C) or solar thermal energy. Moreover, they employ natural and environment-friendly refrigerants. Therefore, the widespread development of ACS will help to solve various energy and environment-related problems.

Although ACS has several advantages but it is often impaired by low performance and bulkiness issues. Consequently, these issues hinder the thermally driven ACS from the widespread commercialization. There are three main ways to improve the system performance such as material's adsorption characteristics improvement, heat transfer improvement in the adsorber bed and system parameters optimization. Therefore, one of the key ways of performance improvement is to enhance the heat and mass transfer in the adsorber bed. Adsorber heat exchanger design improvement and thermal conductivity enhancement of adsorbent are two common techniques to ensure good heat transfer in the bed.

In this present work, a performance study of two adsorbents namely Maxsorb III and spherical activated carbon (SAC) using ethanol and methanol as a refrigerant has been done. From the performance comparison of SAC-ethanol and SAC-methanol pair, it is found that SAC-ethanol pair is better than SAC-methanol pair over 80℃ of desorption temperature whereas below 80℃ SAC-methanol pair shows better performance. Conversely, SAC-ethanol pair performs

comparatively well than Maxsorb III-ethanol pair for a wide range of desorption temperature 60℃-100℃. However, for wide-scale application of adsorption cooling system, Maxsorb III is treated in high regard since the production of SAC is still in a rudimentary stage.

Extensive literature review on the heat transfer improvement in the adsorber bed has been made to highlight the importance of heat exchanger design parameters on system performance. Moreover, different types of existing heat exchanger design have been reviewed. Review study showed that commonly used heat exchanger type in adsorption system is finned and tube type adsorber.

The main objective of this study was to find out the optimum fin shape for finned tube type adsorber. Therefore, a two-dimensional axisymmetric CFD model has been developed for the performance investigation of finned tube type adsorber employing activated carbon Maxsorb III and ethanol pair. The operating conditions of the cooling system were considered 15, 20 and 80℃ for evaporation, cooling and heating temperatures, respectively. The developed CFD model showed good agreement between experimental and simulated temperature and pressure profiles.

Then, the cycle time optimization has been done for finned type adsorber using Maxsorb III-ethanol working pair with the developed CFD model. The cycle time was considered in the range of 600 to 1400 s. The optimum cycle time was found 800 s and the corresponding evaluated SCP and COP were found to be 488 W/kg and 0.61, respectively.

Finally the performance investigation has been carried out for different fin specifications. In this regard, five different domains were considered for activated carbon-ethanol pair for the cycle time of 800 s. In case-1, fin pitch was considered constant 3.7 mm while fin height was varied 5, 10 and 15 mm. In case-2, fin height was 10 mm constant but fin pitch was varied 2, 3.7 and 5.5 mm. In both cases, fin thickness was constant 0.53 mm. The optimum fin specifications are found 3.7 mm for fin pitch and 10 mm for fin height considering the five studied domains and the corresponding evaluated SCP and COP were 568 W/kg and 0.63, respectively.

Chapter 1

1 Introduction

1.1 Background of the study

Cooling system has great importance in growing and sustainable global economy. It contributes significantly to food and drug conservation, thermal comfort, etc. All refrigeration systems are included in this sector. Almost 3 billion refrigeration systems are currently in operation worldwide. Besides, this sector is growing rapidly in developing counties where the demand for cooling is increasing sharply. Therefore, it is indispensable to ensure this growth sustainably and this should have minimum impact on environment and global climate.

According to International Institute of Refrigeration (IIR), greenhouse gases (GHG) emissions from refrigeration sector represent 7.8% of total emissions including direct and indirect emissions. Direct emissions of refrigerants mostly happen during its maintenance or when a refrigeration appliance is used for a long time and it is almost end of its life span. Besides, emissions can be caused by leakage during its operation. CFCs (chlorofluorocarbons), HCFCs (hydrochlorofluorocarbons) and HFCS (hydrofluorocarbons) are the refrigerants which have significant contributions to global warming as their global warming potential is high. Therefore, employing refrigerants with high global warming potential (GWP) such as CFCs, HCFCs and HFCs gases produced 37% of the total GHG emissions of refrigeration sector (IIR, 2017).

Energy is required to drive the refrigeration systems and indirect emissions are occurred during the production of that energy as a by-product. Indirect emissions are the remaining 63% of the total GHG emissions of the refrigeration sector (IIR, 2017).

One of the probable ways to reduce these indirect emissions is the reduction of energy consumption by refrigeration systems. In that case, it is needed to improve the energy efficiency of refrigeration technologies; however, it is limited by the laws of thermodynamics. Besides, there are some constraints related to cost. Another way is to limit the energy losses by employing energy recovery systems or better insulation. Rational use of air conditioning can reduce energy consumptions also.

However, indirect emissions mainly depend on the primary energy sources such as fossil, renewable or nuclear used for electricity production. It is depended on national energy policies. As our fossil fuel stock is limited, therefore, to consider energy conservation, electricity production from fossil fuels should be minimized. Approximately 17% of the worldwide electricity consumption is currently accounted for the refrigeration sector.

In this context, considering energy and environmental conservation, an alternative cooling system should be developed. Adsorption cooling systems (ACS) can be a feasible alternative to vapor compression cooling systems. They can be driven by low-grade waste heat (below $100^{o}C$) or solar thermal energy (Umair et al., 2014). Moreover, they employ natural and environment-friendly refrigerants such as water (Pan et al., 2016), ethanol (Brancato et al., 2015), methanol (El-Sharkawy et al., 2009), ammonia (Li et al., 2010), CO_2 (Jribi et al., 2014), etc. Therefore, the widespread development of adsorption cooling system will help to solve various energy and environment-related problems. Figure 1.1 represents the energy sources which can be used to run the adsorption cooling system and also various applications of this system.
The overview of adsorption cooling system has been discussed in the following sections.

1.2 Sorption system vs. vapor compression system

The most widely used cooling cycle in practice is the vapor compression cycle. A conventional vapor compression system includes four main components: Evaporator, a mechanical

compressor, condenser and expansion valve. Figure 1.2 shows the schematic diagram of vapor compression system. The commonly used refrigerants in vapor compression cooling cycles are: R134a for mobile air-conditioning, R410a for domestic air conditioning, and R-600a for the home refrigerator which are not very eco-friendly and subject to environmental threat.

The basic components of adsorption cooling system are almost same as the vapor compression system. The main difference between these two systems is that thermal compressor is used in adsorption cooling system while the mechanical compressor is used in case of vapor compression system. Besides, refrigerants used in adsorption system are natural and environmentally amiable. The other differences are in operating conditions as well as working fluids used in those systems. Therefore, adsorption cooling systems have several advantages regarding being environmentally friendly, providing thermal comfort by using low-grade thermal energy.

On the other hand, absorption heat pump cycle is also similar to the vapor compression cycle except for the method of raising the pressure of the refrigerant vapor. In the absorption system, the compressor is replaced by an absorber which dissolves the refrigerant in a suitable liquid. Then a liquid pump is used to increase the pressure and a generator which drives off the refrigerant vapor from the high-pressure liquid. The generator can be run by adding heat. Though some work is needed to drive the liquid pump, however, for a given quantity of refrigerant, it is much smaller than required by the mechanical compressor in the vapor compression cycle. In an absorption system, a suitable combination of refrigerant and absorbent is used. The most used combinations are ammonia (refrigerant) and water (absorbent), and water (refrigerant) and lithium bromide (absorbent).

Commonly used working pairs in the adsorption cooling system are silica gel-water, zeolite-water and carbon with methanol or ethanol. On the other hand, in absorption cooling system, lithium bromide-water, methanol-water are used as working pairs. Table 1.1 shows the coefficients of performance of different types of heat pump systems for cooling applications (Damir et al., 2008).

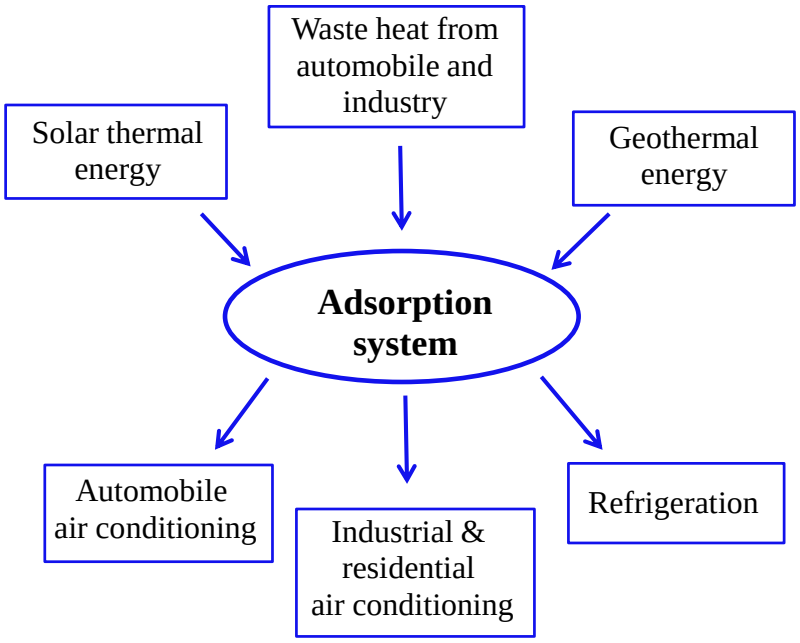

Figure 1.1 Energy sources and applications of adsorption cooling system.

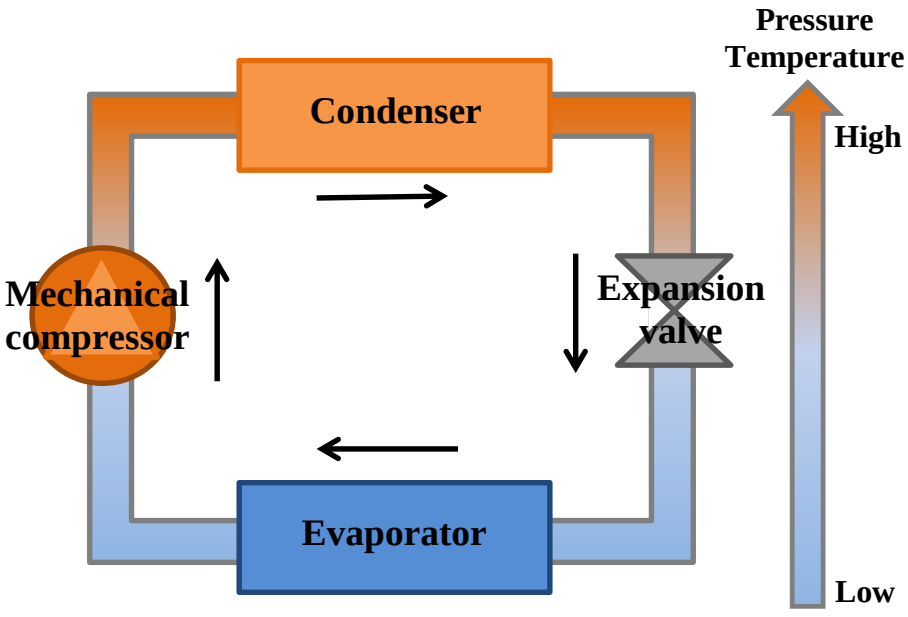

Figure 1.2 Conventional vapor compression system.

Table 1.1 Coefficient of performances of heat pump systems for cooling application (Damir et al., 2008)

Types of heat pump	**Working pair**	**COP**
adsorption	Carbon–methanol	0.12–1.06
	Zeolite–water	0.28–1.4
	Silica gel–water	0.25–0.65
absorption	Methanol-water	0.7–1.1
	Lithium bromide–water	
Vapor compression		3–4

1.3 Adsorption cooling system

1.3.1 Adsorption phenomena

Adsorption is a surface phenomenon and it occurs at the interface of two phases (solid and vapor) by dint of cohesive forces such as Van der Waals forces and hydrogen bonding (Ruthven, 1984). The adsorbing substance is the adsorbent, and the material adsorbed on that substance is the adsorbate which is known as a refrigerant when it is used for cooling purposes.

By the force nature involved during adsorption process, adsorbents can be classified into three different types such as physical, chemical and composite adsorbents. Each type of adsorbents has different characteristics, advantages and disadvantages. The performances of adsorbents which are used in physisorption are depended mostly on the surface characteristics such as surface area, micro-pores and macro-pores, size of granules in powders or crystals in pellets. Activated carbon, zeolite and silica gel are commonly used physical adsorbents for adsorption heat pump systems. Adsorbents having special attraction towards polar substances like water are called hydrophilic adsorbents. This type of absorbents is mostly used for dehumidification or drying applications. The examples of hydrophilic adsorbents are silica gel, zeolites and porous or active alumina. On the other hand, adsorbents having more affinity for oil and gases rather than water

are termed as hydrophobic adsorbents or non-polar adsorbents. Activated carbons, polymer adsorbents are types of hydrophobic adsorbents. The composite adsorbents are made from porous media with a combination of metal chlorides and expanded graphite as a binder (Py et al., 2002).

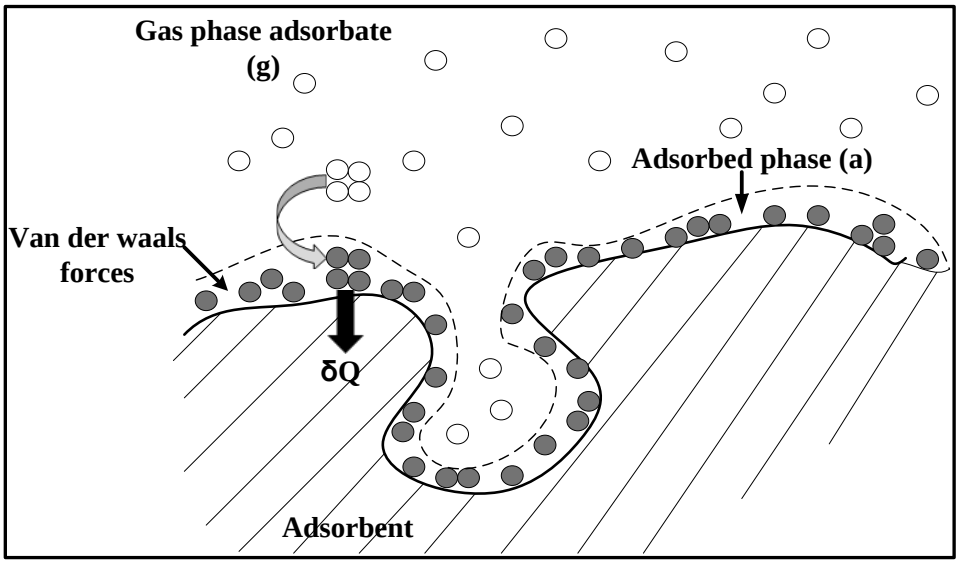

Figure 1.3 Adsorption phenomenon **(**Chakraborty et al., 2006).

1.3.2 Working principle of adsorption cooling system

Adsorption cooling system uses adsorption phenomena to achieve heating/cooling effect. A pair of solid adsorbent beds is used to adsorb and desorb the refrigerant vapor by changing the temperature of the bed. Adsorption cooling system mainly consists of four main components: a pair of solid adsorbent beds, a condenser, an expansion valve and an evaporator. A pair of solid adsorbent beds does the similar work as the mechanical compressor in a vapor compression system. As it is operated by thermal energy, therefore, it is called a thermal compressor. The thermal compressor works through four processes which are pre-heating, desorption, pre-cooling and adsorption and these four processes make one adsorption cycle. In the pre-heating process, the bed is disconnected from the evaporator and hot water is circulated in the adsorption bed. The purpose of preheating is to increase the pressure of the bed from the evaporator pressure to the condenser pressure. When the pressure in the bed increases and becomes higher than that in

the condenser, then it is connected to the condenser and the desorption process starts. Refrigerant vapor is desorbed from the adsorber bed because of additional heat supplied to the bed and moves to the condenser. After the desorption gets finished, the bed is disconnected from the condenser and cooling water is circulated in the bed which is called the pre-cooling process. This process is continued until the pressure of the bed becomes lower than that of the evaporator pressure. When the adsorber bed is connected to the evaporator, the evaporated refrigerant is adsorbed in the bed. During the adsorption process, cooling water is continuously supplied to the bed to remove the heat of adsorption. To attain the uninterrupted cooling effect in the adsorption cooling system, commonly two or more adsorbent beds are needed to use at the same time (Figure 1.4). The working principle of the adsorption cooling system is almost same as the vapor compression system except for the thermal compressor part. In the condenser, the refrigerant vapor is condensed and becomes liquid. Then, the liquid refrigerant is expanded by dint of an expansion valve. Then, the low-pressure liquid refrigerant when passes through an evaporator, it takes heat from the space and the refrigerant liquid becomes vapor.

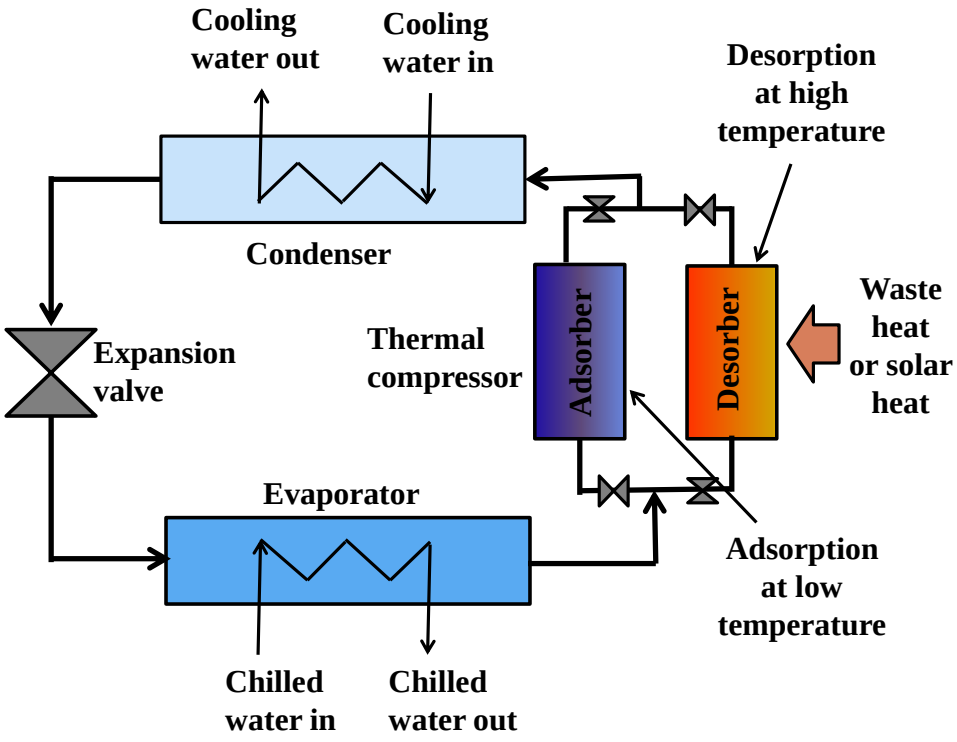

Figure 1.4 Schematic of a two-bed adsorption cooling system.

1.3.3 Important parameters to assess the performance of ACS

The coefficient of performance (COP) and specific cooling power (SCP) are the two most important parameters to evaluate the performance of adsorption cooling system. COP indicates the ratio of the cooling produced by the system and thermal energy supplied to the system whereas SCP refers the ratio of cooling capacity to the mass of adsorbent in the adsorber bed.

The coefficient of performance and the specific cooling power of the adsorption cooling system can be calculated by using equation (1.1) and (1.3) respectively.

$$\mathrm{COP} = \frac{Q_{chill}}{Q_{des}} \tag{1.1}$$

Where Q_{chill} and Q_{des} are the produced cooling effect (J) and the amount of heat energy supplied during the desorption process, respectively.

Q_{chill} can be defined by the following equation:

$$Q_{chill} = h_{fg} \cdot \int_{ads\_start}^{ads\_end} m_{ads}\, dt \tag{1.2}$$

Here h_{fg} represents the heat of evaporation and m_{ads} is the adsorbed refrigerant mass.

$$\mathrm{SCP} = \frac{Q_{chill}}{m_{adsorbent}\, \tau_{cycle}} \tag{1.3}$$

Where $m_{adsorbent}$ is the mass of dry adsorbent (kg) and τ_{cycle} is the cycle time (s).

As SCP has a relation with adsorbent mass as well as the cooling power, therefore, it is an important parameter to determine the size of the system. Besides, higher SCP value indicates that the system is compact whereas low SCP means that the system is bulky.

1.3.4 Commercialized adsorption cooling systems

Adsorption cooling system has drawn the considerable attention as a green and sustainable cooling for the last few decades. Some companies have already developed this kind of cooling system commercially. Mycom, Sortech, Invensor, Union Industry, SolabCool, Bry-Air, Adref-Noa are the companies that successfully developed adsorption cooling systems. Figure 1.5 represents the photograph of commercialized adsorption systems. A small compact adsorption chiller is now available in Japan market which is developed by German manufacturer company, Invensor. The adsorption chiller has a cooling capacity in the range of 7 to 10 kW with compact measurements like 110 cm long, 137 cm high and 75 cm wide. This chiller can be driven by low grade heat sources of temperatures around 60-70°C which is available from renewable energy or waste heat. Therefore, this kind of system enables the use of low-temperature waste heat from cogeneration systems. This kind of chiller also helps to lessen maintenance-related work and costs as it requires very less maintenance. Because of its excellent performance, it has already acquired a significant market share in Germany and other European countries.

Figure 1.5 Photograph of commercialized adsorption heat pumps.

1.4 Review of adsorbent-refrigerant pairs for ACS

Adsorbent-refrigerant pair is a vital part of ACS. Several researchers have made considerable efforts for last few decades to investigate the performance of ACS employing various types of adsorbent-refrigerant pairs. A brief review of the adsorbent-refrigerant pairs used commonly in ACS is given in the following subsections.

1.4.1 Silica gel-water pair

Silica gel is a type of amorphous synthetic silica. It is a rigid, continuous net of colloidal silica, connected to very small grains of hydrated SiO_4. Two common types of silica gel are A type and B type. The pore diameters of A type and B type silica gel are nearly 3 nm and 0.7 nm, respectively and the specific surface area is about 100-1000 m^2/g. Silica gel-water is a low temperature working pair which can be run by around 75^oC heat source (Wang et al., 2010).

Due to the capability of using low grade heat sources, Adsorption cooling systems using silica gel-water working pair was studied in Japan in the 1980s. A transient simulation model for solar powered adsorption cooling cycle employing silica gel-water pair was proposed by Sakoda and Suzuki (1984). The same authors (Sakoda and Suzuki, 1986) also investigated the performances of solar-powered adsorption refrigeration system and reported COP of 0.2 which is attainable by using solar collector with dimensions of 500×500×50 mm. Later, Saha et al. (1995) investigated analytically the effects of operating conditions on the performances of silica gel-water based adsorption chiller. They claimed that 50^oC hot water also can be used to run the system if the cooling water temperature is less than 25ºC. A lumped model and distributed transient model for silica gel-water adsorption system were investigated by Chua et al. (1999) and a good agreement was reported between the simulation and experimental data. A multi-stage based adsorption cooling cycles using silica gel-water pair was developed and analyzed by Saha et al. (1997). They found the optimum COP values for hot water temperature range of 50 to 55ºC in case of three-stage mode where it was between 80 to 85ºC for single stage multi-bed mode.

1.4.2 Zeolite-water pair

Zeolite is a type of alumina silicate crystal composed of alkali or alkali soil. The porosity of the alumina silicate is between 0.2 and 0.5 nm. Natural zeolites are about 40 types and the commonly used zeolite types for adsorption system are chabazite, sodium–chabazite, cowlesite and faujasite. Artificially synthesized zeolites types are around 150 and their named is given by one letter or a group of letters, such as type A, type X, type Y, type ZSM, etc. In case of artificial zeolite, microspores with uniform size can be created by using artificial synthesized process, and different sizes can be obtained by changing the manufacturing methods. The main types used for adsorption system are 4A, 5A, 10X and 13X zeolite molecular sieves.

Solar powered air-conditioning and refrigeration system employing zeolite-water pair was investigated nearly a few decades ago. Design and performance prediction of a novel zeolite-water adsorption chiller was investigated by Wang et al. (2006). Their reported performance of the system was 5 kW for cooling power and 0.25 for COP. The refrigerating power of the machine can be reached up to 10 kW for the evaporation temperature of 6.5 ºC for the cycle time of 1320 s and the SCP reached to 200 W/kg for that corresponding cycle time. A mobile adsorption air conditioner by using zeolite-water pair was developed by Vasta et al. (2012). The reported COP of the system was about 0.4 while the SCP was approximately 600 W/kg. A prototype of adsorption cooling system using zeolite-water pair was presented by Zhang (2000) which was driven by waste heat from a diesel engine. They reported that the proposed system can achieve COP and specific cooling power (SCP) of 0.38 and 2.57 W/kg, respectively. The performance of a zeolite FAM Z01-water pair adsorption chiller investigated by Li et al. (2014) and they reported the optimum COP for the heat source temperature of nearly 65ºC.

1.4.3 Activated carbon-ethanol pair

Ethanol is an environment friendly refrigerant. Besides, it is a non-toxic substance. Another benefit to use ethanol as a refrigerant is that it has comparatively higher vapor pressure even at low temperature.

An innovative adsorption chiller employing pitch based ACF of type A-20 as adsorbent and ethanol as refrigerant was studied by Saha et al. (2007). ACF is a fibrous adsorbent and the advantages of using ACF are fast adsorption rate, high porosity and ease of handling while compared with granular adsorbents. This system can utilize low-temperature waste heat sources (60 to 95ºC) effectively. They reported COP of 0.6 for a cycle time of 600-700 s.

El-Sharkawy et al. (2008) investigated the activated carbon-ethanol pair for solar powered adsorption cooling system experimentally. The activated carbon was named as Maxsorb III which is a highly porous activated carbon. They reported that the maximum adsorption capacity of Maxsorb III was 1.2 kg/kg. It is found from the theoretical calculations that the Maxsorb III-ethanol pair based adsorption cycle could achieve a specific cooling effect of about 420 kJ/kg for the evaporator temperature of 7ºC and heat source temperature of 80ºC.

1.4.4 Activated carbon-methanol pair

One of the most commonly used working pairs for adsorption system is activated carbon-methanol pair due to the large adsorption quantity and lower adsorption heat (about 1800-2000 kJ/kg). However, the disadvantage with activated carbon-methanol pair is of operating condition under sub-atmospheric pressure.

The study on activated carbon-methanol pair was started in Europe in the year of 1980. An activated carbon-methanol based adsorption system driven by renewable energy for ice production application was studied by Pons and Guilleminot (1986). Later, Douss and Meunier (1988) investigated the probability of active carbon type AC135 as adsorbent and methanol as a refrigerant for refrigeration application. It is reported that the experimental COP of the adsorption cycle reached 0.5 with regeneration temperature difference equal to 65ºC. El-Sharkawy et al. (2009) investigated the adsorption characteristics of methanol on to two types of activated carbons, namely, Maxsorb III and Tsurumi activated charcoal. The Dubinin-Radushkevich (D-R) equation is found the suitable model to correlate the adsorption isotherms of the two assorted pairs. Experimental results showed that the Maxsorb III-methanol pair has

better adsorption properties over Tsurumi activated carbon-methanol pair.

1.4.5 Activated carbon-ammonia pair

Latent heat of Ammonia is relatively high which is nearly 1365 kJ/kg at -30^{o}C. However, ammonia often suffers with the problem of toxicity and corrosiveness. Its maximum adsorption capacity in activated carbon is approximately 0.29 g/g (Wang et al., 2006) and the adsorption data was fitted using D-A equation where the fitting coefficients were W_o = 0.29, k = 3.57 and n = 1.38. The adsorption capacity of ammonia on activated carbon fiber was studied (Busofit) by Vasiliev et al. (1997) where they performed the adsorption process for 120 minutes and found the maximum adsorption capacity as 0.61 kg/kg. Busofit is advantageous for high rate of adsorption/desorption. In addition, it has uniform surface pore distribution (0.6–1.6 nm), small number of macropores (100–200 nm) with its specific surface area of 0.5 m^2/g and small number of mesopores with its specific surface area 50 m^2/g (Vasiliev et al., 2007). Qajar et al. (2015) used different carbon samples treated with concentrated nitric acid at 25^{o}C and measured the adsorption uptakes of ammonia. They reported that the maximum adsorption uptake of ammonia on the carbons prior to nitric acid treatment was 10 mol/kg for NPC-PEG-AC at 25^{o}C and 1 bar. Nitric acid treatment of NPCPEG- AC has caused to rise total uptake of ammonia to 17 mol/kg.

The adsorption characteristics of ammonia onto packed multi-walled carbon nanotubes (MWCNTs) was conducted by Yan et al. (2015) and they found that the pure MWCNT is not preferable adsorbent for the adsorption refrigeration system due to its low adsorption capacity which is 90.05 mg/g_{CNT} .

1.4.6 Metal organic framework-ethanol pair

Adsorption isotherm and kinetics for metal organic framework (MIL-101Cr) and ethanol pair has been investigated by Saha et al. (2015). The authors performed experiments for adsorption temperature ranges from 30^{o}C to 70^{o}C and relative pressure within 0.1 to 0.9. The authors reported adsorption of ethanol onto MIL-101 Cr is 1.1 kg/kg at 30^{o}C adsorption temperature. Toth equation is used to fit the adsorption isotherm curves of this pair.

In another work, Ma et al.(2016) used MIL-101 (MIL-101-3) and ethanol as their working pair and their reported maximum adsorption of ethanol onto MIL-101 is 0.74 kg/kg at 25^{o}C. The authors also reported maximum desorption temperature of the pair as 54.0^{o}C. The cooling capacity of (MIL-101-3)-ethanol pair is reported as 283 kJ/kg at the desorption temperature of 80^{o}C which is approximately two times higher than the activated carbon-ethanol pair.

1.5 Obstacles & solutions of adsorption cooling system

Although thermally powered adsorption heat pump systems have several benefits such as effective utilization of low-grade thermal energy, environment-friendly and simple structure; however, it has some challenges as well which obstruct this system from mass production. As a result, vapor compression systems are still prevalent in the sector of cooling market.

The drawbacks of the adsorption system are as follows:

- low COP value
- low SCP value
- intermittently working principles
- large volume and weight relative to mechanical heat pump systems (Damir et al., 2008).

Consequently, for mass production of adsorption heat pump, the key challenges are to make the system compact, to increase the COP as well as SCP and to minimize the cost. Extensive research is continuously being performed for improving the adsorption system performance.

The primary research areas to overcome the above challenges are:

- Material science study which covers finding the innovative materials and improvement of material's adsorption properties
- Heat and mass transfer enhancement in adsorber bed

- System performance optimization in which system control and operation control are included.

1.5.1 Material properties improvement

Adsorbents used in adsorption cooling systems are usually in the form of spherical pellets, rods, moldings, or monoliths with a hydrodynamic radius of between 0.25 to 5 mm. It is very important in case of adsorption materials to be thermally as well as mechanically stable. Another important parameter for adsorption material is pore diameter. As small pore diameters results in the higher surface area, therefore, small pore diameters are good for higher adsorption capacity. To ensure fast transport of the refrigerant vapors, the adsorbents need to have a distinct pore structure (Freni et al., 2015).

1.5.2 Heat and mass transfer improvement in adsorber bed heat exchanger

To get a high-performance adsorption system, heat and mass transfer improvement in the adsorber bed is very fundamental requirement. To ensure good heat and mass transfer inside the bed, one of the key adsorber heat exchanger design requirements is to reduce the heat capacity ratio of the adsorber heat exchanger material and the applied adsorbent. This will help to improve the COP of the system and also enhances the specific cooling power of the system. Another important design requirement is to ensure the low cost. Except the low cost, there are two important sets of adsorber design requirements which are dynamic performance design requirements and reliability design requirements (Freni et al., 2015).

The dynamic performance design requirements are as follows (Freni et al., 2015):

(a) To ensure high heat transfer coefficient between the heat transfer fluid and the adsorbent.

(b) Overall mass diffusion coefficient should be high.

(c) It is also required to maintain the velocity of refrigerant vapor low in the connecting ducts between adsorber and evaporator or condenser as this will be helpful to minimize the pressure losses.

The reliability design requirements are as follows (Freni et al., 2015):

(a) It should be highly stable against the hydrothermal aging.

(b) Mechanical stability is also important and should be high against loading, transport and operating conditions.

(c) Should be non-corrosive under loading, transport and operating conditions.

(d) As this system goes through the adsorption and desorption phases many times, therefore, there should not be release of any inert gases on repetition of adsorption–desorption cycles.

To achieve the dynamic performance requirements, there could be two possible design phenomena:

- Consolidated adsorbent bed and
- Adsorber bed heat exchanger design

1.5.3 Adsorption cycle performance improvement

The performance of the basic adsorption cooling cycle is low and the cooling output is not continuous. To make the practical system and improve the efficiency of the system, many advanced adsorption cooling cycles have been developed which are the heat recovery cycle, mass recovery cycle etc.

1.5.3.1 Heat recovery cycle

The heat recovery cycle is an important advanced adsorption cycle. Two or more adsorbers are needed to use the heat recovery in the system. In this cycle, when the adsorption and desorption phase are finished, the heat is transferred to the cold adsorber from the hot adsorber by

circulating heat transfer fluid between them in a closed loop. From the experimental results, it is showed that the COP of the system can be enhanced up to 25% with the heat recovery cycle (Wang et al., 2001)

1.5.3.2 Mass recovery cycle

To improve the cooling output and COP of the system, the mass recovery cycle uses refrigerant mass recovery between the two adsorbers. Figure 1.6 represents a conceptual diagram of the mass recovery cycle for an adsorption system. After the adsorption and desorption phases are finished, the high-pressure adsorber is connected to the low-pressure adsorber in a closed loop. The refrigerant from the high-pressure adsorber will go to the low-pressure adsorber because of the pressure difference between the two adsorbers. Therefore, refrigerant will be re-adsorbed by the adsorbent in the low pressure adsorber. The adsorption amount can be improved through the mass recovery process and it also helps to enhance the cooling capacity and COP of the system. From the experimental results, it is found that COP increase of more than 10% is possible by the mass recovery cycle (Wang et al., 2001). The performance of the three-bed adsorption chiller with mass recovery scheme was compared with that of the three-bed chiller without mass recovery by Khan et al. (2007). It is found that cooling effect as well as solar/waste heat recovery efficiency of the chiller with mass recovery scheme is superior to those of three-bed chiller without mass recovery for heat source temperatures between 60 and 90^{o}C.

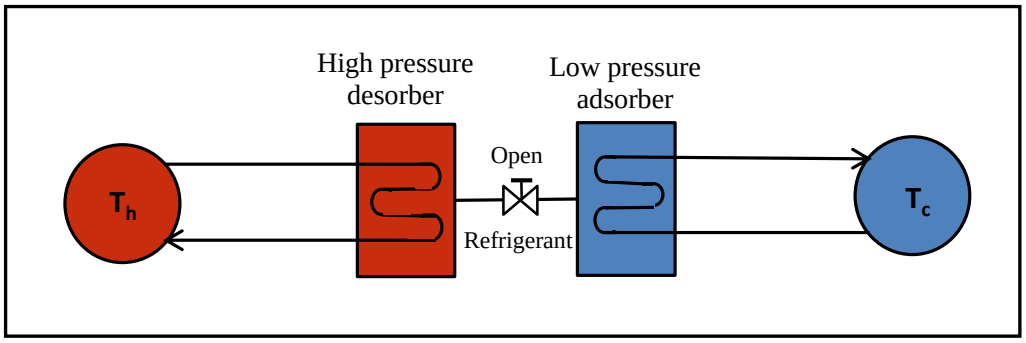

Figure 1.6 Conceptual diagram of mass recovery cycle.

1.6 Concluding remarks

The conclusion of this chapter is as follows:

- Adsorption cooling system has great significance in view point of energy and environmental conservation as it can be run by waste heat or renewable energy and employs environment friendly refrigerants. Therefore, it has potential to be a feasible alternative of vapor compression system.
- However, still adsorption cooling system has few challenges which make the use of this system limited. Consequently, the performance improvement is essential for widespread utilization of this system.
- The three mains ways for performance improvement have been discussed which are as material's adsorption characteristic's improvement, heat transfer improvement in the adsorber bed and system parameters optimization.

1.7 Nomenclature

h_{fg}	heat of evaporation [J kg^{-1}]
$\dot{m}$	mass flow rate [kg s^{-1}]
m	mass [kg]
Q	thermal energy [J]
t	time [s]
Subscripts	
ac	activated carbon
ads	adsorbed
chill	chill
des	desorption
Acronyms	
ACS	adsorption cooling system
COP	coefficient of performance
SCP	specific cooling power

1.8 References

Brancato, V., Frazzica, A., Sapienza, A., Gordeeva, L., & Freni, A. (2015). Ethanol adsorption onto carbonaceous and composite adsorbents for adsorptive cooling system. Energy, 84, 177–185. https://doi.org/10.1016/j.energy.2015.02.077

Chakraborty, A., Saha, B. B., Koyama, S., & Ng, K. C. (2006). On the thermodynamic modeling of the isosteric heat of adsorption and comparison with experiments. Applied Physics Letters, 89(17). https://doi.org/10.1063/1.2360925

Chua, H. T., Ng, K. C., Malek, A., Kashiwagi, T., Akisawa, A., & Saha, B. B. (1999). Modeling the performance of two-bed, silica gel-water adsorption chillers. International Journal of Refrigeration, 22(3), 194–204. https://doi.org/10.1016/S0140-7007(98)00063-2

Demir, H., Mobedi, M., & Ülkü, S. (2008). A review on adsorption heat pump: Problems and solutions. Renewable and Sustainable Energy Reviews, 12(9), 2381–2403. https://doi.org/10.1016/j.rser.2007.06.005

Douss, N., & Meunier, F. (1988). Effect of operating temperatures on the coefficient of performance of active carbon-methanol systems. Heat Recovery Systems and CHP, 8(5), 383–392. https://doi.org/10.1016/0890-4332(88)90042-7

El-Sharkawy, I. I., Hassan, M., Saha, B. B., Koyama, S., & Nasr, M. M. (2009). Study on adsorption of methanol onto carbon based adsorbents. International Journal of Refrigeration, 32(7), 1579–1586. https://doi.org/10.1016/j.ijrefrig.2009.06.011

El-Sharkawy, I. I., Saha, B. B., Koyama, S., He, J., Ng, K. C., & Yap, C. (2008). Experimental investigation on activated carbon-ethanol pair for solar powered adsorption cooling applications. International Journal of Refrigeration, 31(8), 1407–1413. https://doi.org/10.1016/j.ijrefrig.2008.03.012

Freni, A., Dawoud, B., Bonaccorsi, L., Chmielewski, S., Frazzica, A., Calabrese, L., & Restuccia, G. (2015). Characterization of Zeolite-Based Coatings for Adsorption Heat Pumps. https://doi.org/10.1007/978-3-319-09327-7

International Institute of Refrigeration. (2017). 35th Informatory Note on Refrigeration Technologies "The impact of the refrigeration sector on climate change." Retrieved from http://www.iifiir.org/userfiles/file/publications/notes/NoteTech_35_EN_Summary_uz7bwths.pdf

Jribi, S., Saha, B. B., Koyama, S., & Bentaher, H. (2014). Modeling and simulation of an activated carbon-CO_2 four bed based adsorption cooling system. Energy Conversion and Management, 78, 985–991. https://doi.org/10.1016/j.enconman.2013.06.061

Khan, M. Z. I., Saha, B. B., Alam, K. C. A., Akisawa, A., & Kashiwagi, T. (2007). Study on solar/waste heat driven multi-bed adsorption chiller with mass recovery. Renewable Energy, 32(3), 365–381. https://doi.org/10.1016/j.renene.2006.02.003

Li, A., Ismail, A. Bin, Thu, K., Ng, K. C., & Loh, W. S. (2014). Performance evaluation of a zeolite-water adsorption chiller with entropy analysis of thermodynamic insight. Applied Energy, 130, 702–711. https://doi.org/10.1016/j.apenergy.2014.01.086

Li, S. L., Xia, Z. Z., Wu, J. Y., Li, J., Wang, R. Z., & Wang, L. W. (2010). Experimental study of a novel $CaCl_2$/expanded graphite-NH_3 adsorption refrigerator. International Journal of Refrigeration, 33(1), 61–69. https://doi.org/10.1016/j.ijrefrig.2009.08.001

Ma, L., Rui, Z., Wu, Q., Yang, H., Yin, Y., Liu, Z., Wang, H. (2016). Performance evaluation of shaped MIL-101-ethanol working pair for adsorption refrigeration. Applied Thermal Engineering, 95, 223–228. https://doi.org/10.1016/j.applthermaleng.2015.09.023

Pan, Q. W., Wang, R. Z., Wang, L. W., & Liu, D. (2016). Design and experimental study of a silica gel-water adsorption chiller with modular adsorbers. International Journal of Refrigeration, 67, 336–344. https://doi.org/10.1016/j.ijrefrig.2016.03.001

Pons, M. and Guilleminot, J. J. (1986). Design of an Experimental Solar-Powered, Solid-Adsorption Ice Maker. Journal of Solar Energy Engineering, 108(4), 332–337. https://doi.org/doi:10.1115/1.3268115

Py, X., Daguerre, E., & Menard, D. (2002). Composites of expanded natural graphite and in situ prepared activated carbons. Carbon, 40(8), 1255–1265. https://doi.org/10.1016/S0008-6223(01)00285-8

Qajar, A., Peer, M., Andalibi, M. R., Rajagopalan, R., & Foley, H. C. (2015). Enhanced ammonia adsorption on functionalized nanoporous carbons. Microporous and Mesoporous Materials, 218, 15–23. https://doi.org/10.1016/j.micromeso.2015.06.030

Ruthven, M. D. (1984). Principles of Adsorption and adsorption Processes. John Wiley and Sons.

Saha, B. B., El-Sharkawy, I. I., Miyazaki, T., Koyama, S., Henninger, S. K., Herbst, A., & Janiak, C. (2015). Ethanol adsorption onto metal organic framework: Theory and experiments. Energy, 79(C), 363–370. https://doi.org/10.1016/j.energy.2014.11.022

Saha, B. B., I. I. El-Sharkawy, A. Chakraborty, S. K. (2007). Study on an activated carbon fiber-ethanol adsorption chiller: Part I - system description and modelling. International Journal of Refrigeration, 30(1), 86–95.

Saha, B. B., Kashiwagi, T. (1997). Experimental investigation on an advanced adsorption refrigeration cycle. ASHRAE Transactions, 103(2), 50–58.

Saha, B. B., Boelman, E.C., Kashiwagi, T. (1995). Computer simulation of a silica gel-water adsorption refrigeration cycle -the influence of operating conditions on cooling output and COP. ASHRAE Transactions, 101(2), 348–357.

Sakoda, A., and M. Suzuki. (1986). Simultaneous Transport of Heat and Adsorbate in Closed Type Adsorption Cooling System Utilizing Solar Heat. Journal of Solar Energy Engineering, 108(3), 239–245. https://doi.org/doi:10.1115/1.3268099

Sakoda, A., Suzuki, M. (1984). Fundamental study on solar powered adsorption cooling system. Journal of Chemical Engineering, 17(1), 52.

Umair, M., Akisawa, A., & Ueda, Y. (2014). Performance evaluation of a solar adsorption refrigeration system with a wing type compound parabolic concentrator. Energies, 7(3), 1448–1466. https://doi.org/10.3390/en7031448

Vasiliev, L. L., Kanonchik, L. E., Kulakov, A. G., Mishkinis, D. A., Safonova, A. M., & Luneva, N. K. (2007). New sorbent materials for the hydrogen storage and transportation. International Journal of Hydrogen Energy, 32(18), 5015–5025. https://doi.org/10.1016/j.ijhydene.2007.07.029

Vasiliev, L.L., D.A. Mishkinis, L.E. Kanonchik, V.V. Khrolenok, A. S. Z. (1997). Activated carbon ammonia and natural gas adsorptive storage. In Ext Abstracts of 23rd Biennial Conference on Carbon, '"Carbon "97", Philadelphia 1, (pp. 334–335).

Vasta, S., Freni, A., Sapienza, A., Costa, F., & Restuccia, G. (2012). Development and lab-test of a mobile adsorption air-conditioner. International Journal of Refrigeration, 35(3), 701–708. https://doi.org/10.1016/j.ijrefrig.2011.03.013

Wang, D. C., Li, Y. H., Li, D., Xia, Y. Z., & Zhang, J. P. (2010). A review on adsorption refrigeration technology and adsorption deterioration in physical adsorption systems. Renewable and Sustainable Energy Reviews, 14(1), 344–353. https://doi.org/10.1016/j.rser.2009.08.001

Wang, D. C., Xia, Z. Z., & Wu, J. Y. (2006). Design and performance prediction of a novel zeolite-water adsorption air conditioner. Energy Conversion and Management, 47, 590–610. https://doi.org/10.1016/j.enconman.2005.05.011

Wang, L. W., Wang, R. Z., Lu, Z. S., Chen, C. J., Wang, K., & Wu, J. Y. (2006). The performance of two adsorption ice making test units using activated carbon and a carbon composite as adsorbents. Carbon, 44(13), 2671–2680. https://doi.org/10.1016/j.carbon.2006.04.013

Wang, R. Z. (2001). Performance improvement of adsorption cooling by heat and mass recovery operation. International Journal of Refrigeration, 24, 602–611. https://doi.org/10.1016/j.ijrefrig.2014.04.018

Yan, T., Li, T. X., Wang, R. Z., & Jia, R. (2015). Experimental investigation on the ammonia adsorption and heat transfer characteristics of the packed multi-walled carbon nanotubes. Applied Thermal Engineering, 77, 20–29. https://doi.org/10.1016/j.applthermaleng.2014.12.001

Zhang, L. Z. (2000). Design and testing of an automobile waste heat adsorption cooling system. Applied Thermal Engineering, 20, 103–114. https://doi.org/10.1016/S1359-4311 (99) 00009-5

Chapter 2

2 Performance Study of Adsorption Cooling System by Employing Activated Carbon with Ethanol and Methanol

This chapter presents the performance study of adsorption cooling system for different working pairs. We particularly focused on carbon based adsorbents such as commercialized activated carbon Maxsorb III and newly developed spherical activated carbon (SAC) employing refrigerants ethanol and methanol. In this study, adsorption isotherm measurement of SAC onto methanol at different temperatures was conducted by gravimetric method and fitted with D-A adsorption isotherm model. Then a comparative study of SAC-ethanol and SAC-methanol has been presented. From the reported results, it suggests that SAC-ethanol pair is better than SAC-methanol pair over 80^{o}C of desorption temperature whereas below 80^{o}C SAC-methanol pair shows better performance than SAC-ethanol pair. In addition, the performance comparison of Maxsorb III-ethanol and SAC-ethanol in terms of specific cooling effect (SCE) for the desorption temperature ranges from 60^{o}C to 100^{o}C has been shown. SAC-ethanol pair performs comparatively well than Maxsorb III-ethanol pair for a wide range of desorption temperature 60 ^{o}C -100^{o}C. However, for wide scale application of adsorption cooling system, Maxsorb III is treated in high regard since the production of SAC is still in rudimentary stage.

2.1 Introduction

Adsorption cooling system is a growing and promising technology for providing thermal comfort in residential and industrial applications in viewpoint of energy and environmental protection. Adsorption cooling system is already commercialized in the market. In the present system, silica gel and zeolite are the popular adsorbents in combination with water. One of the main advantages to select water as a refrigerant is its large evaporation heat. However, activated carbons are also very promising adsorbents especially for cooling applications because of its large adsorption capacity with different types of refrigerants. Ammonia (Tamainot et al., 2009) and alcohols are the most commonly used refrigerants with activated carbons for adsorption heat pump applications (El-Sharkawy et al., 2009 and 2014). Recently, researchers are attempted to study other refrigerants such as ethanol (El-Sharkawy et al., 2014) and methanol (El-Sharkawy et al., 2009) with activated carbon.

Though many researchers have studied activated carbons intensively for adsorption cooling system applications, however, commercialized adsorption heat pump with activated carbon is still rare. Therefore, researchers extended their research to develop new type of activated carbon which can be employed with ethanol or methanol refrigerant. To step towards this target, our research group has already developed a new spherical activated carbon (SAC) which has large surface area and optimum pore size (Miyazaki et. al., 2017). The adsorption performance of SAC employing ethanol as refrigerant has been checked previously and very promising performance was reported in case of ethanol adsorption (El-Sharkawy et al., 2015). The adsorption characteristics of methanol onto SAC have also been investigated experimentally in this study.

The objective of this chapter is to find out the adsorption characteristic of methanol onto SAC and compare the performance of adsorption cooling system in terms of specific cooling effect (SCE) for Maxsorb III-ethanol, Maxsorb III-methanol, SAC-ethanol and SAC-methanol pair.

2.2 Adsorbents

2.2.1 Commercialized activated carbon

Commercialized activated carbon Maxsorb III is a highly porous activated carbon which was produced by Kansai Coke & Chemicals Co. Ltd., Japan. The properties of Maxsorb III are furnished in Table 2.1.

Table 2.1 Elemental composition and thermo-physical properties of Maxsorb III (El-Sharkawy et al., 2014).

Elemental composition						**Porosity**		
C [wt.%]	H [wt.%]	N [wt.%]	$O_{(diff.)}$ [wt.%]	O/C	Ash [wt.%]	Total surface area [m^2/g]	Micropore volume [cm^3/g]	Average pore width [nm]
95.13	0.14	0.25	4.35	0.034	0.13	3045	1.70	1.12

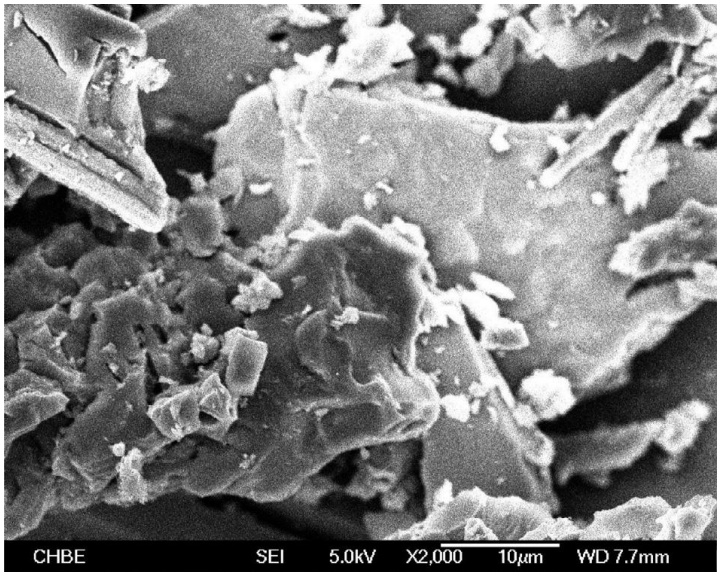

Figure 2.1 SEM picture of activated carbon Maxsorb III (Wai et al., 2012).

2.2.2 Newly developed adsorbent

Our research group has targeted to develop a high-performance adsorption cooling system employing SAC-ethanol pair. Therefore, it was essential to find out the optimum pore characteristics of SAC for ethanol adsorption. From the grand-canonical monte carlo (GCMC) simulation, it was found that the optimum pore size of 1.6 nm is good for ethanol adsorption, however, the micropore size of the commercialized activated carbon was nearly 1.1 mm. Then, our group has developed a new spherical activated carbon with micropore size of 1.6 mm from the spherical phenol resin (Average particle diameter: 15 μm) as an origin (Miyazaki et. al., 2017). Figure 2.2 shows the original phenol resin material and SEM images of spherical activated carbon (SAC) after carbonization and activation by KOH. From SEM images it is evident that SAC kept its original spherical shape after the activation process.

The chemical compositions and pore characteristics of SAC sample are presented in Table 2.2. Pore characteristics have been extracted from N_2 adsorption at 77 K. The total surface area of SAC is nearly 3000 m^2/g, which is close to the highest level of commercialized activated carbons.

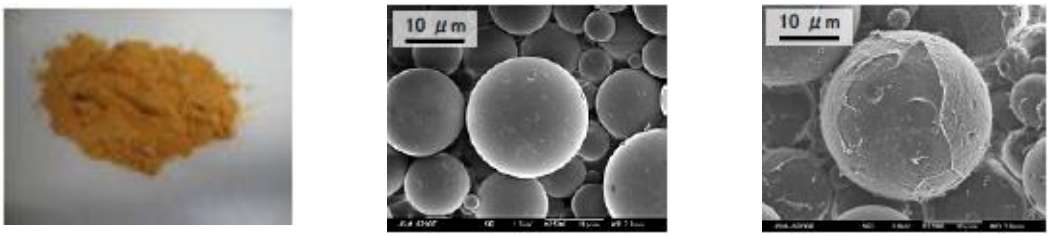

Spherical phenol resin **After carbonization** **After activation by KOH**

Figure 2.2 Original materials and SEM images of spherical activated carbon (Miyazaki et al., 2017).

Table 2.2 Characteristics of SAC (Miyazaki et al., 2017)

Elemental composition						**Porosity**			
C [wt.%]	H [wt.%]	N [wt.%]	$O_{(diff.)}$ [wt.%]	O/C	Ash [wt. %]	Total surface area [m^2/g]	Micropore volume [cm^3/g]	Total Pore volume [cm^3/g]	Average pore width [nm]
95.18	0.22	0.26	4.34	0.034	-	2992	2.29	2.52	1.62

2.3 Adsorption Characteristics

2.3.1 Adsorption Isotherms

Adsorption isotherm measurement of SAC-methanol pair at 30°C and 40°C temperature has been conducted by gravimetric experimental apparatus as shown in Figure 2.3.

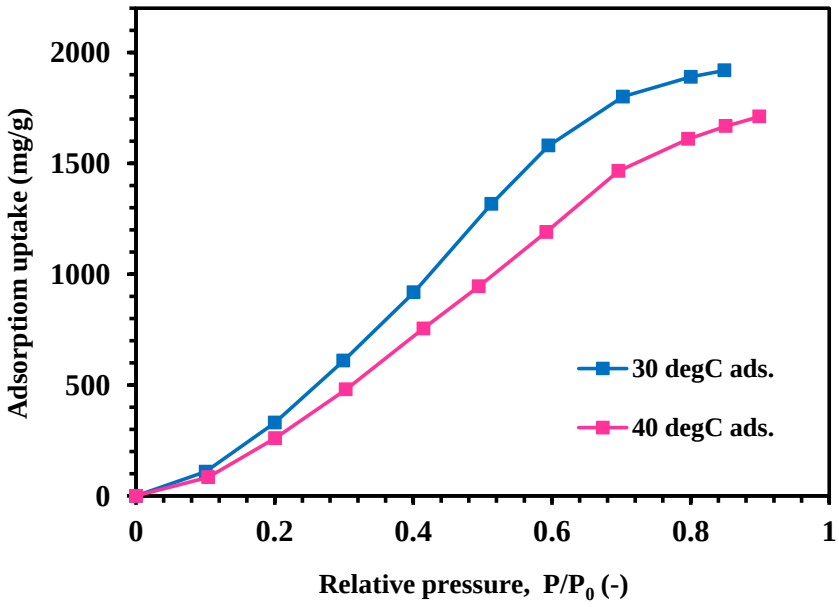

Figure 2.3 Adsorption isotherm curves of SAC-methanol pair at 30 and 40°C temperature.

The Dubinin-Astakhov (D-A) equation Eq. (2.1) is used to fit the adsorption isotherms of SAC-methanol pair.

$$W = W_0 \exp\left(-\left(\frac{RT}{E}\ln\left(\frac{p_s}{p}\right)\right)^n\right) \quad (2.1)$$

Where, W represents the equilibrium uptake and W_0 is the maximum uptake. P denotes the equilibrium pressure and p_s is the saturation pressure corresponding to the adsorption temperature T. E and n indicates characteristic energy and heterogeneity parameter, respectively. The fitting parameters of D-A equation for SAC-methanol pair was found W_0 = 1.87 kg/kg, n = 1.6 and E = 59 kJ/kg.

Adsorption uptake measurement in case of Maxsorb III-ethanol and SAC-ethanol pair has been done by gravimetric method previously. D-A equation is also used to fit the adsorption isotherms of these two pairs. The value of $W_{0,}$ n and E for Maxsorb III-ethanol pair were found by El-Sharkawy et al. (2014) which are 1.2 kg/kg, 1.8 and 139.5 kJ/kg, respectively. The value of $W_{0,}$ n and E for SAC-ethanol pair were reported 1.98 kg/kg, 1.5 and 90 kJ/kg, respectively (Miyazaki et al., 2017).

To predict the adsorption isotherm for Maxsorb III-methanol, Dubinin-Radushkevich (D-R) equation has been used. D-R equation has been presented as follows.

$$W = W_0 \exp(-D(T\ln(\frac{P_s}{P})^2)) \quad (2.2)$$

Where, W represents the equilibrium uptake and W_0 is the maximum uptake. P denotes the equilibrium pressure and p_s is the saturation pressure corresponding to the adsorption temperature T. The value of $W_{0,}$ D for Maxsorb III-methanol pair was reported 1.24 kg/kg, 0.000004022 K^{-2}, respectively (El-Sharkawy et al., 2009).

Figure 2.4 shows the adsorption isotherm curve predicted by D-A equation for the Maxsorb III-ethanol in the range of 20^{o}C to 80^{o}C temperature. Figure 2.5 and 2.6 presents the adsorption isotherms for SAC-ethanol pair and SAC-methanol pair, respectively. Adsorption isotherm Curves for Maxsorb III-methanol pair predicted by D-R equation are shown in Figure 2.7.

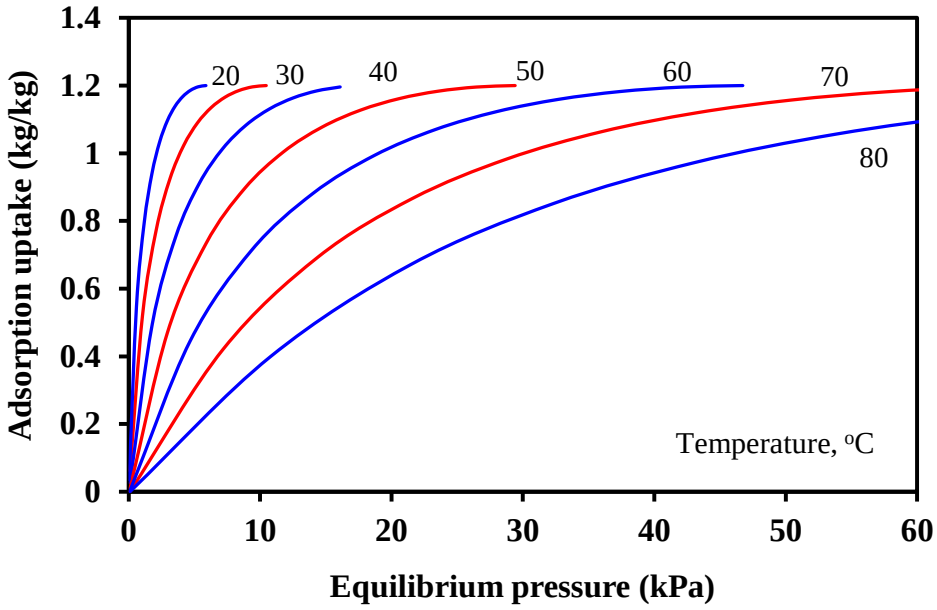

Figure 2.4 Adsorption isotherms predicted by D-A equation for Maxsorb III-ethanol pair (El-Sharkawy et al., 2014).

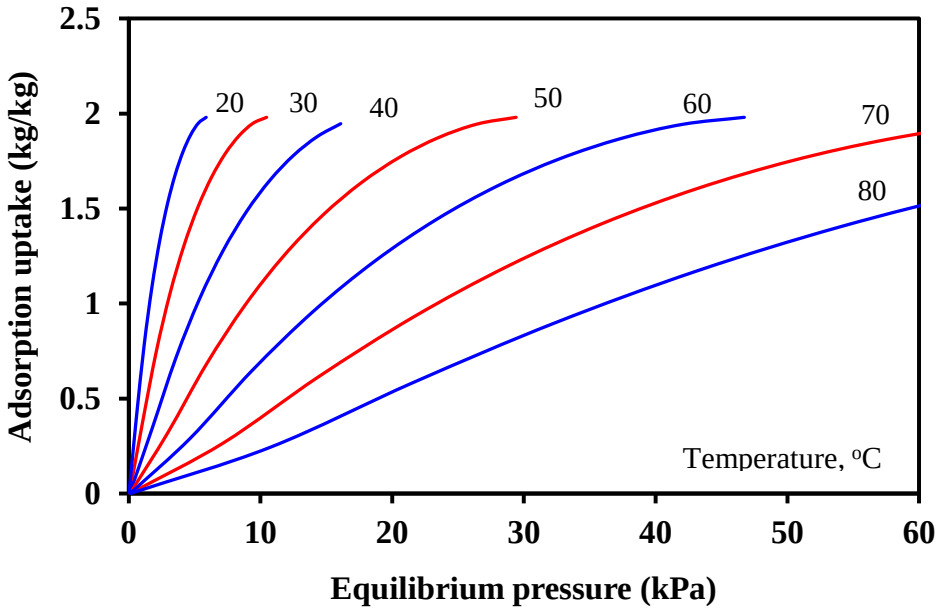

Figure 2.5 Adsorption isotherms of SAC-ethanol pair predicted by D-A equation (Miyazaki et al., 2017).

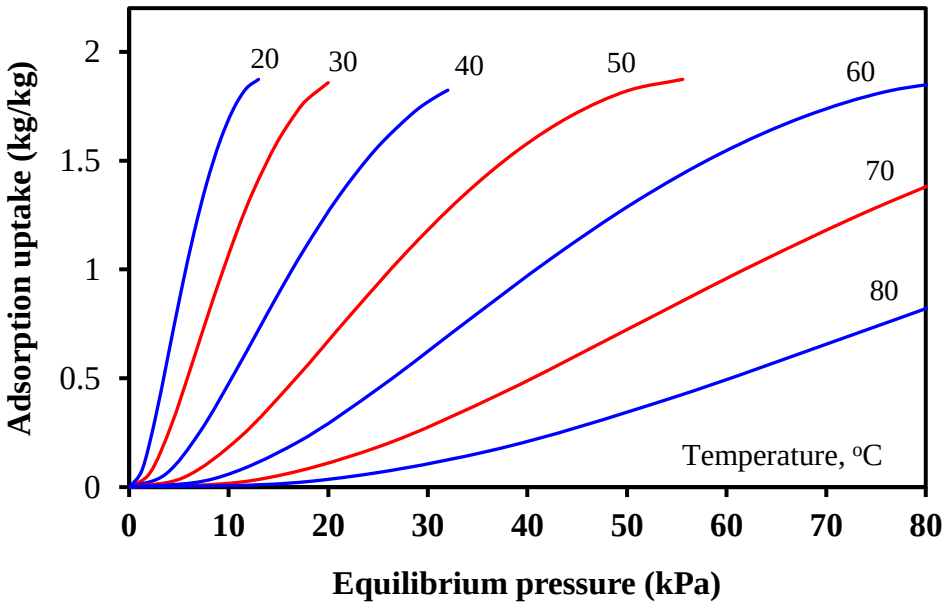

Figure 2.6 Adsorption isotherm curves of SAC-methanol pair predicted by D-A equation.

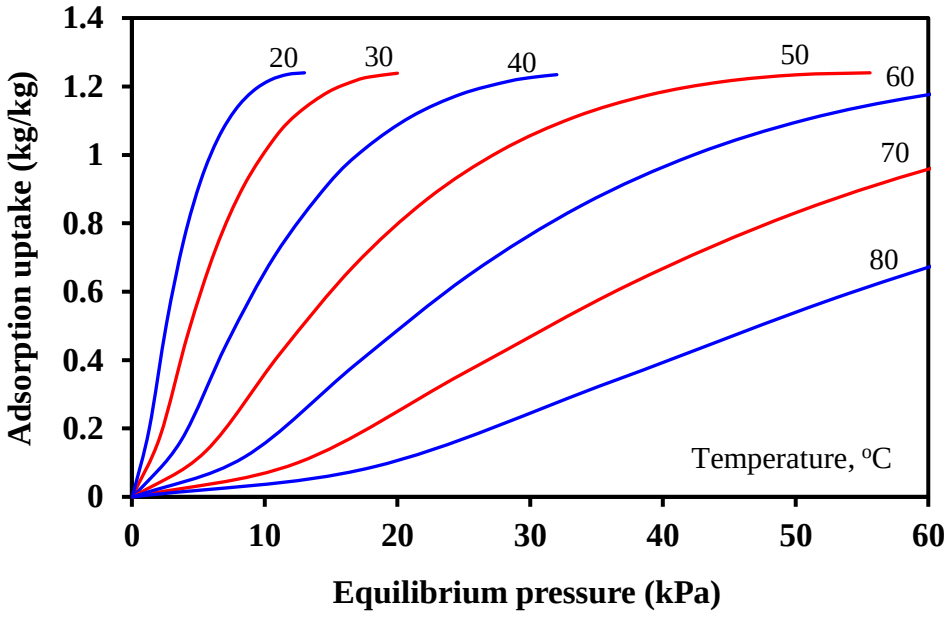

Figure 2.7 Adsorption isotherms of Maxsorb III-methanol pair predicted by D-R equation (El-Sharkawy et al., 2009).

2.4 Performance comparison

Figure 2.8 displays the comparison of ethanol and methanol adsorption onto SAC at 30°C temperature. The maximum ethanol adsorption onto SAC at 30°C is nearly 2030 mg/g while the adsorption amount is about 1900 mg/g in case of methanol. Besides, the effective adsorption amount in the relative pressure range from 0.1 to 0.3 is 722 mg/g in case of ethanol while the amount is 500.6 mg/g for methanol. Therefore, it is evident from the figure that ethanol adsorption is higher than methanol onto SAC. As ethanol has more hydrophobic properties than methanol because of a longer carbon chain, thus, hydrophobic porous carbons prefer to adsorb ethanol more. The shapes of adsorption isotherms, concave and convex curves also propose those properties.

Figure 2.9 demonstrates the comparison between adsorption uptake difference of adsorption cooling cycles employing SAC-ethanol and SAC-methanol pairs at the evaporator, adsorption and desorption temperatures of 10, 30 and 70°C, respectively. It can be seen from Figure 2.9 that adsorption uptake difference of SAC-ethanol pair is about 15% higher in comparison with SAC-methanol pair.

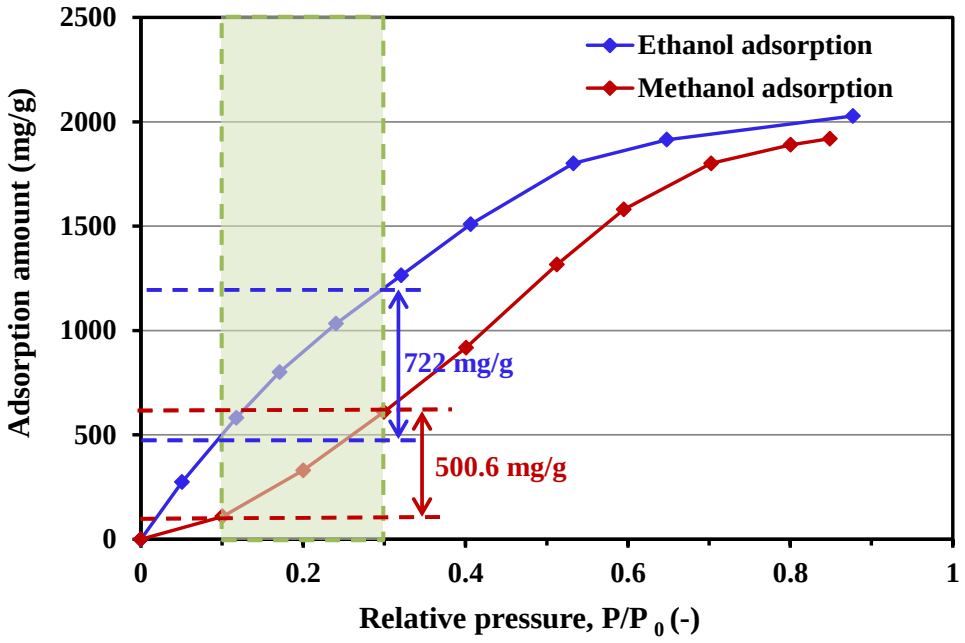

Figure 2.8 Ethanol and methanol adsorption onto SAC at 30°C temperature.

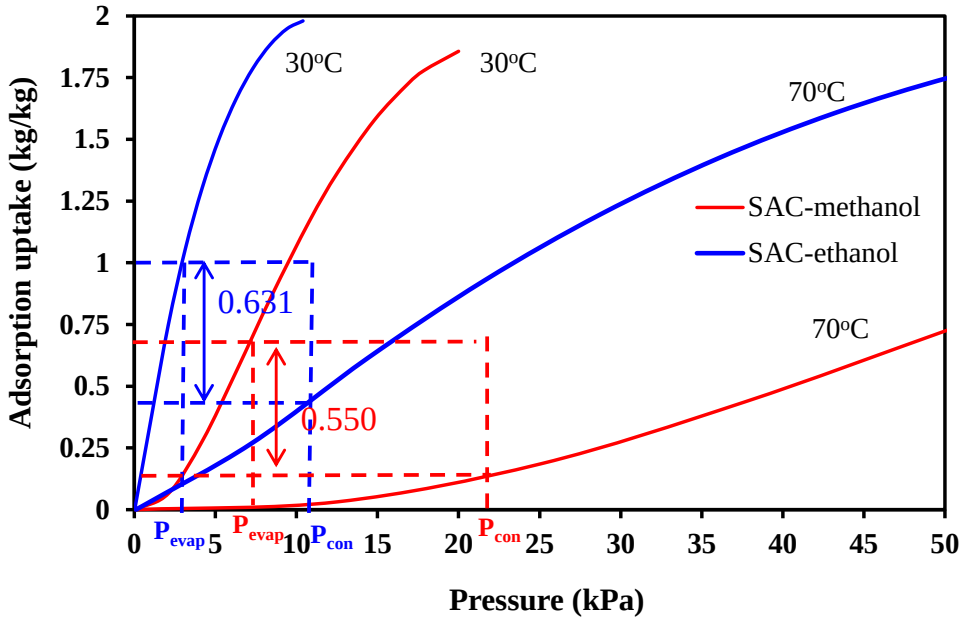

Figure 2.9 Comparison of adsorption uptake of adsorption cooling cycle for SAC-ethanol and SAC-methanol pairs.

Figure 2.10 shows the SCE variation with desorption temperature for SAC-ethanol and SAC-methanol pairs. As can be seen from Figure 2.10 that SAC-methanol pair shows better SCE than that of SAC-ethanol pair below 80^{o}C desorption temperature. After 80^{o}C desorption temperature, the performance of SAC-methanol is almost constant. On the other hand, SAC-ethanol pair shows better performance for desorption temperature more than 80^{o}C. Though it is found in Figure 2.9 that methanol adsorption is lower than ethanol at 70^{o}C desorption temperature. The reason of good performance of SAC-methanol pair below 80^{o}C temperature is that the heat of evaporation in case of methanol is higher than that of ethanol. In this case, SAC-ethanol pair is better than SAC-methanol pair as methanol is toxic as a refrigerant as well as SAC-methanol pair does not show significant performance difference comparing with SAC-ethanol pair.

Figure 2.11 shows the performance comparison of newly developed adsorbent SAC, and commercially available activated carbon Maxsorb III using ethanol as a refrigerant for desorption temperature 50 to 100^{o}C. From the comparison results, it is found that SAC-ethanol pair shows comparatively good performance than Maxsorb III-ethanol pair.

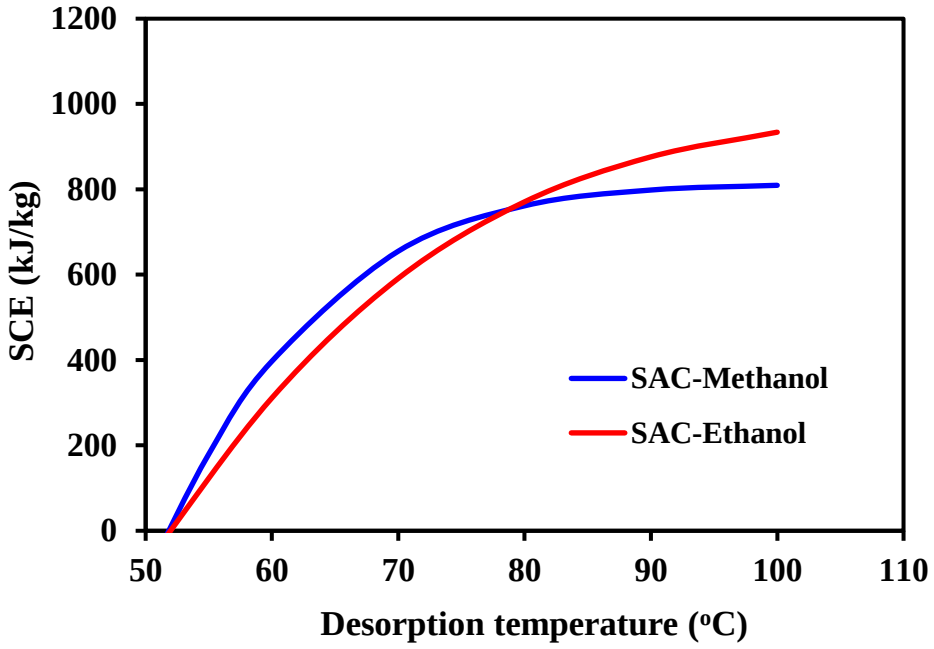

Figure 2.10 Specific cooling effect (SCE) vs. desorption temperature of SAC-ethanol and SAC-methanol pairs.

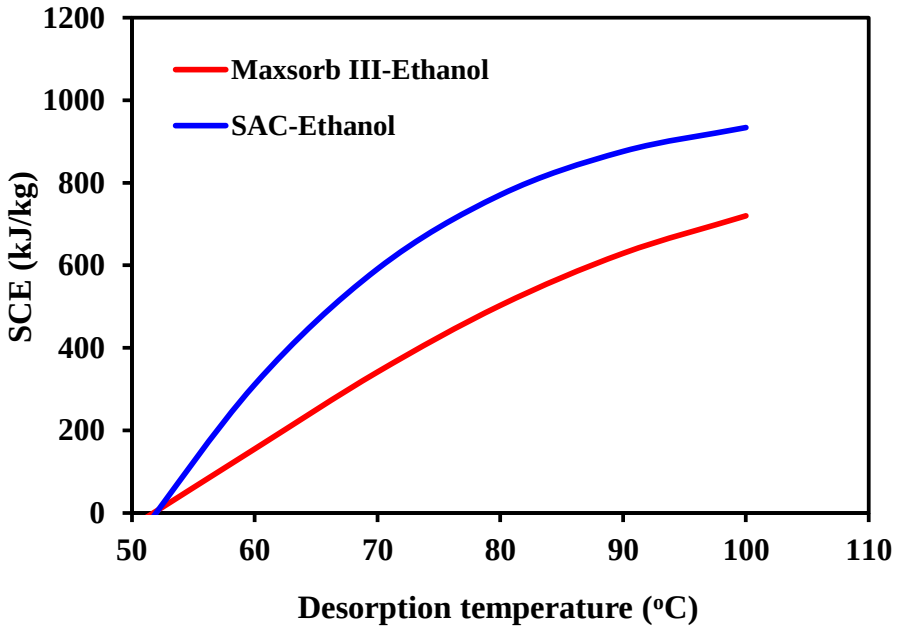

Figure 2.11 Comparison of specific cooling effect (SCE) of SAC-ethanol and Maxsorb III-ethanol pair.

2.5 Conclusion

The conclusions of this chapter are as follows:

- Adsorption equilibriums of SAC and Maxsorb III employing refrigerant ethanol and methanol have been presented.
- Performance comparison of SAC-methanol and SAC-ethanol pair has been done in terms of SCE for the desorption temperature 60 to 100^{o}C. SAC-methanol pair shows a little better performance than that of SAC-ethanol pair below 80^{o}C desorption temperature. After 80^{o}C desorption temperature, the performance of SAC-ethanol pair is significantly better.
- From the performance comparison of newly developed spherical activated carbon (SAC) and commercially available activated carbon type Maxsorb III using ethanol as a refrigerant, it is found that SAC-ethanol pair shows much better performance than Maxsorb III-ethanol pair.
- In our simulation study described in chapter 4 and 5, we chose ethanol as a refrigerant instead of methanol as methanol is toxic. Besides, Maxsorb III is considered as an adsorbent though SAC shows better performance. The reason is that Maxsorb III is commercially available and low cost compared with SAC as SAC still is in research and development stage.

2.6 Nomenclature

n	heterogeneity parameter $[-]$
p	equilibrium pressure [kPa]
p_s	saturation pressure [kPa]
R	gas constant
T	temperature [K]
W	equilibrium uptake[kg/kg]
W_0	maximum uptake[kg/kg]

Acronyms

GCMC	grand-canonical monte carlo

SAC	spherical activated carbon
SCE	specific cooling effect
SEM	scanning electron microscope

2.7 References

El-Sharkawy, I. I., Uddin, K., Miyazaki, T., Baran Saha, B., Koyama, S., Kil, H. S., Yoon, S. H., Miyawaki, J. (2015). Adsorption of ethanol onto phenol resin based adsorbents for developing next generation cooling systems. International Journal of Heat and Mass Transfer, 81, 171–178. https://doi.org/10.1016/j.ijheatmasstransfer.2014.10.012

El-Sharkawy, I. I., Uddin, K., Miyazaki, T., Saha, B. B., Koyama, S., Miyawaki, J., & Yoon, S. H. (2014). Adsorption of ethanol onto parent and surface treated activated carbon powders. International Journal of Heat and Mass Transfer, 73, 445–455. https://doi.org/10.1016/j.ijheatmasstransfer.2014.02.046

El-Sharkawy, I. I., Hassan, M., Saha, B. B., Koyama, S., & Nasr, M. M. (2009). Study on adsorption of methanol onto carbon based adsorbents. International Journal of Refrigeration, 32(7), 1579–1586. https://doi.org/10.1016/j.ijrefrig.2009.06.011

Miyazaki, T., Miyawaki, J., Tomonori, O., Yoon, S. H., Saha, B. B., & Koyama, S., (2017). Study toward high-performance thermally driven air-conditioning systems. In AIP Conference Proceedings. American Institute of Physics. https://doi.org/https://doi.org/10.1063/1.4968250

Tamainot, Z., Metcalf, S. J., Critoph, R. E., Zhong, Y., & Thorpe, R. (2009). Carbon-ammonia pairs for adsorption refrigeration applications: ice making, air conditioning and heat pumping. International Journal of Refrigeration, 32(6), 1212–1229. https://doi.org/10.1016/j.ijrefrig.2009.01.008

Wai S. L., Azhar B. I., Baojuan X., Kim C. N., and W. G. C. (2012). Adsorption Isotherms and Isosteric Enthalpy of Adsorption for Assorted Refrigerants on Activated Carbons. Journal of Chemical Engineering & Data, 57(10), 2766–2773. https://doi.org/10.1021/je3008099

Chapter 3

3 Heat Transfer Enhancement in Adsorber Bed

Heat transfer enhancement in adsorber bed has a huge prominence in the performance improvement of adsorption cooling system. This chapter presents comprehensive discussions on various ways of heat transfer enhancement inside the adsorber bed which are consolidated adsorbent, binder based coatings and different heat exchanger types. This study also focuses on different types of heat exchanger geometries used as an adsorber bed previously to enhance the heat transfer in the bed. Finally, the performance of adsorption cooling system using different types of heat exchangers for silica gel and activated carbon has been shown.

3.1 Introduction

The performance of adsorption cooling system (ACS) strongly depends on heat and mass transfer characteristics inside the adsorber bed. Heat transfer and mass transfer are related to each other strongly. Heat transfer improvement in the adsorber bed can accelerate the adsorption and desorption process which is one of the key ways to improve the system performance (which can shorten the cycle time). Besides, if the heat transfer inside the bed is not good during the adsorption time, it will not be possible to reach its highest adsorption capacity. Moreover, during desorption time, full desorption of refrigerant vapor will not be possible. Therefore, it can be said that adsorption system performance has a direct relation to the heat transfer characteristics of adsorber bed. An adsorber bed is consists of a heat exchanger and adsorbent. Therefore, heat

exchanger design and adsorbent's heat transfer properties both are crucial for heat transfer enhancement inside the bed.

3.2 Literature reviews on heat transfer enhancement

Poor heat transfer characteristics in the adsorber bed are one of the main reasons for low system performances which hinder this system form widespread utilization. Researchers have been making several attempts for last few years to improve the heat transfer characteristics of adsorber bed which are consolidated adsorbent, heat exchanger design improvement, and coated heat exchanger. They found that all these methods can contribute to enhance the heat transfer in the bed.

Figure 3.1 shows the heat transfer process inside an adsorber bed and contribution of these three methods to boost up the heat transfer in the bed.

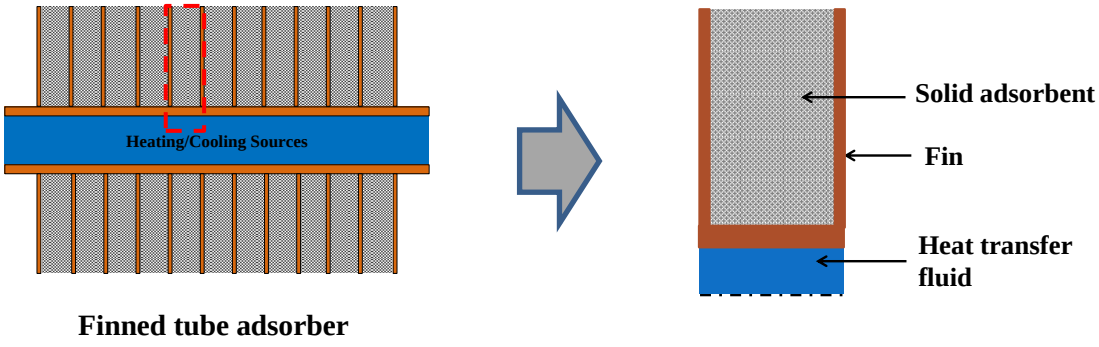

Figure 3.1 Heat transfer process inside an adsorber.

In an adsorber bed, heat transfer occurs in several steps such as (i) during desorption process, first heat is transferred in convection process from heat transfer fluid to the metallic wall of heat exchanger (ii) then, heat is transferred through the metallic wall by conduction process (iii) after that, there is contact resistance between metallic wall and the adsorbent. Heat transfer is occurred in convection process from metallic wall to the adsorbent, (iv) then mainly by conduction

process, heat is transferred from one adsorbent particle to another adsorbent particle (Wang et al, 1998). Therefore, the overall heat transfer performance of an adsorber bed depends on these four steps. To improve heat transfer in case of step (i), heat exchanger design can play an important role in enhancing the heat transfer surface area. For maintaining good heat transfer in step (ii), the metallic wall thickness should be as low as possible after assuring the strength of heat exchanger (Wang et al., 1998). To reduce the thermal resistance at the interface of the metallic wall and the adsorbent (iii), coated heat exchanger has been introduced. It can ensure good contact between metallic wall and the adsorbent, and improve the heat transfer between these two. Solid adsorbents are porous materials with low thermal conductivity, and the thermal contact resistance between adsorbent particles are also high which contribute to making the overall thermal conductivity of adsorbent low (Zhu & Wang, 2002) (Rezk et al., 2013). To maximize the conduction heat transfer in step (iv), the consolidated adsorbent can show a crucial role. During adsorption process, heat transfer will be occurred in the same way but in reverse direction.

3.2.1 Consolidated adsorbents

The powder type adsorbents were used at the beginning of the adsorption cooling system. However, it is discovered by researchers that in case of powder adsorbents the thermal conductivity is not good. Conduction is one of the leading ways of heat transfer from one adsorbent particle to another adsorbent particle of adsorbent. Therefore, the effective method to improve the heat transfer inside the adsorbent is the thermal conductivity enhancement. It can be achieved by adding the right thermal conductive materials and making the adsorbent consolidated or applying both together. By making the adsorbent consolidated, the density of the adsorbent can be enhanced. Figure 3.2 shows the process of making of consolidated composite adsorbent block; first, activated carbon and expanded graphite are dried in the oven to eliminate the moisture content. Then dried activated carbon and expanded graphite in specific ratios is mixed with the binder solution. After that, the mixture is compressed by applying pressure. Finally, the composite adsorbent is dried in the oven to remove the water vapor. The density of the composite block can be varied by changing the applied pressure (El-Sharkawy et al., 2016).

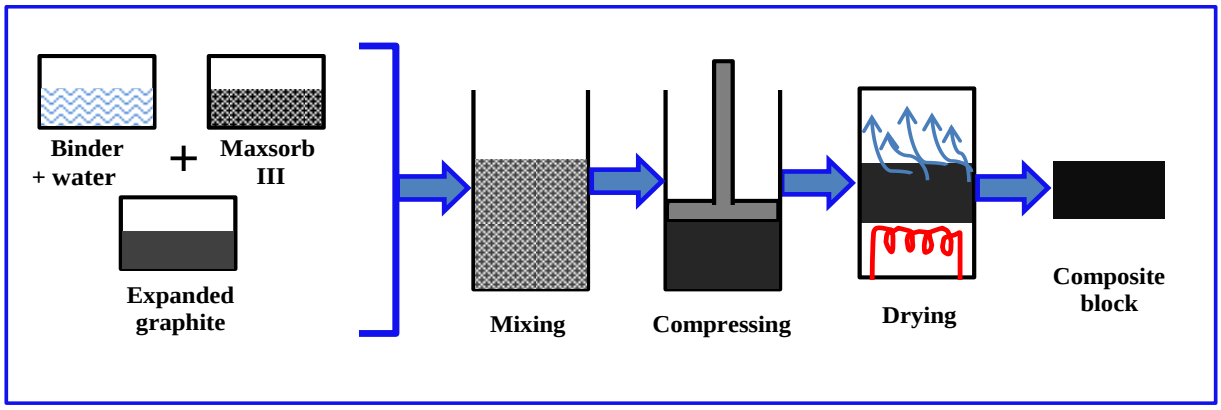

Figure 3.2 Producing processes of consolidated composite activated carbon block (El-Sharkawy et al., 2016).

Several researchers already reported the thermal conductivity improvement through composite adsorbents (Tamainot & Critoph, 2001; Wang et al., 2011; Py et al., 2002; Tian et al., 2012). A consolidated composite adsorbent based on activated carbon with a host matrix of expanded graphite treated with sulfuric acid (ENG-TSA) was developed by Wang et al. (2012) and they reported that the highest effective thermal conductivity of the composite activated carbon is 150 times higher than ordinary granular activated carbon and the value was 34.2 $Wm^{-1}K^{-1}$. Jin et al. (2013) reported the comparison of the thermal conductivity of granular activated carbon, consolidated activated carbon with a chemical binder and consolidated activated carbon with expanded natural graphite. Their reported thermal conductivity in case of granular activated carbon and consolidated activated carbon with chemical binder are approximately 0.36 $Wm^{-1}K^{-1}$ and 0.4 $Wm^{-1}K^{-1}$ respectively while the value of thermal conductivity for consolidated activated carbon with expanded natural graphite ranges from 2.08 $Wm^{-1}K^{-1}$ to 2.61 $Wm^{-1}K^{-1}$. The thermal conductivity of a composite desiccant adsorbent based on silica gel with expanded natural graphite treated with sulfuric acid (ENG-TSA) was reported by Zheng et al. (2014) and they showed thermal conductivity of composite desiccant adsorbent could be increased 270 times comparing to that of pure silica gel.

Previously in our laboratory, a composite adsorbent block has been developed by comprising activated carbon powder namely Maxsorb III, expanded graphite and a binder, and compared with the Maxsorb III powder (El-Sharkawy et al., 2016). From experimental results, it is found that thermal conductivity of the developed composite adsorbent can be improved 11 times higher comparing to the Maxsorb III powder. They reported the highest value of thermal conductivity 0.74 $Wm^{-1}K^{-1}$ at composite packing density of 650 kg m^{-3}. It is evident from Figures 3.3 that thermal conductivity of the composite adsorbent is increased with the increase of adsorbents packing density.

Thermal conductivity of composite adsorbents can be enhanced with the percentage increase of expanded graphite as shown in Figures 3.4. From experimental results, it is showed that thermal conductivity of composite adsorbent for 10% expanded graphite was 0.15 $Wm^{-1}K^{-1}$ while the thermal conductivity value reaches to 0.61 $Wm^{-1}K^{-1}$ for 40% expanded graphite (El-Sharkawy et al., 2016).

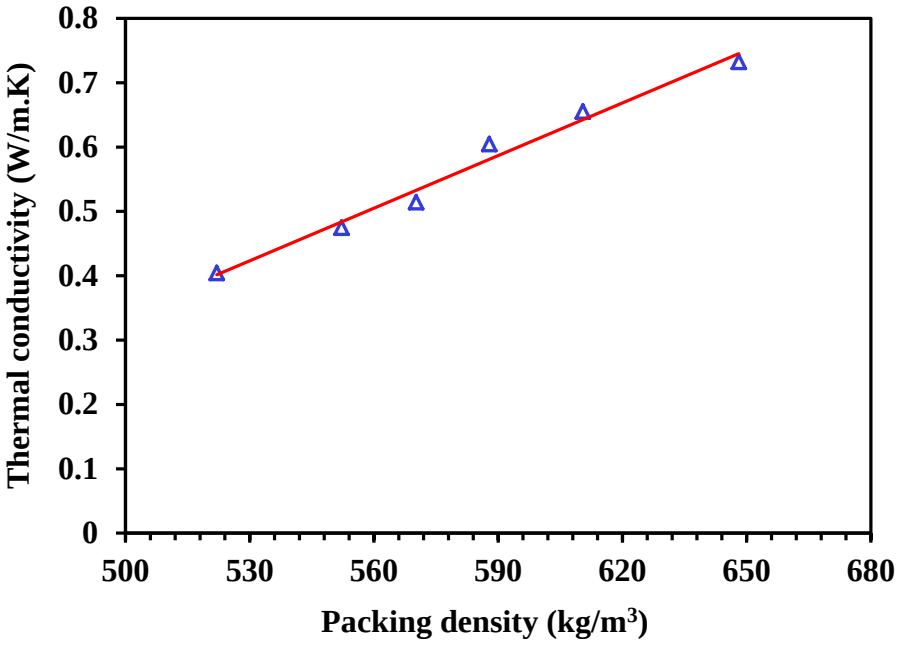

Figure 3.3 Thermal conductivity of composite block (50% Maxsorb III, 40% EG, 10% binder) with the increase of packing density (El-Sharkawy et al., 2016).

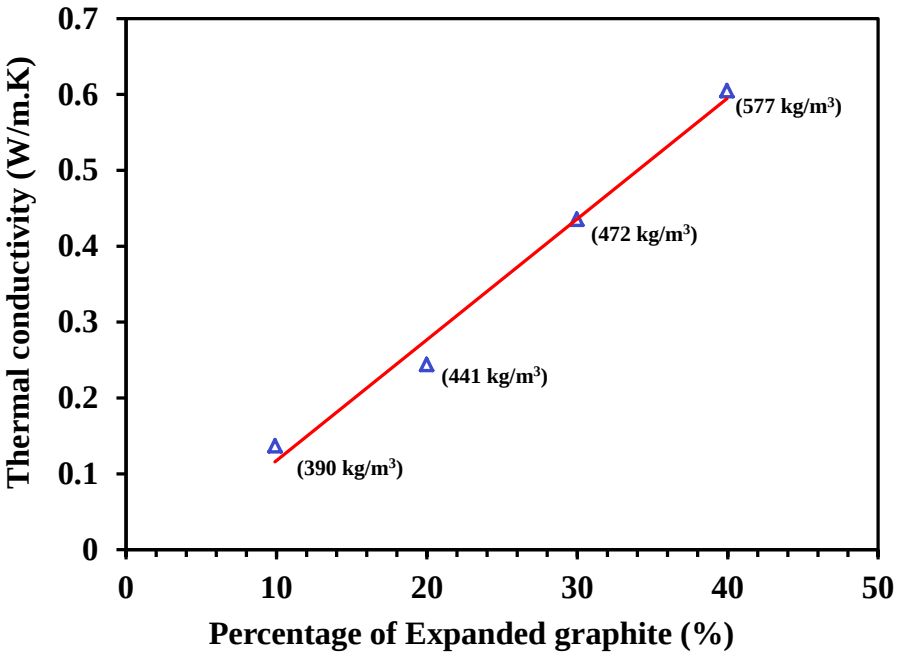

Figure 3.4 Thermal conductivity improvement with the percentage increase of expanded graphite (El-Sharkawy et al., 2016).

3.2.2 Heat exchanger design improvements

Heat exchanger design plays a crucial role to maintain the good heat transfer in the adsorber bed. An optimum heat exchanger design is required to achieve good performance of the adsorber heat exchanger. Weak heat transfer to and from the solid adsorbent bed makes the SCP of the adsorption cooling system low. Low SCP leads to the large size of the systems, contributes for making the use of this technology limited. Therefore, heat transfer enhancement in the bed with the use of extended surfaces of heat exchanger becomes a major concern. In this case, heat exchanger geometries play a vital role. Mahdavikhah and Niazmand (2013) reported the effects of plate finned heat exchanger specifications on the adsorption system performance. The authors showed the relation of COP and SCP with fin height (FH) for different fin spaces (FS) [Figure 3.5]. In case of plate finned heat exchanger, they found that variation of fins spacing has less influence on COP compared to the fin height. For a particular fins spacing, COP enhances with

the increase of fin height. The reason is with the increases of fin height, the quantity of adsorbate increases, which leads to an increase in the cooling energy. Though the amount of heat required for the cycle increases with the fin height increases, however, the cooling energy compensates the heat input and increases the COP. From the Figure 3.5, it is noticeable that with increase of fin height, COP increases while SCP decreases. Therefore, either higher COP or higher SCP can be chosen. Thus, heat exchanger geometry specifications have a significant practical importance in the adsorption cooling system design (Mahdavikhah & Niazmand, 2013).

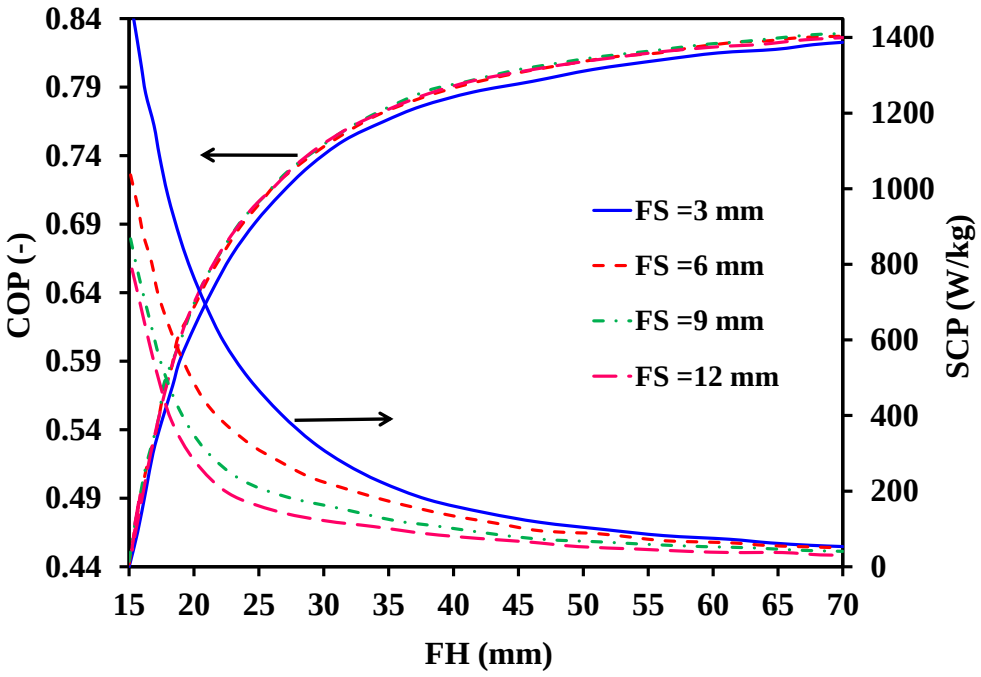

Figure 3.5 Effects of heat exchanger parameters on COP and SCP (Mahdavikhah & Niazmand, 2013).

3.2.3 Binder based-coatings

Another method to improve the heat transfer between the heat exchanger and the adsorbent is a binder-based coating of the adsorber heat exchanger. In case of loose grain and consolidated adsorbents, heat transfer resistance is high at the interface of the heat exchanger and adsorbent. One of the critical advantages of the coated adsorber is that it can reduce heat and mass transfer

resistance by maintaining good contact of adsorbent layer and heat exchanger surface (Freni et al., 2015).

There are two types of coating methods, one is dip coating, and another one is spray coating. Coating thickness usually can be varied up to 0.5 mm. In dip coating method, the heat exchanger is immersed in a liquid solution that is made of active powder and an organic or inorganic binder. Then, a thermal treatment is used to remove the excess solvent. Thus, a compact adsorbent layer is obtained (Freni et al., 2015). Blank and dip coated heat exchanger has been shown in Figure 3.6.

The advantages of dip coating methods (Freni et al., 2015) are as follows:

i. In dip coating method, complex heat exchanger geometries can be coated effortlessly and also uniform coating thickness can be maintained.
ii. By changing the preparative parameters such as temperature and slurry viscosity, coating thickness can be varied and obtained up to 0.5 mm.

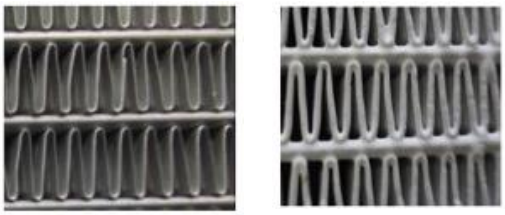

(a) (b)

Figure 3.6 (a) Blank heat exchanger (b) dip coated heat exchanger (Freni et al., 2015).

Several researchers already applied the coating method on adsorber heat exchanger and checked the influence of coating on adsorption system performance (Dawoud et al., 2007; Kummer et al., 2015; Dawoud et al., 2013). Restuccia et al. (2002) developed a tube heat exchanger which is coated with thin zeolite layer by applying the dip-coating method, and they ensured that this coated heat exchanger can assure good heat and mass transfer with the improvement of heat transfer coefficient at the interface of metal and adsorbent.

Waszkiewicz et al. (2009) developed a coated annular fin heat exchanger by using hydrophobic zeolite and cellulose methyl ether binder, and they found noticeable heat transfer enhancement by coating method.

Freni et al. (2015) prepared a 0.1 mm thick coated finned flat-tubes aluminum heat exchanger by applying dip coating technique. The preparation steps of dip coating are shown in Figure 3.7. For coating purposes, SAPO-34 zeolite and silane-based binder have been used. They found good performance, specific cooling power 657 W/Kg_{ads} for 5 min cycle time. Besides, Freni et al. (2013) developed another coating methodology where they used inorganic clay as a binder for AQSOA Z02 material.

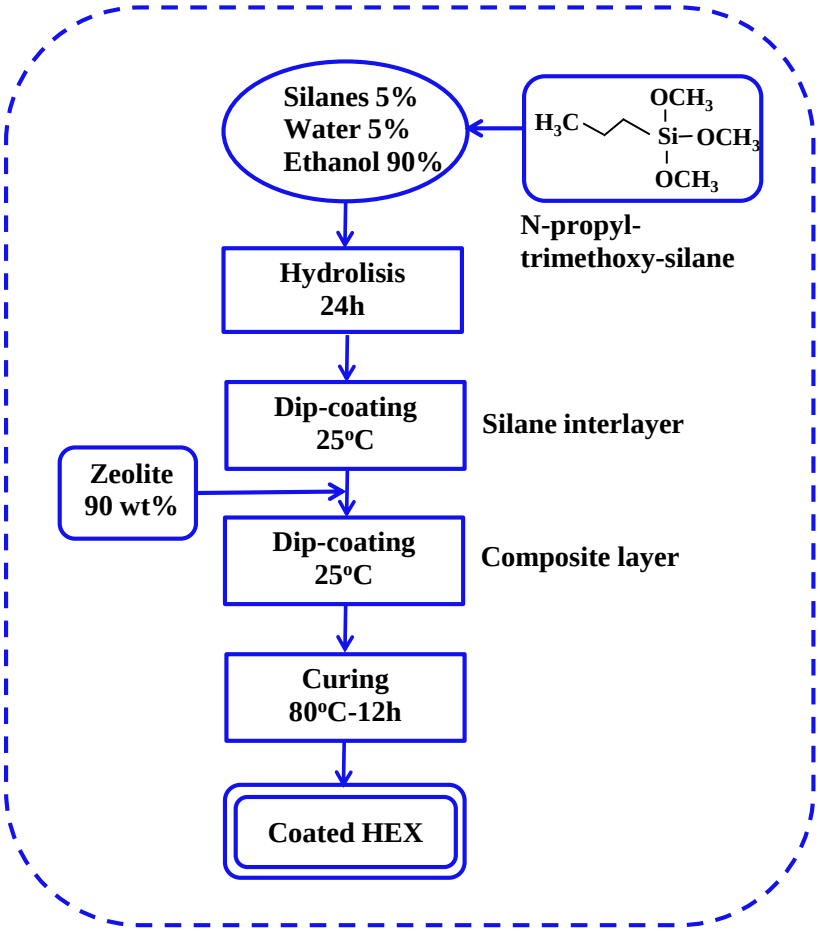

Figure 3.7 Flow-chart of the dip-coating process (Freni et al., 2015).

3.3 Various adsorber bed heat exchanger

3.3.1 Existing heat exchanger types for ACS

The design of adsorber bed heat exchanger is critical. An adsorber heat exchanger should be designed explicitly concerning several things that are as follows:

- Heat capacity ratio between heat exchanger material and the applied adsorbent should be low.
- Overall heat transfer coefficient has to be high between heat transfer fluid and the adsorbent (Freni et al., 2015). High heat transfer coefficient will be cooperative to shorten the adsorption/desorption time. Thus, the system will be compact (Wang et al., 1998).
- High mass diffusion coefficient (Freni et al., 2015).
- The metal part of heat exchanger should be low to ensure cost-effectiveness (Wang et al., 1998).
- Ensure lightweight adsorber heat exchanger to decrease sensible heat transfer losses (Saha et al., 2006).

Besides, there are some reliability design requirements such as high stability in contradiction of hydrothermal aging, high mechanical stability and corrosion free characteristics against loading and different operating conditions (Freni et al., 2015).

However, there are still no conclusive suggestions about the appropriate heat exchanger type for adsorption cooling and refrigeration system (Sharafian and Bahrami, 2014). Therefore, to find out the suitable heat exchanger design, various types of heat exchangers have been selected by researchers as an adsorber to check the heat transfer characteristics experimentally. The heat exchanger types which are already used as an adsorber bed (Figure 3.8) for adsorption air-conditioning and refrigeration systems are as follows:

(a) finned tube (Yang et al., 2006) (b) plate fin (Wang et al., 1998; Liu et al., 2005) (C) flat tube with corrugated fin (Chang et al., 2007) (d) round finned tube (Makimoto et al., 2011) (e) shell and tube without baffles (Oliveira et al., 2006) (f) spiral plate (Wang et al., 1998) (g) plate-finned

tube (Wang et al., 2001b) (h) simple tube (Tamainot and Critoph, 2003) (Critoph 2002) (i) flat-pipe (j) plate type (k) annulus tube (l) hairpin.

Though several types of heat exchanger have been used previously to check the performance as an adsorber, however, in recent times, the use of heat exchanger types like spiral plate, simple tube, flat pipe, plate type, annulus tube and hairpin is very limited. Due to the good heat transfer performance, most commonly used heat exchanger types nowadays are fin and tube, and shell and tube. Fin and tube type heat exchanger includes many varieties such as fin tube, round finned tube, plate fin tube, corrugated fin with flat tube etc.

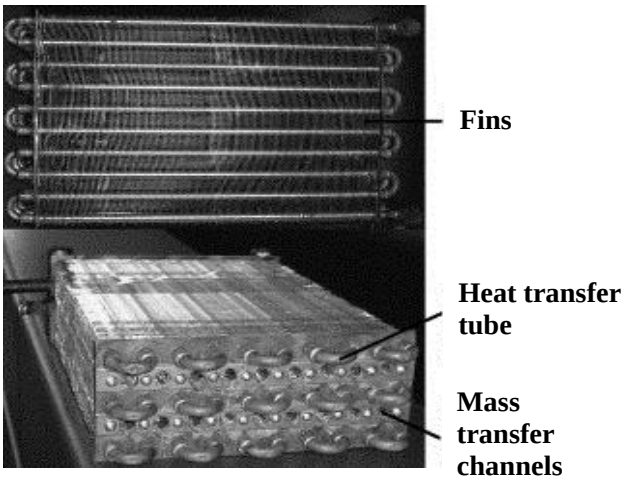

(a) Finned tube adsorber (Yang et al., 2006)

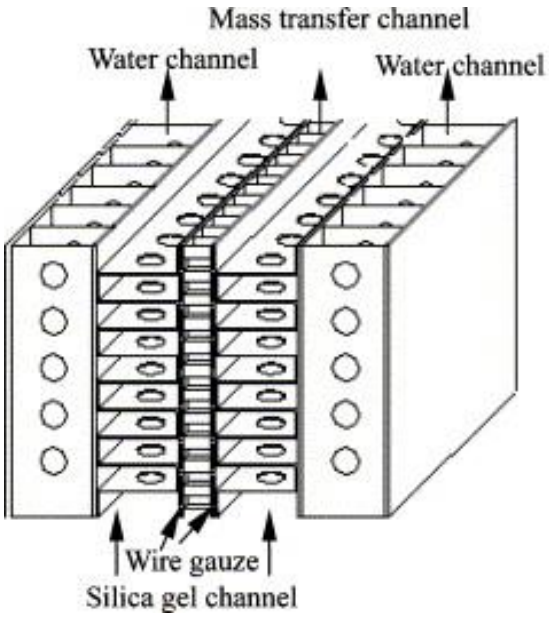

(b) Plate fin (Liu et al., 2005)

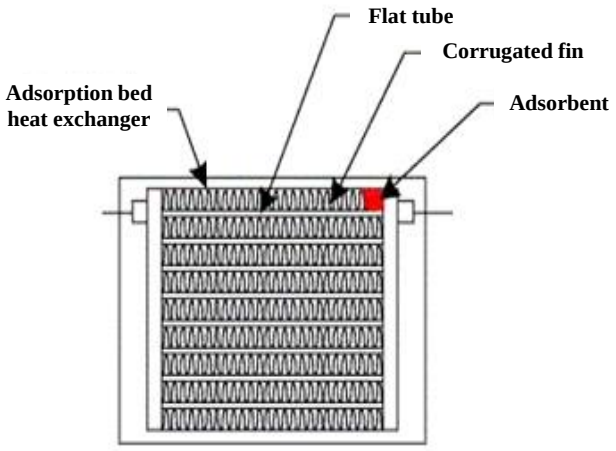

(C) Flat tube with corrugated fin (Chang et al., 2007)

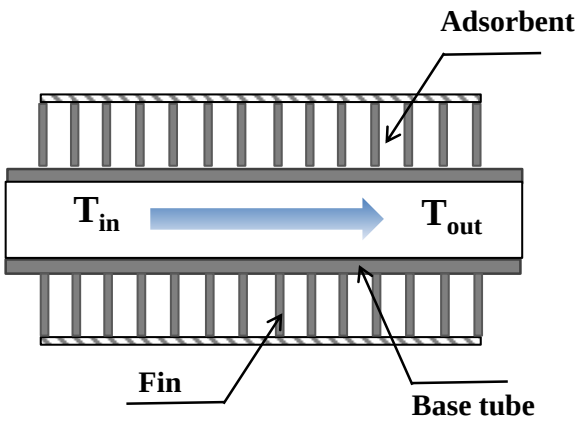

(d) Round finned tube (Makimoto et al., 2010 and 2011)

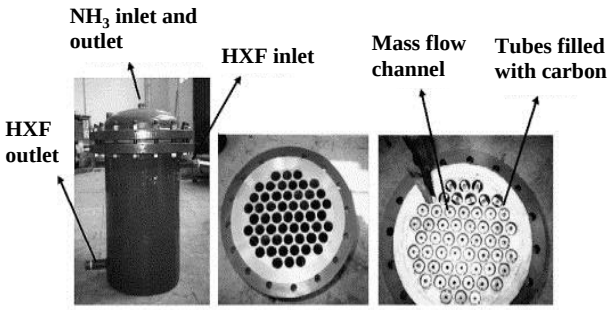

(e) Shell and tube without baffles (Oliveira et al., 2006)

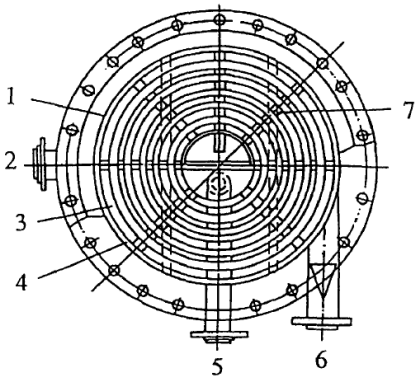

1. spiral plate 2. vapor outlet 3. solid adsorbent 4.fluid flow passage 5. thermal fluid out 6. thermal fluid in 7. support rod.

(f) Spiral plate (Wang et al., 1998)

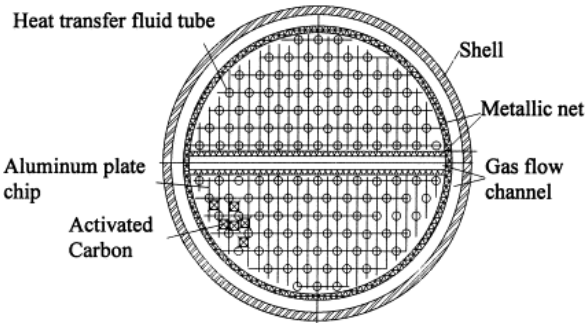

(g) Plate-finned tube (Wang et al., 2001a)

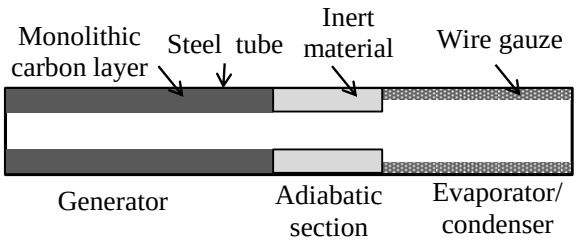

(h) Simple tube (Critoph et al., 2002)

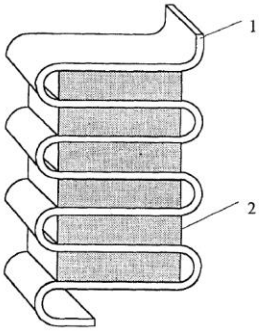

1. Thermal fluid flow channel 2. adsorbent embedded

(i) Flat-pipe (Wang et al., 1998)

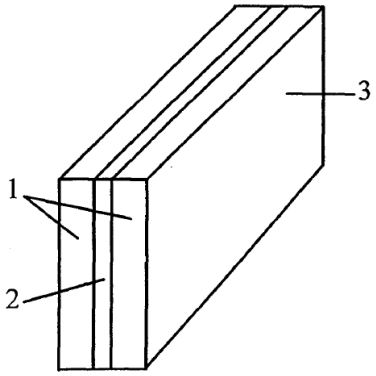

1. adsorbent embedded 2. thermal fluid passage 3. metallic sealing wall.

(j) Plate type (Wang et al., 1998)

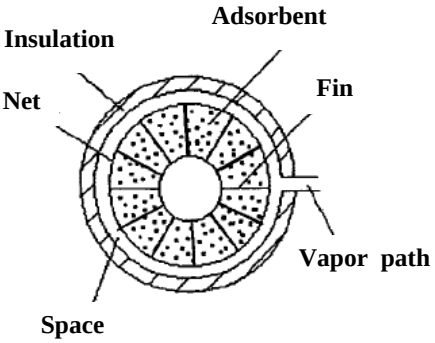

(k) Annulus tube (Pons et al.,1996) (Zhang, 2000)

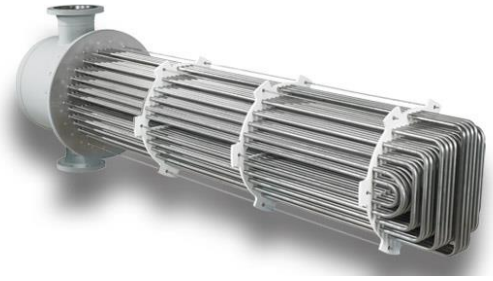

(l) Hairpin (Douss and Meunier, 1989)

Figure 3.8 Different heat exchanger types used in adsorption cooling and refrigeration system.

3.3.2 Performance comparison of various adsorber heat exchanger

The performance of adsorption cooling and refrigeration system strongly depends on heat exchanger shape; however, operating conditions such as cycle time, evaporator temperature, heat source temperature, adsorption temperature also influence the system performance. The effects of operating conditions on system performance have not discussed in this study and it is not very critical to find out for a specific type of heat exchanger. Therefore, the main focus of this study is to discuss the performances of different types of heat exchangers for available low-grade waste heat (nearly 100^{o}C temperature heat source). To assess the performance of adsorption system, two important parameters are the coefficient of performance (COP) and specific cooling power (SCP). Volumetric cooling power (VCP) is also a very important parameter to ensure whether the heat exchanger design is compact or not.

The commonly used adsorbents in adsorption cooling system are silica gel, zeolite and activated carbon (Sharafian and Bahrami, 2014). However, it has been tried to compare the performance of different types of heat exchanger employing silica gel-water, activated carbon-methanol and activated carbon-ethanol pairs as these working pairs are suitable for below 100^{o}C waste heat. The performance of different heat exchanger types are summarized in Table 3.1.

From the literature review, it is found that for silica-gel water working pairs, the chosen heat exchanger types are plate-fin, fin-tube and corrugated fin with the flat tube. Within these types, fin-tube specially corrugated fin and flat tube shows relatively high COP than plate fin types for below 85^{o}C temperature. However, plate fin heat exchanger shows better SCP.

In case of activated carbon and methanol pair, several types of heat exchanger have been used by researchers which are plate-fin, finned tube, spiral plate, and plate fin shell tube. From the performance analysis, it is shown that plate fin, and plate fin shell tube heat exchanger design show good COP value comparing with finned tube and spiral plate for nearly 100^{o}C heat source temperature. However, finned tube type adsorber shows good SCP value which is 396.6 W/kg at 85^{o}C desorption temperature.

The performance of adsorption cooling system employing activated carbon powder-ethanol pair has been investigated for two different types of heat exchanger which are round finned tube, and corrugated fin by Makimoto et al. (2010) and Jerai et al. (2015) respectively. From results, it is found that the COP in case of round-finned tube is better rather than corrugated fin for activated carbon-ethanol pair. However, corrugated fin shows better SCP comparing with round fin tube.

Table 3.1 Performance of adsorption cooling system for different heat exchanger types

Adsorbent	**Refrigerant**	**Adsorber heat exchanger type**	**Operating conditions**	**COP**	**SCP/ CP**	**References**
Silica gel	water	plate-fin	heat source-85^{o}C,cooling water-28^{o}C	0.419	278 [W/kg]	(Liu et al., 2005)(Liu et al., 2005)
Silica gel	water	plate-fin	hot water-80^{o}C, cooling water-30^{o}C	0.34	130 [W/kg]	(Akahira et al., 2005)
Silica gel	water	tube-fin	hot water-84.3^{o}C, cooling water-30.4^{o}C	0.41	94 [W/kg]	(Wang et al., 2005a)(Wang et al., 2005b)
Silica gel	water	finned tube	hot water-85^{o}C, cooling water-28^{o}C	0.339	158 [W/kg]	(Yang et al., 2006)
Silica gel	water	tube-fin	hot water-66^{o}C, cooling water-30.5^{o}C	0.385	6.0 [kW]	(Wang et al., 2007)

Silica gel	water	corrugated fins with flat tube	hot water-80^{o}C, cooling water-30^{o}C	0.45	176 [W/kg]	(Chang et al., 2007)
Activated carbon	ammonia	shell and tube without baffles	heat source/generation temp-85^{o}C	0.06	1.7 [kg/h ice]	(Oliveira et al., 2006)
Activated carbon	methanol	plate-fin	des temp-80^{o}C ads temp-30^{o}C	0.44	-	(Wang et al., 2001b)
Activated carbon	methanol	finned tube	des temp-85^{o}C	0.19	396.6 [W/kg]	(Lim and Abdullah, 2010)
Activated carbon	methanol	spiral plate	des temp-100^{o}C ads temp-25^{o}C	-	14 [kg/day ice]	(Wang et al., 1998)
Activated carbon	methanol	shell tube	Heating temp-110^{o}C	0.057	11 [W/kg]	(Li et al., 2010)
Activated carbon	methanol	spiral plate	heat source temp-100^{o}C	0.13	2.6 [kg/day ice]	(Wang et al., 2001)
Activated carbon	methanol	plate-fin shell and tube	heat source temp-100^{o}C	0.4	150 [W/kg]	(Wang et al., 2001)
Activated carbon	ethanol	corrugated fin	hot water-90^{o}C, cooling water-30^{o}C	0.2	358.3 [W/kg]	(Jerai et al., 2015)
Activated carbon	ethanol	round-finned tube	hot water-80^{o}C, cooling water-20^{o}C	0.4	503 [W]	(Makimoto et al., 2011)

3.4 Concluding remarks

- An extensive review has been done on heat transfer improvement in the adsorber bed. The three main ways of heat transfer improvement have been discussed which are consolidated or consolidated composite adsorbent, heat exchanger design optimization and coated heat exchanger.
- A review study of existing heat exchanger geometries for adsorption cooling system indicates that finned and tube type adsorber is the commonly used heat exchanger type.
- For silica gel-water working pair, finned-tube type heat exchanger specially corrugated fin and flat tube shows relatively high COP than plate fin types for 85^{o}C desorption temperature.
- In case of activated carbon and methanol pair, plate fin, and plate fin shell tube type heat exchanger show good COP value comparing with finned tube and spiral plate for nearly 100^{o}C heat source temperature. However, finned tube type adsorber shows good SCP value which is 396.6 W/kg at 85^{o}C desorption temperature.
- For activated carbon-ethanol pair, it is found that the COP in case of round-finned tube is better rather than corrugated fin; however, corrugated fin shows better SCP comparing with round fin tube.

3.5 Nomenclature

Acronyms

ACS	adsorption cooling system
AHP	adsorption heat pump
COP	coefficient of performance
CP	cooling power
SCP	specific cooling power
VCP	volumetric cooling power

3.6 References

Akahira, A., Alam, K. C. A., Hamamoto, Y., Akisawa, A., & Kashiwagi, T. (2005). Experimental investigation of mass recovery adsorption refrigeration cycle. International Journal of Refrigeration, 28, 565–572. https://doi.org/10.1016/j.ijrefrig.2004.10.001

Chang, W. S., Wang, C. C., & Shieh, C. C. (2007). Experimental study of a solid adsorption cooling system using flat-tube heat exchangers as adsorption bed. Applied Thermal Engineering, 27, 2195–2199. https://doi.org/10.1016/j.applthermaleng.2005.07.022

Critoph, R. E. (2002). Multiple bed regenerative adsorption cycle using the monolithic carbon-ammonia pair. Applied Thermal Engineering, 22, 667–677. https://doi.org/10.1016/S1359-4311(01)00118-1

Dawoud, B. (2013). Water vapor adsorption kinetics on small and full scale zeolite coated adsorbers; A comparison. Applied Thermal Engineering, 50(2), 1645–1651. https://doi.org/10.1016/j.applthermaleng.2011.07.013

Dawoud, B., Vedder, U., Amer, E. H., & Dunne, S. (2007). Non-isothermal adsorption kinetics of water vapour into a consolidated zeolite layer. International Journal of Heat and Mass Transfer, 50, 2190–2199. https://doi.org/10.1016/j.ijheatmasstransfer.2006.10.052

Douss, N., & Meunier, F. (1989). Experimental study of cascading adsorption cycles. Chemical Engineering Science, 44(2), 225–235. https://doi.org/10.1016/0009-2509(89)85060-2

El-Sharkawy, I. I., Pal, A., Miyazaki, T., Saha, B. B., & Koyama, S. (2016). A study on consolidated composite adsorbents for cooling application. Applied Thermal Engineering, 98, 1214–1220. https://doi.org/10.1016/j.applthermaleng.2015.12.105

Freni, A., Bonaccorsi, L., Calabrese, L., Caprì, A., Frazzica, A., & Sapienza, A. (2015). SAPO-34 coated adsorbent heat exchanger for adsorption chillers. Applied Thermal Engineering, 82, 1–7. https://doi.org/10.1016/j.applthermaleng.2015.02.052

Freni, A., Dawoud, B., Bonaccorsi, L., Chmielewski, S., Frazzica, A., Calabrese, L., & Restuccia, G. (2015). Characterization of Zeolite-Based Coatings for Adsorption Heat Pumps. https://doi.org/10.1007/978-3-319-09327-7

Freni, A., Frazzica, A., Dawoud, B., Chmielewski, S., Calabrese, L., & Bonaccorsi, L. (2013). Adsorbent coatings for heat pumping applications: Verification of hydrothermal and mechanical stabilities. Applied Thermal Engineering, 50, 1658–1663. https://doi.org/10.1016/j.applthermaleng.2011.07.010

Jerai, F., Miyazaki, T., Saha, B. B., & Koyama, S. (2015). Overview of Adsorption Cooling System based on Activated Carbon-Alcohol Pair. Evergreen Joint Journal of Novel Carbon Resource Sciences & Green Asia Strategy, 2(1), 30–40.

Jin, Z., Tian, B., Wang, L., & Wang, R. (2013). Comparison on thermal conductivity and permeability of granular and consolidated activated carbon for refrigeration. Chinese Journal of Chemical Engineering, 21(6), 676–682. https://doi.org/10.1016/S1004-9541(13)60525-X

Kummer, H., Füldner, G., & Henninger, S. K. (2015). Versatile siloxane based adsorbent coatings for fast water adsorption processes in thermally driven chillers and heat pumps. Applied Thermal Engineering, 85, 1–8. https://doi.org/10.1016/j.applthermaleng.2015.03.042

Li, S. L., Xia, Z. Z., Wu, J. Y., Li, J., Wang, R. Z., & Wang, L. W. (2010). Experimental study of a novel CaCl2/expanded graphite-NH3 adsorption refrigerator. International Journal of Refrigeration, 33(1), 61–69. https://doi.org/10.1016/j.ijrefrig.2009.08.001

Lim, L. S., & Abdullah, M. O. (2010). Experimental Study of an Automobile Exhaust Heat-Driven Adsorption Air- Conditioning Laboratory Prototype by Using Palm Activated Carbon- Methanol Experimental Study of an Automobile Exhaust Heat-Driven Adsorption by Using Palm Activated Carbon-Methanol. HVAC&R Research, 16(2), 221–231.

Liu, Y. L., Wang, R. Z., & Xia, Z. Z. (2005). Experimental performance of a silica gel-water adsorption chiller. Applied Thermal Engineering, 25, 359–375. https://doi.org/10.1016/j.applthermaleng.2004.06.012

Liu, Y., Wang, R., & Xia, Z. (2005). Experimental study on a continuous adsorption water chiller with novel design. International Journal of Refrigeration, 28, 218–230. https://doi.org/10.1016/j.ijrefrig.2004.09.004

Mahdavikhah, M., & Niazmand, H. (2013). Effects of plate finned heat exchanger parameters on the adsorption chiller performance. Applied Thermal Engineering, 50, 939–949. https://doi.org/10.1016/j.applthermaleng.2012.08.033

Makimoto, N., Miyazaki, T., & Koyama, S. (2011). The effect of heating water temperature on the performance of an adsorption cooling system using activated carbon powder/ethanol pair. In 13th CSS-EEST symposium.

Makimoto, N., Hu, B., & Koyama, S. (2011). A study on thermophysical characteristices of activated carbon powder / ethanol pair in adsorber. In International Sorption Heat Pump Conference, Italy (pp. 433–442).

Makimoto, N., Kariya, K., & Koyama, S. (2010). Numerical analysis on adsorption characteristics of activated carbon/ethanol pair in finned tube type adsorber. Trans. of the JSRAE, 27(4), 383–392.

Oliveira, R. G., Silveira, V., & Wang, R. Z. (2006). Experimental study of mass recovery adsorption cycles for ice making at low generation temperature. Applied Thermal Engineering, 26, 303–311. https://doi.org/10.1016/j.applthermaleng.2005.04.021

Pons, M., Laurent, D., & Meunier, F. (1996). Experimental temperature fronts for absorptive heat

pump applications. Applied Thermal Engineering, 16, 395–404. https://doi.org/10.1016/1359-4311(95)00025-9

Py, X., Daguerre, E., & Menard, D. (2002). Composites of expanded natural graphite and in situ prepared activated carbons. Carbon, 40(8), 1255–1265. https://doi.org/10.1016/S0008-6223(01)00285-8

Restuccia, G., Freni, A., & Maggio, G. (2002). A zeolite-coated bed for air conditioning adsorption systems: Parametric study of heat and mass transfer by dynamic simulation. Applied Thermal Engineering, 22(6), 619–630. https://doi.org/10.1016/S1359-4311(01)00114-4

Rezk, A., Al-Dadah, R. K., Mahmoud, S., & Elsayed, A. (2013). Effects of contact resistance and metal additives in finned-tube adsorbent beds on the performance of silica gel/water adsorption chiller. Applied Thermal Engineering, 53, 278–284. https://doi.org/10.1016/j.applthermaleng.2012.04.008

Saha, B. B., Koyama, S., El-sharkawy, I. I., Kuwahara, K., Kariya, K., & Ng, K. C. (2006). Experiments for measuring adsorption characteristics of an activated carbon fiber/ethanol pair using a plate-fin heat exchanger. HVAC&R Research, 12(3b).

Sharafian, A., & Bahrami, M. (2014). Assessment of adsorber bed designs in waste-heat driven adsorption cooling systems for vehicle air conditioning and refrigeration. Renewable and Sustainable Energy Reviews, 30, 440–451. https://doi.org/10.1016/j.rser.2013.10.031

Tamainot-Telto, Z., & Critoph, R. E. (2003). Advanced solid sorption air conditioning modules using monolithic carbon-ammonia pair. Applied Thermal Engineering, 23, 659–674. https://doi.org/10.1016/S1359-4311(02)00238-7

Tamainot-Telto, Z., & Critoph, R. E. (2001). Monolithic carbon for sorption refrigeration and heat pump applications. Applied Thermal Engineering, 21, 37–52. https://doi.org/10.1016/S1359-4311(00)00030-2

Tian, B., Jin, Z. Q., Wang, L. W., & Wang, R. Z. (2012). Permeability and thermal conductivity of compact chemical and physical adsorbents with expanded natural graphite as host matrix. International Journal of Heat and Mass Transfer, 55, 4453–4459. https://doi.org/10.1016/j.ijheatmasstransfer.2012.04.016

Wang, D. C., Shi, Z. X., Yang, Q. R., Tian, X. L., Zhang, J. C., & Wu, J. Y. (2007). Experimental research on novel adsorption chiller driven by low grade heat source. Energy Conversion and Management, 48, 2375–2381. https://doi.org/10.1016/j.enconman.2007.03.001

Wang, D. C., Xia, Z. Z., Wu, J. Y., Wang, R. Z., Zhai, H., & Dou, W. D. (2005a). Study of a novel silica gel-water adsorption chiller. Part I. Design and performance prediction. International Journal of Refrigeration, 28, 1073–1083. https://doi.org/10.1016/j.ijrefrig.2005.03.001

Wang, D. C., Xia, Z. Z., Wu, J. Y., Wang, R. Z., Zhai, H., & Dou, W. D. (2005b). Study of a novel silica gel-water adsorption chiller. Part II. Experimental study. International Journal of Refrigeration, 28(7), 1084–1091. https://doi.org/10.1016/j.ijrefrig.2005.03.001

Wang, L. W., Metcalf, S. J., Critoph, R. E., Thorpe, R., & Tamainot-Telto, Z. (2012). Development of thermal conductive consolidated activated carbon for adsorption refrigeration. Carbon, 50(3), 977–986. https://doi.org/10.1016/j.carbon.2011.09.061

Wang, L. W., Tamainot-Telto, Z., Thorpe, R., Critoph, R. E., Metcalf, S. J., & Wang, R. Z. (2011). Study of thermal conductivity, permeability, and adsorption performance of consolidated composite activated carbon adsorbent for refrigeration. Renewable Energy, 36, 2062–2066. https://doi.org/10.1016/j.renene.2011.01.005

Wang, R. Z. (2001a). Adsorption refrigeration research in Shanghai Jiao Tong University. Renewable & Sustainable Energy Reviews, 5, 1–37. https://doi.org/10.1016/S1364-0321(00)00009-5

Wang, R. Z. (2001b). Performance improvement of adsorption cooling by heat and mass recovery operation. International Journal of Refrigeration, 24, 602–611. https://doi.org/10.1016/j.ijrefrig.2014.04.018

Wang, R. Z., Wu, J. Y., Xu, Y. X., & Wang, W. (2001). Performance researches and improvements on heat regenerative adsorption refrigerator and heat pump. Energy Conversion and Management, 42, 233–249. https://doi.org/10.1016/S0196-8904(99)00189-2

Wang, R. Z., Wu, J. Y., Xu, Y. X., Teng, Y., & Shi, W. (1998). Experiment on a continuous heat regenerative adsorption refrigerator using spiral plate heat exchanger as adsorbers. Applied Thermal Engineering, 18, 13–23. https://doi.org/10.1115/1.2888135

Wang, R. Z., Xu, Y. X., Wu, J. Y., & Wang, W. (1998). Experiments on heat-regenerative adsorption refrigerator and heat pump. International Journal of Energy Research, 22, 935–941. https://doi.org/10.1002/(SICI)1099-114X(199809)22:11<935::AID-ER409>3.0.CO;2-3

Waszkiewicz, S. D., Tierney, M. J., & Scott, H. S. (2009). Development of coated, annular fins for adsorption chillers. Applied Thermal Engineering, 29, 2222–2227. https://doi.org/10.1016/j.applthermaleng.2008.11.004

Yang, G.Z., Xia, Z. Z., Wang, R. Z., Keletigui, D., Wang, D. C., Dong, Z. H., & Yang, X. (2006). Research on a compact adsorption room air conditioner. Energy Conversion and Management, 47, 2167–2177. https://doi.org/10.1016/j.enconman.2005.12.005

Zhang, L. Z. (2000). Design and testing of an automobile waste heat adsorption cooling system. Applied Thermal Engineering, 20, 103–114. https://doi.org/10.1016/S1359-4311(99)00009-5

Zheng, X., Wang, L. W., Wang, R. Z., Ge, T. S., & Ishugah, T. F. (2014). Thermal conductivity,

pore structure and adsorption performance of compact composite silica gel. International Journal of Heat and Mass Transfer, 68, 435–443. https://doi.org/10.1016/j.ijheatmasstransfer.2013.09.075

Zhu, D., & Wang, S. (2002). Experimental investigation of contact resistance in adsorber of solar adsorption refrigeration. Solar Energy, 73, 177–185. https://doi.org/10.1016/S0038-092X(02)00042-7

Chapter 4

4 CFD Modeling of Finned Tube Type Adsorber Bed

This chapter presents a two-dimensional axisymmetric CFD model developed for the performance investigation of finned tube type adsorber using activated carbon and ethanol as the working pair. The operating conditions of the cooling system were about 15, 20 and 80^{o}C for evaporation, cooling and heating temperatures, respectively. The simulated temperature profiles for different adsorbent thicknesses were validated with those from experimental data measured in our laboratory. Moreover, the error in mass and energy balance were 3% and 7.88%, respectively. Besides, the performance investigation has been performed for cycle time ranging from 600 to 1400 s. The optimum cycle time was 800 s and the corresponding evaluated SCP and COP were found to be 488 W/kg and 0.61, respectively. The developed CFD model will be used for fin height and fin pitch optimization and can be extended to other adsorbent-adsorbate based adsorption cooling system.

4.1 Introduction

Adsorber bed design optimization is very difficult to perform experimentally due to higher cost and huge time requirement. Several researchers (Critoph, 1998) (Wang et al., 2006) (Saha et al., 2007) (Ali and Chakraborty, 2015) performed a simulation to investigate the performance of adsorption cooling system (ACS) for different adsorbent-adsorbate pairs with lump-sum modeling. Though these simulations provide more realistic performance comparing to ideal

cooling cycle performance, however, the assumptions in that modeling such as the same temperature in the bed is not realistic.

In contrast, CFD simulation can provide detailed heat and mass transfer distribution inside the adsorber bed. Moreover, CFD simulation can provide faster bed design at lower cost to realize higher SCP and COP. Due to the several advantages associated with CFD simulation, it has accrued a lot of interest recently. A transient two-dimensional simulation of combined heat and mass transfer in the adsorber bed of a silica gel-water adsorption cooler is presented by Niazmand and Dabzadeh (2012). The authors showed the effect of fin height, fin spacing and cycle time on COP and SCP for annular fin adsorber. A three dimensional non-equilibrium model of combined heat and mass transfer employing water and composite sorbent SWS-1L has been developed by Mahdavikhah and Niazmand (2013) to predict the dynamic performance of ACS. The authors examined the effects of plate fin heat exchanger configurations on the system performance and they mentioned that adsorber bed geometry has great importance in designing of ACS. Ramji et al. (2014) presented three-dimensional modeling and CFD simulations of activated carbon-methanol adsorber for mobile air-conditioning applications. A two-dimensional CFD simulation has been performed for silica-gel water pair by Caglar. The author showed the comparison of adsorbent bed with fin and finless tube. Besides, the influences of various fin configurations on heat transfer inside the bed have studied by the author (Çağlar 2016).

However, from the literature it is found that very few CFD simulation works have been done on activated carbon and ethanol pair. Recently, Jribi at el. (2017) showed the temperature change in the activated bed packed heat exchanger during the adsorption process. Besides, the author showed the temperature profile with and without the heat of adsorption. Mitra et al. (2018) reported the effects of heat exchanger aspect ratio and adsorbent particle size on the dynamic adsorption characteristics. However, in both cases, the authors did not show the simulation results for all cycle phases such as adsorption, pre-heating, desorption and pre-cooling process which is very important to investigate the adsorption system performance accurately. Moreover, the authors did not address the effect of cycle time in their study.

This study presents the mathematical model and CFD simulation of finned tube type adsorber/desorber bed employing activated carbon-ethanol pair for adsorption cooling applications. Simulation results are compared with experimental data for all the adsorption cycle phases considering similar operating conditions. Good agreement is found between experimental and simulated temperature and pressure profiles. Moreover, heat and mass balance are examined for the system. Finally, performance optimization is done in terms of cycle time ranging from 600 s to 1400 s. The optimum cycle time was found 800 s and the corresponding evaluated SCP and COP were found to be 488 W/kg and 0.61, respectively. Besides cycle time, our developed CFD model can be used to optimize the operating conditions and adsorber heat exchanger configurations such as fin pitch, fin height and fin thickness. Moreover, this developed model can be extended for other adsorbent-adsorbate pair.

4.2 CFD modeling

Performance investigation of finned tube type adsorber employing activated carbon and ethanol pair was carried out experimentally in our laboratory earlier (Makimoto at el., 2010) (Makimoto at el., 2011). The experimental apparatus consists of an adsorber, an evaporator and a condenser connected with stainless steel tubes. The temperatures and pressures in all components are measured by K-type thermocouples and pressure gages, respectively. Two copper finned tubes were incorporated inside the adsorber. The finned tube heat exchanger consists of 190 circular fins attached to an annular tube having a length of 700 mm. Fin height, fin pitch and fin thickness were 10, 3.7 and 0.53 mm, respectively. Porous activated carbon was filled between two consecutive fins and sealed with a mesh sheet. The annular tube was 1.5 mm thick with an inner diameter of 26 mm. Ethanol was considered as a refrigerant. Besides, water was used as a heat transfer fluid and passed through the annular tube. The adsorbent temperatures at 1 and 5 mm thicknesses were recorded experimentally by using K-type thermocouples shown as T_1 and T_5 in Figure 4.1.

Under similar experimental conditions, the transient CFD simulation was performed using Ansys-Fluent software v.18.1. Geometry and meshing were created by using Ansys Design

Modeler and Ansys Meshing, respectively. The details of the CFD modeling were presented as follows.

4.2.1 Assumptions

The assumptions used in the simulation are as follows:

- The adsorbent layer height is equal to the height of the fins.
- The porous media is considered as homogenous.
- Darcy model is adopted for flow through porous media.
- A thermal equilibrium model is assimilated for porous media i.e. the adsorbent and ethanol vapor are at same temperature.
- The variation of the heat of adsorption with the ethanol uptake is not considered, therefore, the average value of the heat of adsorption is used.

4.2.2 Geometry and meshing

Figure 4.1 shows the finned tube type adsorber and computational domain. As the finned tube heat exchanger has a symmetric axis; therefore, the geometry can be reduced to 2D. The computational domain considered in this simulation is 2D-axisymmetric and the half space between the two fins as this geometry has several symmetry planes.

To perform the simulation, we used fine meshing and divided the computational domain (11.5 mm x 1.85 mm) into 748 elements with 897 nodes. The following mesh quality is reported from Fluent.

- Minimum orthogonal quality = 0. 9721 where orthogonal quality ranges from 0 to 1 and values close to 0 represents low quality.
- Maximum ortho skew = 0.0279 where ortho skew ranges from 0 to 1 and values close to 1 correspond to low quality.
- Maximum Aspect Ratio = 1.75883

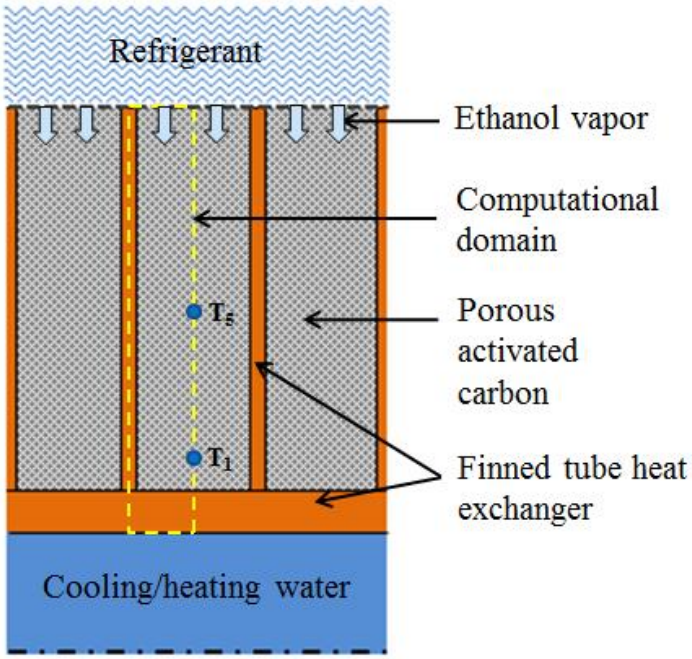

Figure 4.1 2D-axisymmetric geometry of finned tube adsorber showing computational domain.

4.2.3 Materials and porous zone properties

4.2.3.1 Materials

The materials used in the simulations were (i) copper material for tube and fins, (ii) ethanol as gas phase refrigerant, and (iii) activated carbon powder of type Maxsorb III packed between the fins. The properties of copper were taken from the fluent database. Real gas properties of ethanol were imported into Fluent from NIST Refprop database. The properties of Maxsorb III were, the particle density ρ_p = 464.1 kg. m^{-3}, adsorbent-adsorbate thermal conductivity λ_p = 0.2 W m^{-1} K^{-1}(Jribi et al., 2017) where the effective thermal conductivity was equal to 0.12 W m^{-1} K^{-1} and specific heat capacity. The solid adsorbent heat capacity of Maxsorb III was investigated lately and the average value for temperatures ranging from 30 to 80°C is 0.9 $kJ.kg^{-1}K^{-1}$ (Uddin et al., 2018). Therefore, the particle heat capacity for average instantaneous uptake of 0.7 g/g considering that the adsorbate is in the liquid phase (Chakraborty et al., 2007) becomes 4.64 $kJ.kg^{-1}K^{-1}$.

4.2.3.2 Porous Zone Properties

The permeability (α) and inertial loss coefficient (β) of porous media were calculated for the average particle diameter of Maxsorb III $D_P = 70\ \mu m$ and adsorbent porosity ε = 0.434 (Jribi et al., 2017) by the following equations (Ansys 2015). The viscous flow resistance inside the porous media is the reciprocal of permeability of adsorbent.

$$\alpha = \frac{{D_p}^2}{150}\frac{\varepsilon^3}{(1-\varepsilon)^2} \tag{4.1}$$

$$\beta = \frac{3.5}{D_P}\frac{(1-\varepsilon)}{\varepsilon^3} \tag{4.2}$$

4.2.4 Boundary conditions

The boundary conditions applied in this simulation are shown in Figure 4.2 and the detailed boundary conditions are explained in section 4.2.4.1 and 4.2.4.2

4.2.4.1 Pressure inlet/wall/pressure outlet conditions

The interface between activated carbon and refrigerant was set as pressure inlet during adsorption process and the refrigerant inlet pressure was set to 3.85 kPa corresponding to the evaporation temperature of 13.1^{o}C. Similarly, the interface is considered as pressure outlet during the desorption process. In addition, desorption is performed at a pressure of 10.35 kPa corresponding to the condensation temperature of 29.8^{o}C. Besides, at the time of preheating and precooling processes, the interface is considered as wall condition. The purpose of precooling is to reduce the bed pressure from condensation pressure to that of evaporation pressure. Therefore, when the bed pressure becomes lower than the evaporator's pressure, the precooling process was ended. Similarly, when the bed pressure becomes higher than that of the condenser, the preheating process was terminated.

4.2.4.2 Convection boundary conditions

We applied convection boundary condition at the tube inner surface. The water temperature was estimated from the average of inlet and outlet temperature of the tube as presented in Figure 4.3. The free stream temperature profile was fitted to polynomial functions (Figure 4.4) and implemented into fluent as a user-defined function (UDF). Moreover, Gnielinski correlation is used to calculate the convection heat transfer coefficient for water flow rate of 3 l/min. Then, the heat transfer coefficient is incorporated into fluent as a UDF for the temperature range 20^{o}C to 80^{o}C. During the preheating and desorption processes, hot water was supplied to give the heat input to the bed. Similarly, cooling water was provided at the tube inner surface to remove the heat from the bed at the time of precooling and adsorption. The heating and cooling processes were applied for 400 s each.

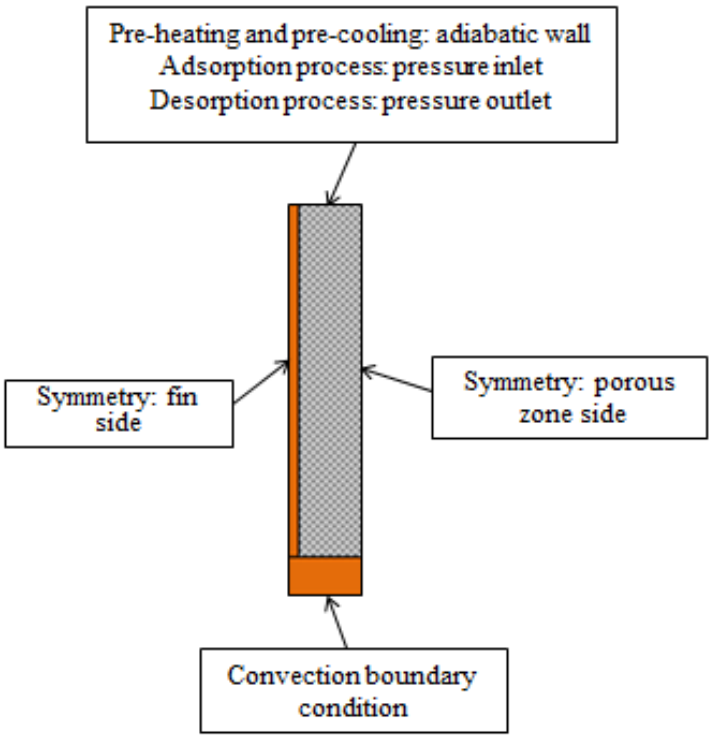

Figure 4.2 Domain boundary conditions.

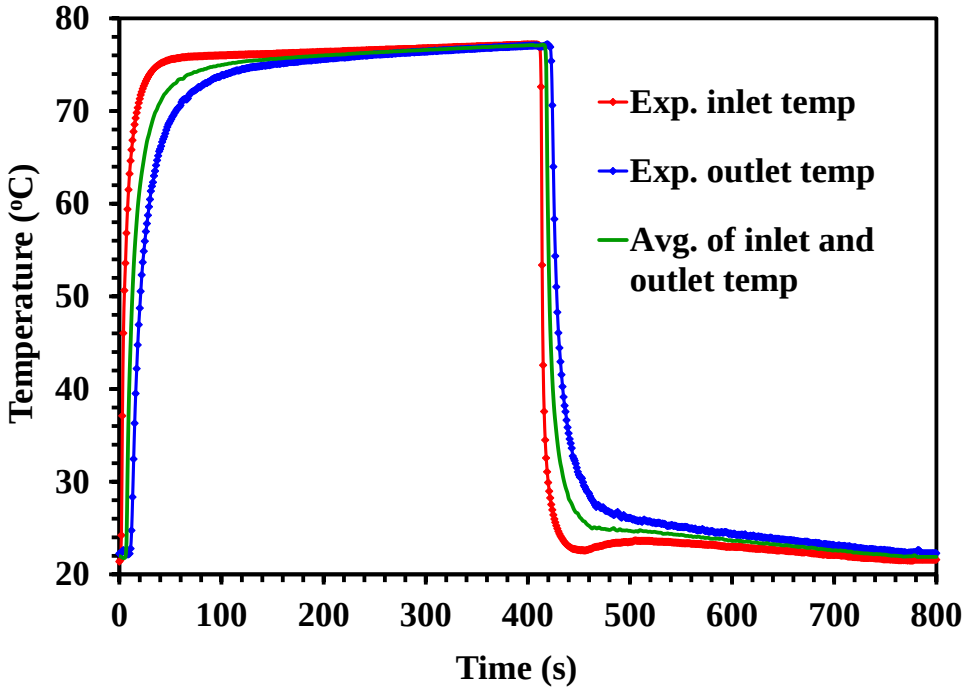

Figure 4.3 Water source temperature profiles at the inlet (red) outlet (blue) and middle tube (green).

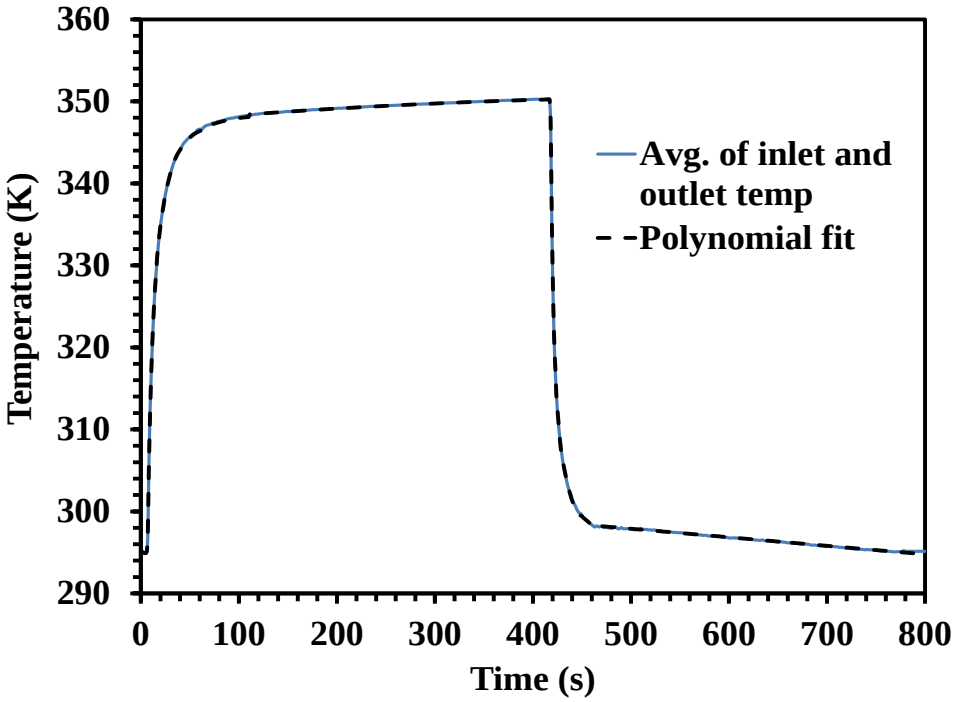

Figure 4.4 Average water temperature profile fitted with polynomial functions.

4.2.5 Governing equations

The main mathematical equations used in fluent are mass, momentum and energy conservation equations. To consider the adsorption phenomena, mass and energy source terms are added to these conservation equations through user-defined functions (UDF).

4.2.5.1 Mass conservation equation in porous media

The mass conservation equation for porous media is given by

$$\frac{\partial(\varepsilon\rho_g)}{\partial t} + \frac{\partial(u\rho_g)}{\partial x} + \frac{\partial(v\rho_g)}{\partial y} = S_m \tag{4.3}$$

Where, *u* and *v* are the superficial velocity of ethanol vapor along x and y direction. S_m is the mass source term denote the adsorbed ethanol gas inside the porous media and is specified as follows :

$$S_m = -(1-\varepsilon)\rho_p \frac{dq}{dt} \tag{4.4}$$

Here, $\frac{dq}{dt}$ represents the adsorption kinetics which is the diffusion of ethanol vapor into the Maxsorb III micropores and will be stated in section 4.2.5.4.

4.2.5.2 Momentum conservation equation

x momentum equation:

$$\frac{1}{\varepsilon}\frac{\partial}{\partial t}(\rho_g u) + \frac{u}{\varepsilon^2}\frac{\partial}{\partial x}(\rho_g u) + \frac{v}{\varepsilon^2}\frac{\partial}{\partial y}(\rho_g u) = -\frac{\partial p}{\partial x} + \frac{\mu}{\varepsilon}\left(\frac{\partial^2 u}{\partial x^2} + \frac{\partial^2 u}{\partial y^2}\right) + \frac{\mu}{\alpha}u + \frac{1}{2}\rho_g \beta|u|u \tag{4.5}$$

y momentum equation:

$$\frac{1}{\varepsilon}\frac{\partial}{\partial t}\left(\rho_g v\right) + \frac{u}{\varepsilon^2}\frac{\partial}{\partial x}\left(\rho_g v\right) + \frac{v}{\varepsilon^2}\frac{\partial}{\partial y}\left(\rho_g v\right) = -\frac{\partial p}{\partial y} + \frac{\mu}{\varepsilon}\left(\frac{\partial^2 v}{\partial x^2} + \frac{\partial^2 v}{\partial y^2}\right) + \frac{\mu}{\alpha}v + \frac{1}{2}\rho_g \beta |v| v \tag{4.6}$$

4.2.5.3 Energy conservation equation

$$\frac{\partial T}{\partial t}\left[\varepsilon\rho_g C_{p,g} + (1-\varepsilon)\rho_p C_{\mathrm{p,s}}\right] + \rho_g C_{p,g}\left(u\frac{\partial T}{\partial x} + v\frac{\partial T}{\partial y}\right) = \lambda_{eff}\left(\frac{\partial^2 T}{\partial x^2} + \frac{\partial^2 T}{\partial y^2}\right) + S_h \tag{4.7}$$

S_h is the heat source term corresponding to the heat released by adsorption process and is given by:

$$S_h = (1-\varepsilon)\rho_p Q_{st}\frac{dq}{dt} \tag{4.8}$$

Here, $Q_{st} = 1002\ \mathrm{kJ.kg^{-1}}$ is the average heat of adsorption for Maxsorb III-ethanol pair (Uddin et al., 2014).

4.2.5.4 Adsorption characteristics

The linear driving force (LDF) equation (Jribi et al., 2016) is used in this modeling as the adsorption rate equation. It is expressed by:

$$\frac{dq}{dt} = k(q^* - q) \tag{4.9}$$

Where k and q^* are the diffusion time constant and equilibrium uptake, respectively. The diffusion time constant is defined by the Arrhenius equation (Eq. 4.10) and the equilibrium uptake was calculated by Dubinin-Astakhov (D-A) adsorption isotherm model (Eq. 4.11).

$$k = Aexp\left(-\frac{E_a}{RT}\right) \tag{4.10}$$

$$q^* = q_s\, exp\left(-\left(\frac{RT}{E} ln\left(\frac{P_s}{P}\right)\right)^n\right) \tag{4.11}$$

Here, $A = 0.2415\ \mathrm{s}^{-1}$, $E_a = 225\ \mathrm{kJ\ kg}^{-1}$, $q_s = 1.2\ \mathrm{kg\ kg}^{-1}$, $E = 139.5\ \mathrm{kJkg}^{-1}$ and $n = 1.8$ denote the pre-exponential factor, activation energy, saturated uptake, characteristic energy and heterogeneity parameter, respectively (El-Sharkawy et al., 2014).

In D-A equation, P_s indicates the saturated pressure (bar) which was calculated by the Antoine equation as presented in equation (4.12).

$$log_{10}P_s = A - \frac{B}{T+C} \tag{4.12}$$

Where $A = 5.247, B = 1598.673$ and $C = -46.424$ are the constant parameters of Antoine equation for ethanol at the temperature range 292.77 to 366.63 K (Ambrose and Sprake, 1970).

4.2.5.5 Performance investigation

To evaluate the specific cooling power (SCP) and coefficient of performance (COP) of the system, the following equations have been used.

$$SCP = \frac{h_{fg} \cdot \int_{ads\_start}^{ads\_end} \dot{m}_{ads}\, dt}{t_{cycle} \cdot m_{ac}} \tag{4.13}$$

$$COP = \frac{Q_{chill}}{Q_{des}} \tag{4.14}$$

Where,

$$Q_{chill} = h_{fg} \cdot \int_{ads\_start}^{ads\_end} \dot{m}_{ads}\, dt \tag{4.15}$$

4.2.5.6 Mass and energy balance equation

The mass balance in the adsorber/desorber bed implies that the mass of refrigerant adsorbed onto the adsorbent is equal to that desorbed from the bed as described in equation (4.16).

$$\int_{ads\_start}^{ads\_end} \dot{m}_{ads}\, dt = \int_{des\_start}^{des\_end} \dot{m}_{des}\, dt \tag{4.16}$$

The energy balance in the adsorption cooling system indicates that the heat released by the condenser and adsorber bed is equal to that adsorbed by the evaporator and desorber bed as expressed by the following equation.

$$Q_{chill} + Q_{des} = Q_{cond} + Q_{ads} \tag{4.17}$$

4.2.6 User-defined functions (UDF) validation

As mentioned in section 4.2.5, we need to incorporate the user-defined functions to perform simulation with adsorption phenomena. However, from the finned tube adsorber simulation, we only can validate the temperature and pressure profile. Therefore, to confirm the adsorption characteristics (adsorption equilibrium uptake and instantaneous uptake), we performed a simulation for Maxsorb III-ethanol pair where adsorption temperature was considered 30^{o}C and pressure 2.26 kPa. Then, we validated our simulation results with the previously measured adsorption data by using rubotherm experimental setup in our laboratory (El-Sharkawy et al., 2014).

Figure 4.5 depicts the comparison between experimental and simulated fractional uptake. A good agreement is found between the two curves as shown in Figure 4.5. The details of this simulation are explained in Appendix A.

$$\text{Fractional uptake} = \frac{q - q_{in}}{q^{*} - q_{in}} \tag{4.18}$$

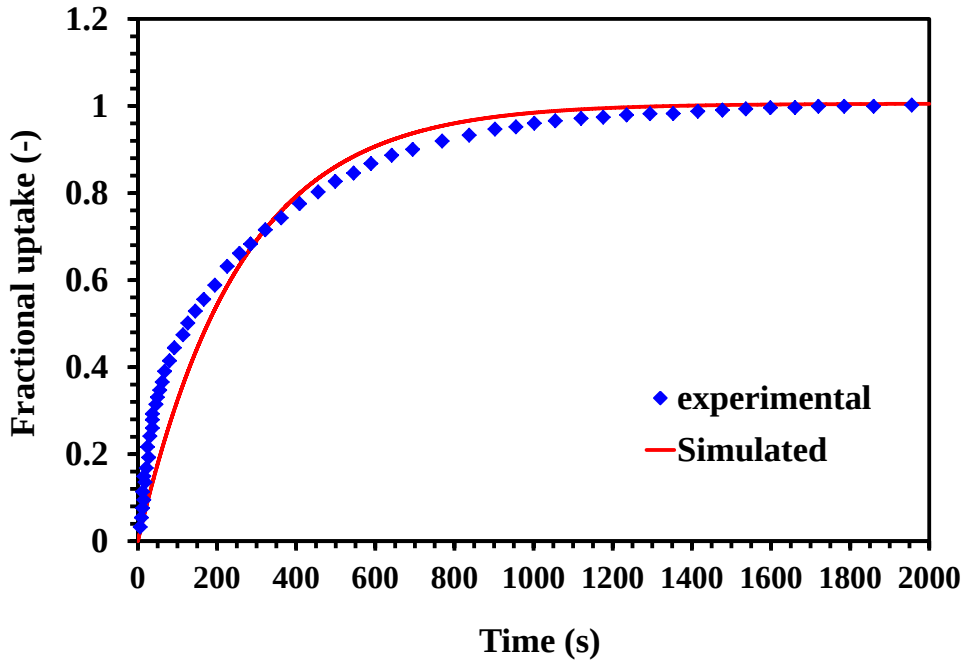

Figure 4.5 Fractional uptake comparison between simulation and experimental data.

4.3 Results and discussion

4.3.1 Simulation results validation with experimental data

4.3.1.1 Pressure profile

Figure 4.6 shows the simulated pressure change vs. experimental pressure profile in the adsorber/desorber bed for two adsorption cycles. The experimental pressure was not constant during adsorption and desorption processes as it was affected by the temperature fluctuation in condenser and evaporator, respectively and this was not considered in this study. In simulated pressure profile, adsorption and desorption occur at constant pressure condition as seen from Figure 4.6. This simulation can obtain the cyclic steady-state pressure within two cycles. Good agreement has been found between experimental and simulated pressure profiles at the beginning of pre-heating and pre-cooling processes.

4.3.1.2 Temperature profiles

Simulated temperature profiles were validated with the experimental data at 1 and 5 mm adsorbent thicknesses (T_1 and T_5) as presented in Figure 4.7. Good agreement was found between the experimental data and the simulated results. In Figure 4.7, simulated temperature profile perfectly matched with that of experimental data at the end of desorption and in pre-cooling process. However, a little deviation is found during the adsorption process and at the starting of desorption. One possible reason for deviation at adsorption process is that Gnielinski correlation under-estimated the heat transfer coefficient from the adsorber bed to the heat transfer water. Consequently, the heat of adsorption was not removed properly from the bed. This makes the simulated bed temperature during adsorption process is higher than that of experimental temperature.

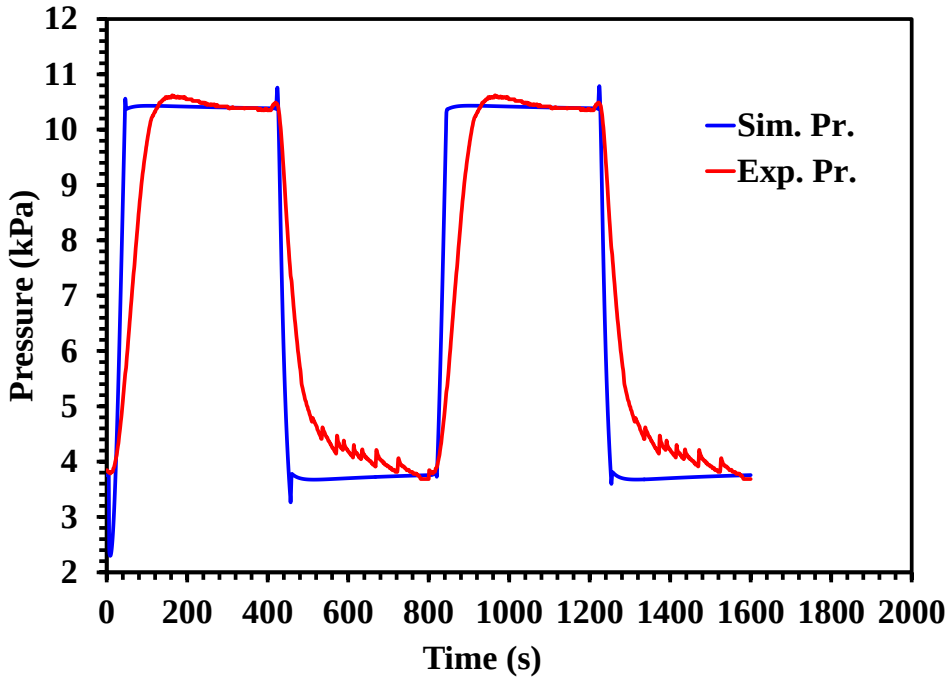

Figure 4.6 Comparison of pressure change in the adsorber/desorber bed: experimental (red) and simulated (blue).

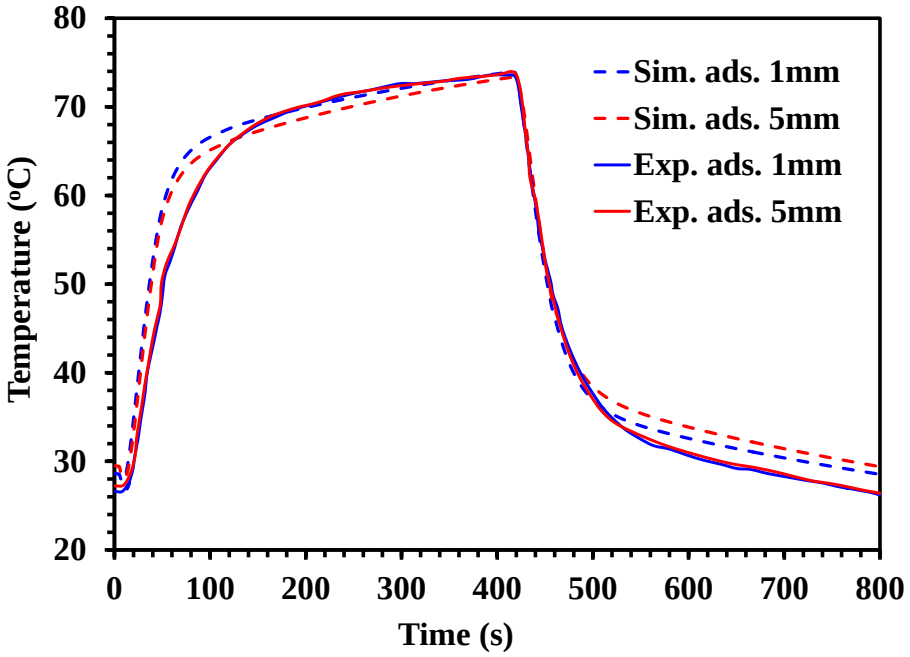

Figure 4.7 Simulated (dashed line) vs. experimental (line) temperature profiles at 1 (blue) and 5 mm (red) adsorbent thicknesses.

4.3.2 Temperature profiles and distribution inside the bed

Figure 4.8 provides the simulated temperature profile at different adsorbent thicknesses from the tube outer surface such as 0, 1, 5 and 8 mm. During pre-heating and pre-cooling processes, the change of temperature is almost same in all these points due to the high heat transfer rate. However, during desorption and adsorption processes, the change of temperature is noticeable at 0, 1 and 5 mm thickness. After 5 mm thickness, the temperature was not changed as heat transfer was not good at the middle of the bed.

Figure 4.9 displays the temperature distribution inside the adsorber bed at different phases of adsorption cycle. In Figure 4.9, due to the high thermal conductivity of copper comparing with adsorbent thermal conductivity, fin and tube have the same temperature at different adsorption phases. Moreover, the adsorbent close to the fin and tube have the same temperature as of tube

and fins while the adsorbent temperature at the middle of the bed is higher during adsorption and precooling processes and lower at the time of desorption and preheating. However, the maximum temperature change inside the bed was within 4-5^{o}C.

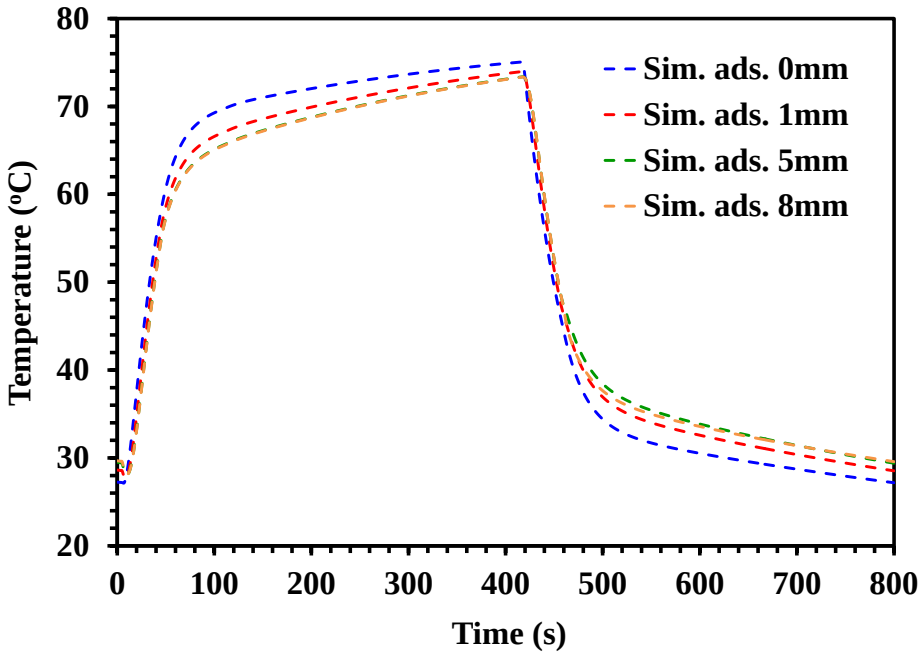

Figure 4.8 Simulated temperature profiles at different adsorbent thickness.

4.3.3 Adsorption characteristics

The profiles of equilibrium uptake (q^*) and instantaneous uptake (q) in the adsorber/desorber bed are displayed in Figure 4.10. The difference between maximum and minimum values of equilibrium uptake Δq^* is 0.51 kg/kg whereas the change in case of instantaneous uptake Δq is 0.314 kg/kg. This means that ethanol adsorption onto activated carbon is only 61.6% of its capacity within the 400s adsorption time. If adsorption is continued for longer cycle time, the total adsorption amount will be increased.

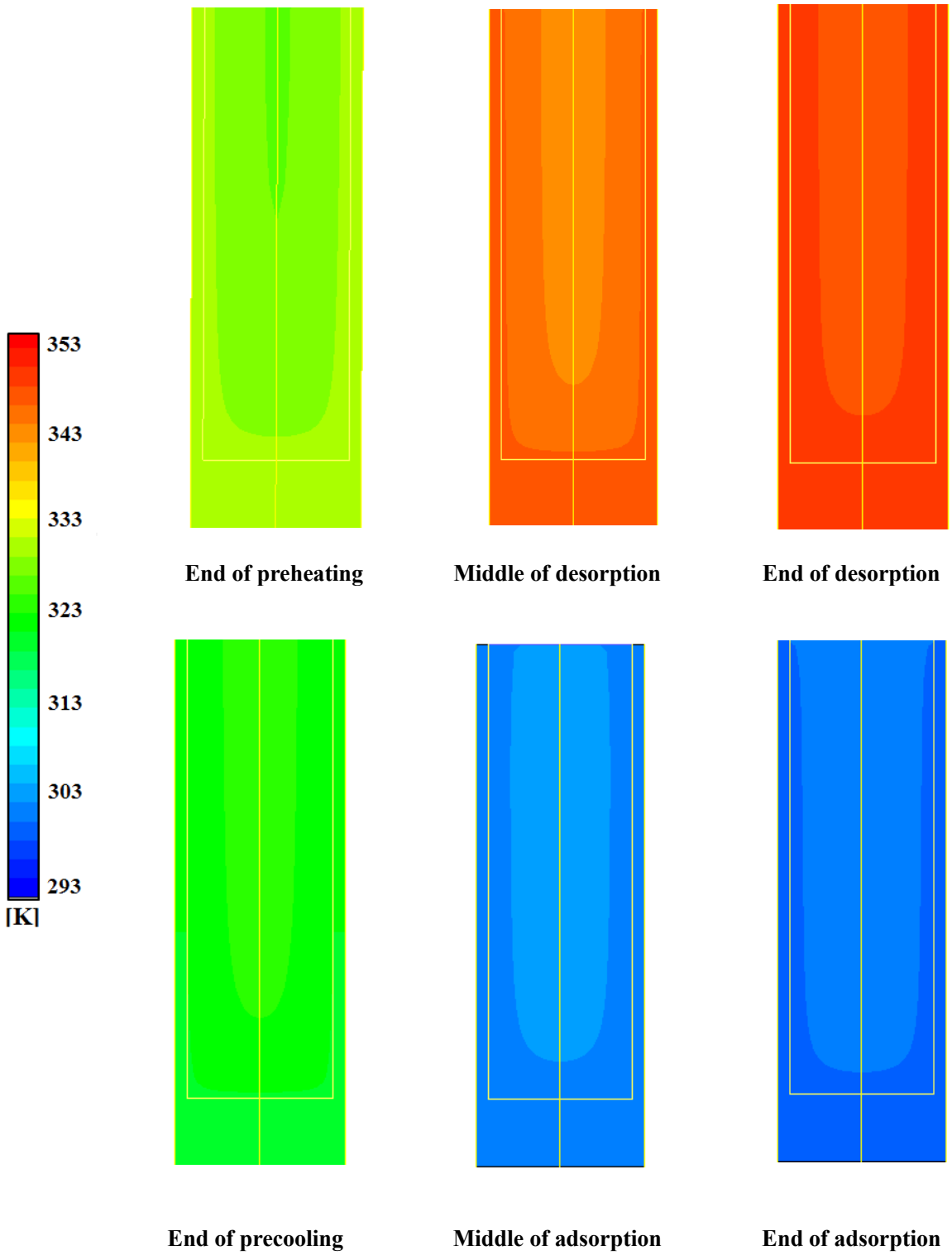

Figure 4.9 Temperature distribution inside the adsorber bed.

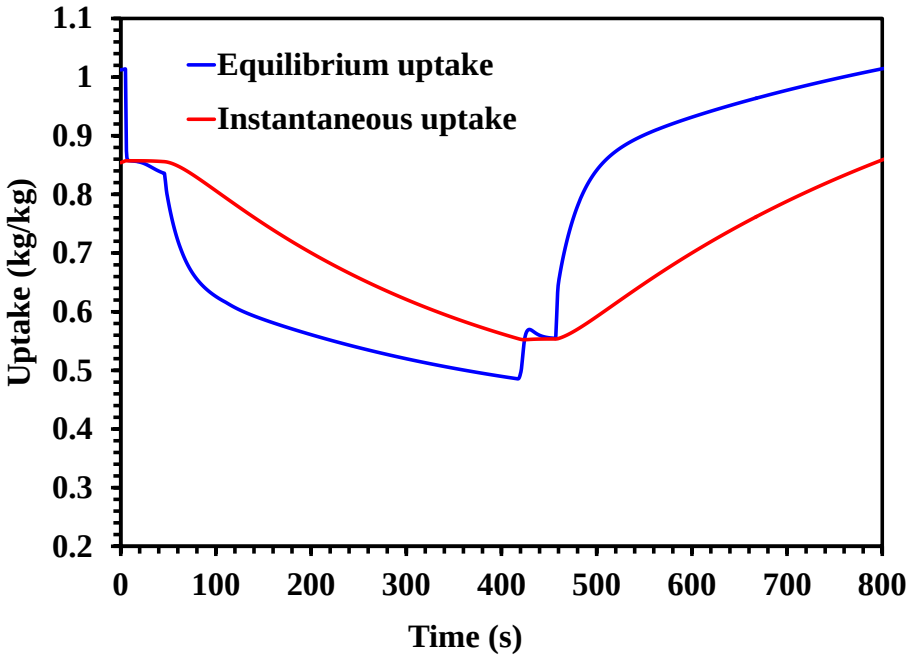

Figure 4.10 Simulated average instantaneous and equilibrium uptakes in the adsorber/desorber bed.

4.3.4 Energy and mass balance

The total amount of heat removed from adsorber and that added to desorber were calculated by integrating the heat transfer profile as shown in Figure 4.11. The values of heat released from condenser and adsorber bed and those adsorbed by desorber and evaporator are used to check the energy balance as shown in equation (4.17) and the error in energy balance is found to be 7.88%. The simulated ethanol flow rate to/from the adsorber/desorber bed is presented in Figure 4.12. The error in mass balance was 3% which is estimated by equation (4.16).

One of the main reasons for mass balance error is that the time for adsorption and desorption was not exactly same in the case of the experiment. The time difference during the experiment was around 12 s. This mass balance error also affects the energy balances. Besides, during adsorption at 20^{o}C temperature, the heat transfer coefficient was underestimated by Gnielinski correlation that is also visible in the Figure. 4.7. Therefore, heat input was higher than the heat removed from the bed.

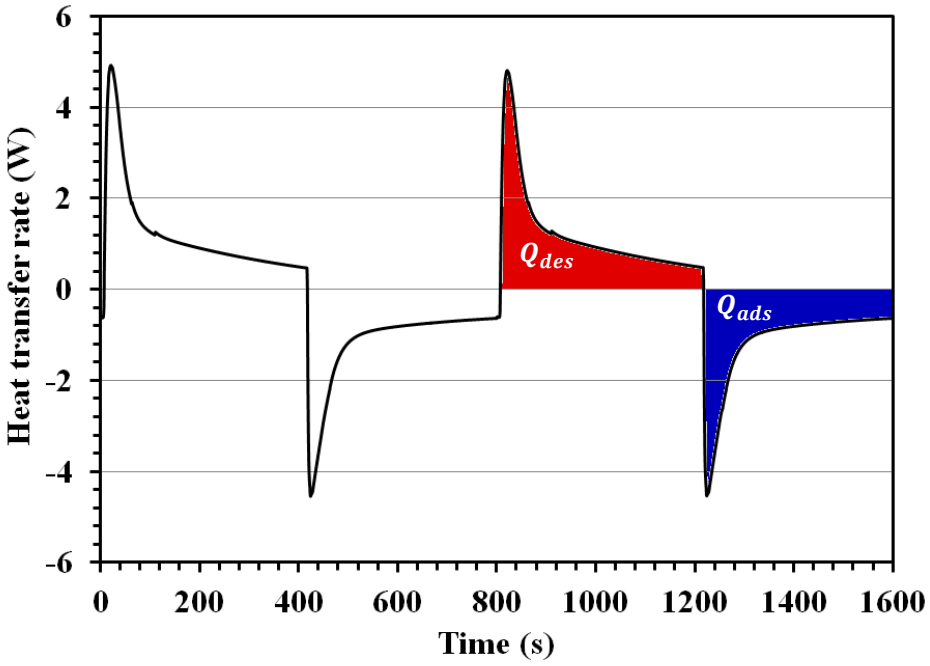

Figure 4.11 Simulated heat transfer rate to and from the finned tube adsorber.

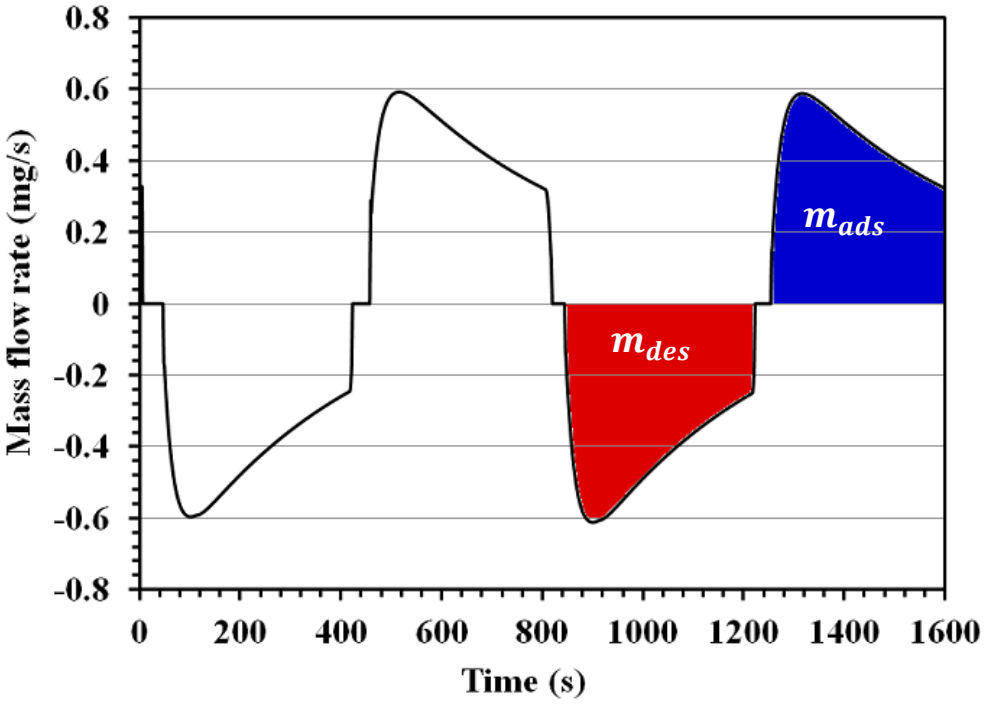

Figure 4.12 Simulated mass flow rate to and from the adsorber for a volume between 2 fins.

4.3.5 Performance investigation

The performance of adsorption cooling system (ACS) has been evaluated in terms of specific cooling power (SCP) and coefficient of performance (COP) by using equation (4.13) and (4.14), correspondingly. The estimated SCP and COP for 800 s cycle time are found 488 W/kg_{ac} and 0.61, respectively. This performance is also relevant to the reported performance for activated carbon-ethanol pair in other studies previously. The specific cooling capacity for activated-carbon ethanol pair considering two different particle size and three different domains has been reported between the range of 424 and 710 W/ kg_{ac} by Mitra et al. (2018). Besides, the performance of activated carbon fiber-ethanol based adsorption cooling system was found 200 W/kg for SCE and 0.65 for COP previously (Saha et al., 2007).

4.4 Effects of cycle time on adsorption system performance

Figure 4.13 shows the performance variation with cycle time. The COP increases with the increase of cycle time. However, the SCP reaches its maximum at a cycle time of 800 s.

With the increase of adsorption time, the cooling effect becomes better as the total adsorbed mass increases. However, the flow rate of adsorbed mass increases sharply at starting of adsorption then decreases as shown previously in Figure 4.10. Therefore the cooling power increases with cycle time increase and reaches its maximum at the cycle time of 800 s. Then, for higher adsorption/desorption time, the cooling power decreases. The COP increases with adsorption/desorption time increase which as the increase in cooling effect generated is higher than the increase of heat consumed to desorb the refrigerant from activated carbon. Besides, with an increase of cycle time, it approaches towards the maximum adsorption amount which helps to reach its highest theoretical COP. As SCP decreases after 800 s, therefore, the optimum cycle time here is considered to 800 s. If a little compromise is done with the SCP then optimum cycle time can be considered in the range of 800 to 1000 s.

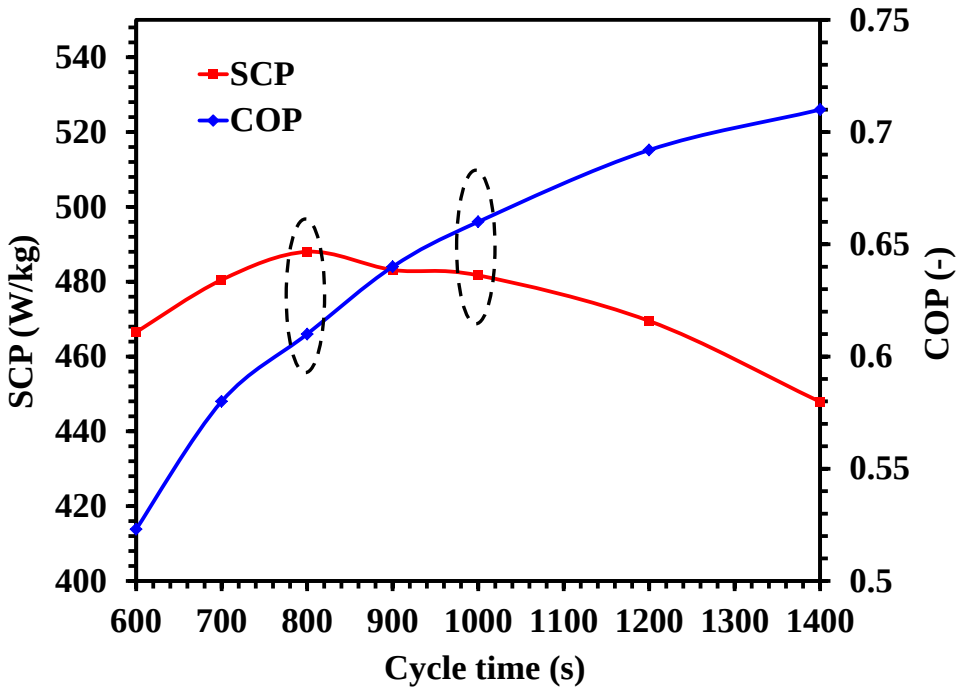

Figure 4.13 The variation of COP and SCP with cycle time.

4.5 Conclusion

CFD modeling of finned tube adsorber employing activated carbon-ethanol as the adsorbent-adsorbate pair has been performed. The simulated pressure and temperature profiles were compared with experimental data of an adsorption cooling system tested in our laboratory for evaporation temperature of 15°C, cooling temperature of 20°C, the heating temperature of 80°C and total cycle time of 800 s. Good agreement was found between experimental and simulation results. The performance of the system was investigated numerically for different adsorption/desorption phase' time ranging from 300 to 700 s. The optimal cycle time for pre-heating and adsorption phases as well as pre-cooling and adsorption phases corresponded to 400 s. At this condition, the cooling power reached 488 W per kilogram of adsorbent and the COP was 0.61. This CFD model will allow performance optimization of the system by optimizing the operating conditions as well as fin dimensions.

4.6 Nomenclature

A	pre-exponential factor [s^{-1}]
C_p	Specific heat capacity at constant pressure [kJ kg^{-1} K^{-1}]
D	diameter [m]
E	energy [kJ]
$\vec{g}$	gravitational acceleration [m s^{-2}]
h_{fg}	heat of evaporation [J kg^{-1}]
k	diffusion time constant [s^{-1}]
n	heterogeneity parameter [$-$]
$\dot{m}$	mass flow rate [kg s^{-1}]
m	mass [kg]
p	pressure [Pa]
R	gas constant [kJ $kmol^{-1}K^{-1}$]
S_m	mass source term [kg $m^{-3}s^{-1}$]
S_h	heat source term [kW m^{-3}]
q	uptake [kg. kg^{-1}]
Q	thermal energy [J]
Q_{st}	heat of adsorption [kJ kg^{-1}]
t	time [s]
T	temperature [K]
u	velocity at *x* direction [m s^{-1}]
v	velocity at *y* direction [m s^{-1}]

Greek

α	permeability [m^2]
β	inertial loss coefficient [m^{-1}]
ε	porosity [$-$]
v_μ	adsorbent' micropore volume [$cm^3.g^{-1}$]
ρ	density [kg m^{-3}]
μ	dynamic viscosity [Pa. s]
λ	Thermal conductivity [W m^{-1} K^{-1}]

Superscripts

$*$	equilibrium

Subscripts

a	apparent, activation
ac	activated carbon
ads	adsorption
$chill$	chill
$cond$	condenser
des	desorption
eff	effective
g	gas phase
in	initial
p	particle
s	solid, saturated

Acronyms

ACS	adsorption cooling system
CFD	computational fluid dynamics
COP	coefficient of performance
SCP	specific cooling power
NIST	National Institute of Standards and Technology

4.7 References

Ali, S. M., & Chakraborty, A. (2015). Thermodynamic modelling and performance study of an engine waste heat driven adsorption cooling for automotive air-conditioning. Applied Thermal Engineering, 90(X), 54–63. https://doi.org/10.1016/j.applthermaleng.2015.06.078

Ambrose, D., & Sprake, C. H. S. (1970). Thermodynamic properties of organic oxygen compounds XXV. Vapour pressures and normal boiling temperatures of aliphatic alcohols. The Journal of Chemical Thermodynamics, 2(5), 631–645. https://doi.org/10.1016/0021-9614(70)90038-8

Ansys. (2015). Ansys Fluent user's guide.

Çağlar, A. (2016). The effect of fin design parameters on the heat transfer enhancement in the adsorbent bed of a thermal wave cycle. Applied Thermal Engineering, 104, 386–393. https://doi.org/10.1016/j.applthermaleng.2016.05.092

Chakraborty, A., Saha, B. B., Koyama, S., & Ng, K. C. (2007). Specific heat capacity of a single

component adsorbent-adsorbate system. Applied Physics Letters, 90(17). https://doi.org/10.1063/1.2731438

Critoph, R. E. (1998). Forced convection adsorption cycles. Applied Thermal Engineering, 18, 799–807. https://doi.org/10.1016/S1359-4311(97)00110-5

El-Sharkawy, I. I., Uddin, K., Miyazaki, T., Saha, B. B., Koyama, S., Miyawaki, J., & Yoon, S. H. (2014). Adsorption of ethanol onto parent and surface treated activated carbon powders. International Journal of Heat and Mass Transfer, 73, 445–455. https://doi.org/10.1016/j.ijheatmasstransfer.2014.02.046

Jribi, S., Miyazaki, T., Saha, B. B., Koyama, S., Maeda, S., & Maruyama, T. (2017). CFD simulation and experimental validation of ethanol adsorption onto activated carbon packed heat exchanger. International Journal of Refrigeration, 74, 343–351. https://doi.org/10.1016/j.ijrefrig.2016.10.019

Jribi, S., Miyazaki, T., Saha, B. B., Koyama, S., Maeda, S., & Maruyama, T. (2016). Corrected adsorption rate model of activated carbon–ethanol pair by means of CFD simulation. International Journal of Refrigeration, 71, 60–68. https://doi.org/10.1016/j.ijrefrig.2016.08.004

Mahdavikhah, M., & Niazmand, H. (2013). Effects of plate finned heat exchanger parameters on the adsorption chiller performance. Applied Thermal Engineering, 50, 939–949. https://doi.org/10.1016/j.applthermaleng.2012.08.033

Makimoto, N., Hu, B., & Koyama, S. (2011). A study on thermophysical characteristices of activated carbon powder / ethanol pair in adsorber. In International Sorption Heat Pump Conference, Italy (pp. 433–442).

Makimoto, N., Kariya, K., & Koyama, S. (2010). Numerical analysis on adsorption characteristics of activated carbon/ethanol pair in finned tube type adsorber. Trans. of the JSRAE, 27(4), 383–392.

Mitra, S., Muttakin, M., Thu, K., & Saha, B. B. (2018). Study on the influence of adsorbent particle size and heat exchanger aspect ratio on dynamic adsorption characteristics. Applied Thermal Engineering, 133, 764–773. https://doi.org/10.1016/j.applthermaleng.2018.01.015

Niazmand, H., & Dabzadeh, I. (2012). Numerical simulation of heat and mass transfer in adsorbent beds with annular fins. International Journal of Refrigeration, 35(3), 581–593. https://doi.org/10.1016/j.ijrefrig.2011.05.013

Ramji, H. R., Leo, S. L., & Abdullah, M. O. (2014). Parametric study and simulation of a heat-driven adsorber for air conditioning system employing activated carbon-methanol working pair. Applied Energy, 113, 324–333. https://doi.org/10.1016/j.apenergy.2013.07.017

Saha, B. B., Chakraborty, A., & Koyama, S. (2007). Study on an activated carbon fiber e ethanol adsorption chiller : Part II - performance evaluation, 30, 96–102.

https://doi.org/10.1016/j.ijrefrig.2006.08.005

Uddin, K., Amirul Islam, M., Mitra, S., Lee, J. boong, Thu, K., Saha, B. B., & Koyama, S. (2018). Specific heat capacities of carbon-based adsorbents for adsorption heat pump application. Applied Thermal Engineering, 129, 117–126. https://doi.org/10.1016/j.applthermaleng.2017.09.057

Uddin, K., El-Sharkawy, I. I., Miyazaki, T., Saha, B. B., Koyama, S., Kil, H. S., Yoon, S. H. (2014). Adsorption characteristics of ethanol onto functional activated carbons with controlled oxygen content. Applied Thermal Engineering, 72, 211–218. https://doi.org/10.1016/j.applthermaleng.2014.03.062

Wang, D. C., Xia, Z. Z., & Wu, J. Y. (2006). Design and performance prediction of a novel zeolite-water adsorption air conditioner. Energy Conversion and Management, 47, 590–610. https://doi.org/10.1016/j.enconman.2005.05.011

Chapter 5

5 Performance Investigation of Finned Tube Type Adsorber for Different Fin Specifications

This chapter presents a performance study of finned tube adsorber for different fin specifications. In this study, five different domains were considered to investigate the performance of adsorption cooling system. In case-1, fin pitch was considered constant 3.7 mm while fin height was adapted 5, 10 and 15 mm. In case-2, fin height was 10 mm constant but fin pitch was varied 2, 3.7 and 5.5 mm. In both cases, fin thickness was constant 0.53 mm. Activated carbon and ethanol was considered as working pair for all the studied domains. Then, two-dimensional axisymmetric CFD simulations were performed to find out the performance of the system in terms of SCP and COP for 800 s cycle time. The operating conditions of the cooling system were 15, 20 and 80^{o}C for evaporation, cooling and heating temperatures, respectively. Simulation results showed that the optimum fin specifications were, fin pitch 3.7 mm and fin height 10 mm, and the corresponding evaluated SCP and COP were found 568 W/kg and 0.63, respectively.

5.1 Introduction

Fin specifications of finned tube type adsorber have great significance in the improvement of adsorption system performance. Therefore, several researchers already made efforts for last few years to find out the out the optimum heat exchanger shape for different working pairs. A transient two-dimensional simulation of combined heat and mass transfer in the adsorber bed of

a silica gel-water adsorption cooler is presented by Niazmand and Dabzadeh (2012). The authors showed the effect of fin height, fin spacing and cycle time on COP and SCP for annular fin adsorber. A three dimensional non-equilibrium model of combined heat and mass transfer employing water and composite sorbent SWS-1L has been developed by Mahdavikhah and Niazmand (2013) to predict the dynamic performance of ACS. The authors examined the effects of plate fin heat exchanger configurations on the system performance and they mentioned that adsorber bed geometry has great importance in designing of ACS. Ramji et al. (2014) presented three-dimensional modeling and CFD simulations of activated carbon-methanol adsorber for mobile air-conditioning applications. A two-dimensional CFD simulation has been performed for silica-gel water pair by Caglar. The author showed the comparison of adsorbent bed with fin and finless tube. The influences of various fin configurations on heat transfer inside the bed have also studied by the author (Çağlar, 2016).

Mitra at el. (2018) reported the effects of heat exchanger aspect ratio and adsorbent particle size on the dynamic adsorption characteristics of activated carbon-ethanol pair considering three different domains and two different particle size. They found the specific cooling capacity within the range of 424 to 710 W/ kg.

This study presents CFD simulation of finned tube type adsorber employing activated carbon-ethanol pair for five different fin specifications. Two-dimensional axisymmetric CFD simulations were performed to find out the performance of the system in terms of SCP and COP for 800 s cycle time. The operating conditions of the cooling system were considered 15, 20 and 80^{o}C for evaporation, cooling and heating temperatures, correspondingly. The optimum fin pitch and fin height were found 3.7 mm and 10 mm, respectively and the corresponding evaluated SCP and COP were 568 W/kg and 0.63, respectively.

5.2 CFD simulation details

This section will provide geometry descriptions, meshing and boundary conditions considered in this study. Also, several assumptions involved in the CFD modeling are explained.

5.2.1 Assumptions

The assumptions used in the simulations are as follows:

- The height of the fins is same as the adsorbent layer height.
- The porous media is considered as homogenous.
- Darcy model is adopted for flow through porous media.
- A thermal equilibrium model is assimilated for porous media which means the adsorbent and ethanol vapor are at same temperature.
- The variation of the heat of adsorption with the ethanol uptake is not considered, therefore, the average value of the heat of adsorption is used.
- Adsorbent packing density is considered constant for all the studied domains.

5.2.2 Domain description

Figure 5.1 shows the physical model of the finned tube type adsorber heat exchanger as well as computational domain.

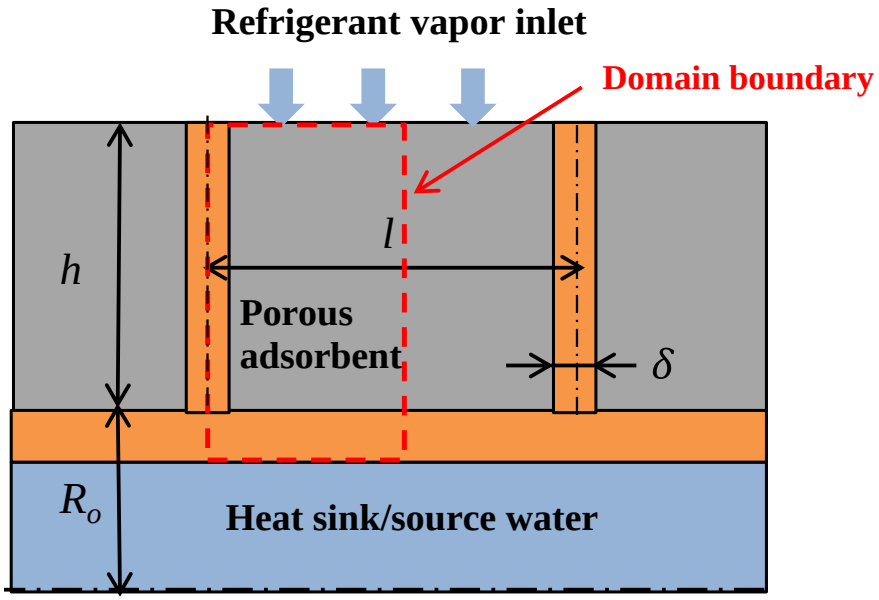

Figure 5.1 Physical model description and calculation domain of finned tube adsorber.

The finned tube heat exchanger is made of copper with the following configurations; the base outer tube radius is R_o, the fin height is h, the fin thickness is δ, the fin pitch is l. In this study, five different domains were considered to investigate the performance of adsorption cooling system. In case-1, fin pitch was considered constant 3.7 mm while fin height was varied 5, 10 and 15 mm. Besides, in case-2, fin height was 10 mm constant but fin pitch was varied 2, 3.7 and 5.5 mm. However, fin thickness was constant 0.53 mm for all cases. Table 5.1 presents the detailed fin specifications for case-1 and case-2.

Table 5.1 The detailed fin specifications for case-1 and case-2

Case-1 (Effect of fin height variation)			
Domain	**I**	**II**	**III**
Fin height, *h* (mm)	**5**	**10**	**15**
Fin pitch, *l* (mm)	**3.7** (constant)		
Fin thickness, δ (mm)	**0.53** (constant)		
Case-2 (Effect of fin pitch variation)			
Domain	**I**	**II**	**III**
Fin height, *h* (mm)	**10** (constant)		
Fin pitch, *l* (mm)	**2**	**3.7**	**5.5**
Fin thickness, δ (mm)	**0.53** (constant)		

5.2.3 Material and porous zone properties

The materials used in the simulations were (i) copper material for the tube and fins, (ii) ethanol as a refrigerant, and (iii) activated carbon powder of type Maxsorb III packed between the fins. The properties of activated carbon Maxsorb III are shown in Table 5.2. The particle density, ρ_p

of activated carbon is estimated by the equation, $\rho_p = \frac{\rho_a}{(1-\varepsilon)}$. The thermal conductivity and heat capacity of Maxsorb III were investigated experimentally by El-Sharkawy et al. (2016) and Uddin et al. (2018), respectively. The constant porous zone properties used in the simulation are shown in Table 5.3.

The properties of copper were used from the Fluent database. Real gas properties of ethanol were imported into Fluent from NIST Refprop database.

Table 5.2 Activated carbon powder properties

Parameter	Value
Adsorbent packing density, ρ_a	275 kg.m^{-3} (Jribi et al., 2016)
Adsorbent skeletal density, ρ_s	2200 kg.m^{-3} (Saha et al., 2011)
Adsorbent particle density, ρ_p	464.14 kg.m^{-3}
Adsorbent average particle diameter, D_p	70 μm (El-Sharkawy et al. 2014)
Adsorbent micropore volume, v_μ	1.7 cm^3.g^{-1} (Saha et al., 2011)

The porous zone properties of the activated carbon powder are characterized by equations (5.1-5.3).

$$\varepsilon = 1 - \frac{\rho_a}{\rho_s} - v_\mu \rho_a \tag{5.1}$$

$$\alpha = \frac{{D_P}^2}{150} \frac{\varepsilon^3}{(1-\varepsilon)^2} \tag{5.2}$$

$$\beta = \frac{3.5}{D_P} \frac{(1-\gamma)}{\varepsilon^3} \tag{5.3}$$

Table 5.3 Porous zone properties

Parameter	Value
Porosity, ε	0.4075
Permeability, α	6.28×10^{-12} m^{-2}
Inertial resistance coefficient, $\boldsymbol{\beta}$	4.37×10^{5} m^{-1}
Specific heat capacity, $C_{p,bed}$	1000 J.kg^{-1}.K^{-1}
Effective thermal conductivity, λ_{eff}	0.066 W.m^{-1}.K^{-1}

5.2.4 Boundary conditions

The boundary conditions applied in this simulation are shown in Figure 5.2 and the detailed boundary conditions are explained in section 5.2.4.1 and 5.2.4.2

5.2.4.1 Pressure inlet/wall/pressure outlet conditions

The interface between activated carbon and refrigerant is set as pressure inlet during adsorption process and the refrigerant inlet pressure was set to 3.85 kPa corresponding to the evaporation temperature of 13.1^{o}C. Similarly, the interface is considered as pressure outlet during the desorption process. Desorption is performed at a pressure of 10.35 kPa corresponding to the condensation temperature of 29.8^{o}C. Besides, at the time of preheating and precooling processes, the interface is considered as wall condition. The purpose of precooling is to reduce the bed pressure from condensation pressure to that of evaporation pressure. Therefore, when the bed pressure becomes lower than the evaporator's pressure, the precooling process was ended. Similarly, when the bed pressure becomes higher than that of the condenser, the preheating process was terminated.

5.2.4.2 Convection boundary conditions

We applied convection boundary condition at the tube inner surface. The supply water temperature was considered constant 20˚C during pre-cooling and adsorption processes and 80˚C during preheating and desorption processes. Moreover, Gnielinski correlation is used to calculate the convection heat transfer coefficient for water flow rate of 3 l/min. Then, the heat transfer coefficient is given into fluent for the water temperature 20^{o}C and 80^{o}C. The heating and cooling processes were continued for 400s each.

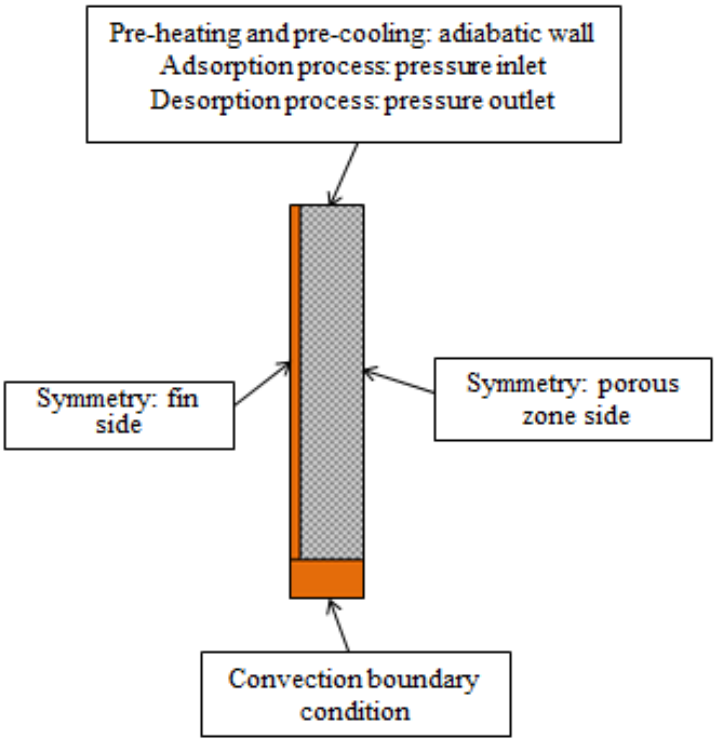

Figure 5.2 Domain boundary conditions.

5.2.5 Governing equations

The governing equations used to perform the simulations are as follows:

5.2.5.1 Mass conservation equation in porous media

The mass conservation equation for porous media is given by

$$\frac{\partial(\varepsilon\rho_g)}{\partial t} + \frac{\partial(u\rho_g)}{\partial x} + \frac{\partial(v\rho_g)}{\partial y} = S_m \tag{5.4}$$

Where, u and v are the superficial velocity of ethanol vapor along x and y direction. S_m is the mass source term denote the adsorbed ethanol gas inside the porous media and is specified as follows :

$$S_m = -(1-\varepsilon)\rho_p \frac{dq}{dt} \tag{5.5}$$

Here, $\frac{dq}{dt}$ represents the adsorption rate which will be stated in section 5.2.5.4.

5.2.5.2 Momentum conservation equation

x momentum equation:

$$\frac{1}{\varepsilon}\frac{\partial}{\partial t}(\rho_g u) + \frac{u}{\varepsilon^2}\frac{\partial}{\partial x}(\rho_g \mathrm{u}) + \frac{v}{\varepsilon^2}\frac{\partial}{\partial y}(\rho_g \mathrm{u}) = -\frac{\partial p}{\partial x} + \frac{\mu}{\varepsilon}\left(\frac{\partial^2 u}{\partial x^2} + \frac{\partial^2 u}{\partial y^2}\right) + \frac{\mu}{\alpha}u + \frac{1}{2}\rho_g \beta|\mathrm{u}|u \tag{5.6}$$

y momentum equation:

$$\frac{1}{\varepsilon}\frac{\partial}{\partial t}(\rho_g v) + \frac{u}{\varepsilon^2}\frac{\partial}{\partial x}(\rho_g v) + \frac{v}{\varepsilon^2}\frac{\partial}{\partial y}(\rho_g v) = -\frac{\partial p}{\partial y} + \frac{\mu}{\varepsilon}\left(\frac{\partial^2 v}{\partial x^2} + \frac{\partial^2 v}{\partial y^2}\right) + \frac{\mu}{\alpha}v + \frac{1}{2}\rho_g \beta|v|v \tag{5.7}$$

5.2.5.3 Energy conservation equation

The energy conservation equation for porous media considering thermal equilibrium condition is given by:

$$\frac{\partial T}{\partial t}\left[\varepsilon\rho_g C_{p,g} + (1-\varepsilon)\rho_p C_{p,bed}\right] + \rho_g C_{p,g}\left(u\frac{\partial T}{\partial x} + v\frac{\partial T}{\partial y}\right) = \lambda_{eff}\left(\frac{\partial^2 T}{\partial x^2} + \frac{\partial^2 T}{\partial y^2}\right) + S_h \quad (5.8)$$

S_h is the heat source term corresponding to the heat released by adsorption process given by:

$$S_h = (1-\varepsilon)\rho_p Q_{st}\frac{dq}{dt} \quad (5.9)$$

Here, $Q_{st} = 1002$ kJ. kg^{-1} is the average heat of adsorption for Maxsorb III-ethanol pair (Uddin et al. 2014).

5.2.5.4 Adsorption characteristics

The linear driving force (LDF) equation (Jribi et al. 2016) is used in this modeling as the adsorption rate equation. It is expressed by:

$$\frac{dq}{dt} = k(q^* - q) \quad (5.10)$$

Where k and q^* are the diffusion time constant and equilibrium uptake, respectively. The diffusion time constant is defined by the Arrhenius equation (Eq.5.11) and the equilibrium uptake was calculated by Dubinin-Astakhov (D-A) adsorption isotherm equation (Eq. 5.12).

$$k = Aexp\left(-\frac{E_a}{RT}\right) \quad (5.11)$$

$$q^* = q_s\, exp\left(-\left(\frac{RT}{E}ln\left(\frac{P_s}{P}\right)\right)^n\right) \quad (5.12)$$

$A = 0.2415$ s^{-1}, $E_a = 225$ kJ kg^{-1}, $q_s = 1.2$ kg kg^{-1}, $E = 139.5$ kJkg^{-1} and $n = 1.8$ denote the pre-exponential factor, activation energy, saturated uptake, characteristic energy and heterogeneity parameter, respectively (El-Sharkawy et al. 2014).

In D-A equation, P_s denotes the saturated pressure (bar) calculated by the Antoine equation.

$$log_{10}P_s = A - \frac{B}{T+C} \quad (5.13)$$

Where $A = 5.247, B = 1598.673$ and $C = -46.424$ are the constant parameters of Antoine equation for ethanol at the temperature range 292.77 to 366.63 K (Ambrose and Sprake 1970).

5.2.5.5 Performance investigation

The performance of adsorption cooling system was investigated in terms of specific cooling power (SCP) and coefficient of performance (COP) using the equation (5.14) and (5.15), respectively.

$$SCP = \frac{h_{fg} \cdot \int_{ads\_start}^{ads\_end} \dot{m}_{ads}\, dt}{t_{cycle} \cdot m_{ac}} \quad (5.14)$$

$$COP = \frac{Q_{chill}}{Q_{des}} \quad (5.15)$$

Where,

$$Q_{chill} = h_{fg} \cdot \int_{ads\_start}^{ads\_end} \dot{m}_{ads}\, dt \quad (5.16)$$

5.3 Solution procedure

5.3.1 Numerical process

CFD simulation was carried out using Ansys-Fluent software v.18.1. Geometry and meshing were created by using Ansys Design Modeler and Ansys Meshing, respectively. Fine good quality meshing is used to perform all the simulations. Besides, suitable initial conditions such as bed temperature, equilibrium uptake and instantaneous uptake value are given to Fluent to initiate the calculation. However, the initial values do not affect the solution results as the

simulation reaches cyclic steady state after completion of first cycle. Time step is used 1 s for all cases. In addition, cycle time is considered 800 s for both cases which we found optimum cycle time for the same operating conditions as showed in chapter 4.

5.3.2 Boundary condition validation

Our CFD model was validated with experimental data as reported in chapter 4. In that study, we used experimental temperature profile for tube inner surface boundary conditions which we cannot be used for different fin specifications study. Therefore, we used simplified convection boundary conditions in this case. We applied 20˚C water during pre-cooling and adsorption processes and 80˚C hot water during preheating and desorption processes. Other all the conditions are almost same as described in chapter 4. Good agreement is found between experimental and simulated temperature profiles at 1 and 5 mm adsorbent thickness as depicted in Figure 5.3. After validating the boundary conditions, the simulations for other domains were performed in the same condition.

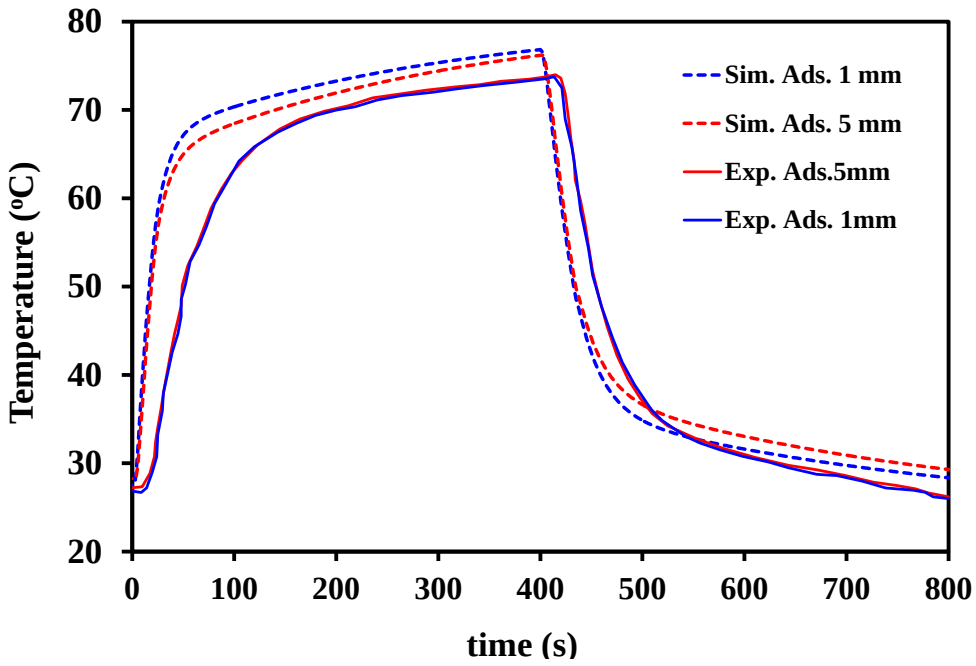

Figure 5.3 Comparison of simulated temperature curve with experimental data for current boundary conditions.

5.4 Results and discussion

5.4.1 Effect of fin height variation

Figure 5.4 shows the average bed temperature profiles for the fin height variation for all phases of adsorption cycle. It is found that the increase of fin height makes the bed temperature lower during desorption process and higher during the adsorption process. That means the heat transfer is not good inside the bed for higher fin heights. Consequently, the heat of adsorption during adsorption process was not removed properly as well as the bed does not get enough heat for desorption process. However, the temperature profile for 10 mm fin height shows interesting behavior during desorption process and the bed temperature of 10 mm fin height is very close to as of 5 mm fin height. Besides, during pre-cooling process, the bed temperature reduction rate is almost same for 5 and 10 mm fin heights while the temperature reduction rate gets slower for 15 mm fin height.

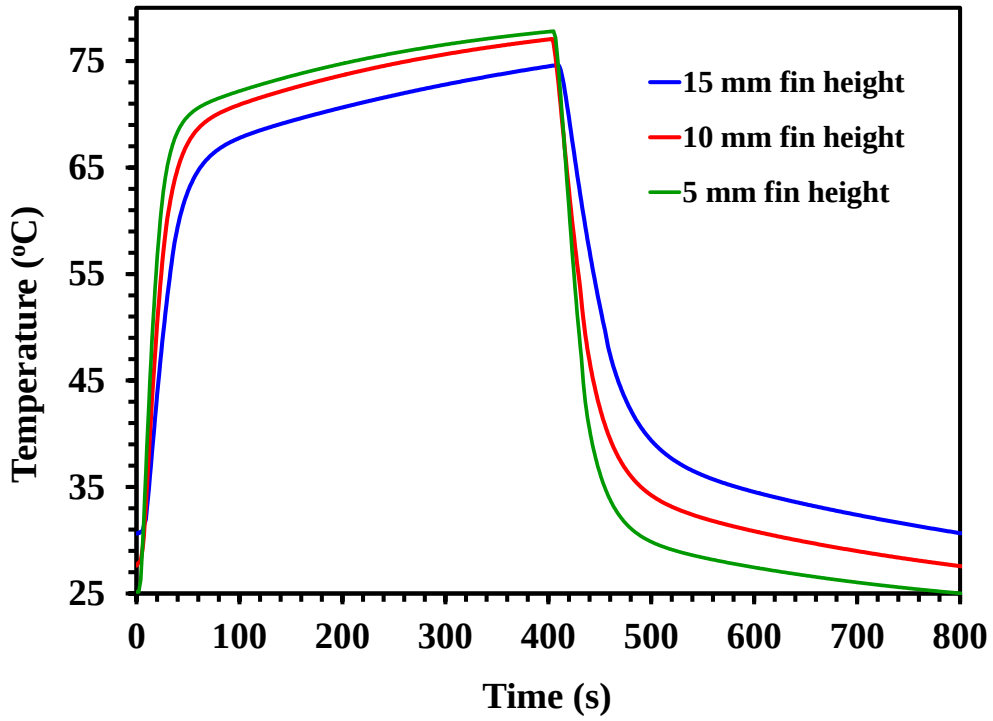

Figure 5.4 Average bed temperature for different fin heights.

Average instantaneous adsorption/desorption for various fin heights is presented in Figure 5.5. The figure depicts that adsorption/desorption rate becomes slower with the increase of fin height while for lower fin height it gets faster. One of the reasons is that the heat transfer inside the bed is not good in case of larger fin heights as can be seen from Figure 5.4, therefore, both adsorption and desorption rate becomes slower. In addition, mass diffusion is also sluggish for larger fin heights as there is some flow resistance due to the higher adsorbent thickness.

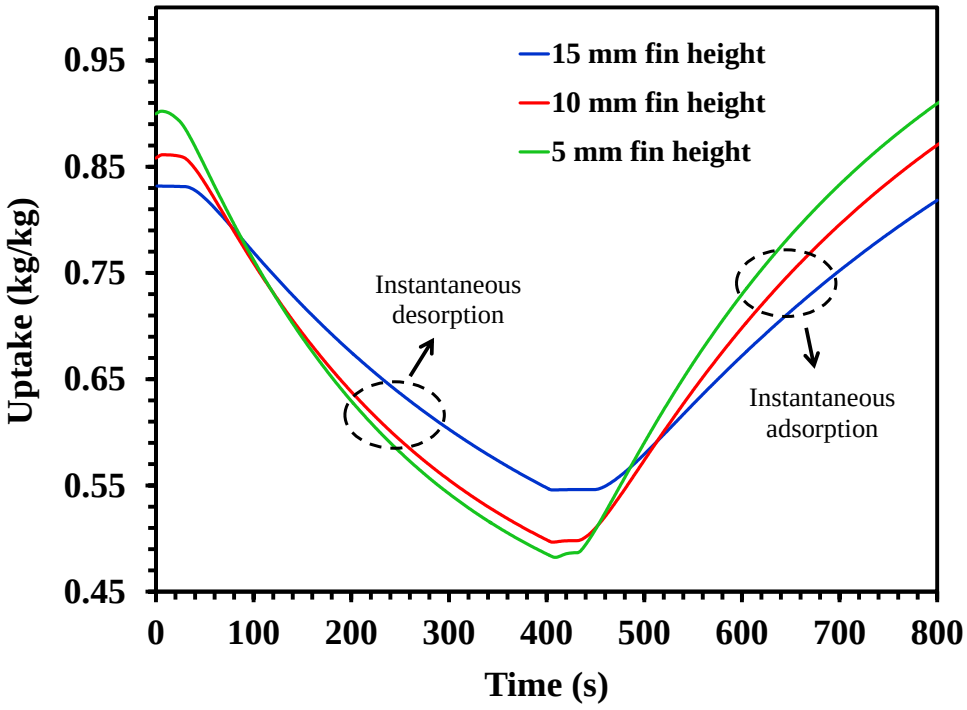

Figure 5.5 Average instantaneous adsorption/desorption for various fin heights.

5.4.2 Effect of fin pitch variation

The effect of fin pitch variation in bed temperature and adsorption/desorption rate is displayed in Figure 5.6 and 5.7, respectively. As presented in Figure 5.6, for larger fin pitch, heat transfer is not good inside the bed and it makes the bed temperature higher in adsorption and lower in desorption process. Besides, for 2 and 3.7 mm fin pitch, the difference of bed temperature is not

that significant during desorption process while the bed temperature is significantly low for 5.5 mm fin pitch.

Figure 5.7 shows the instantaneous adsorption/desorption for the variation of fin pitches. It is found that the maximum adsorption uptake value is almost same for the fin pitch variation, however, there are some differences in the highest desorption value which is very significant in case of 5.5 mm fin pitch. As we mentioned that the heat transfer in the middle of the bed is not good in case of 5.5 mm fin pitch during desorption process, therefore, it affects the highest desorption value.

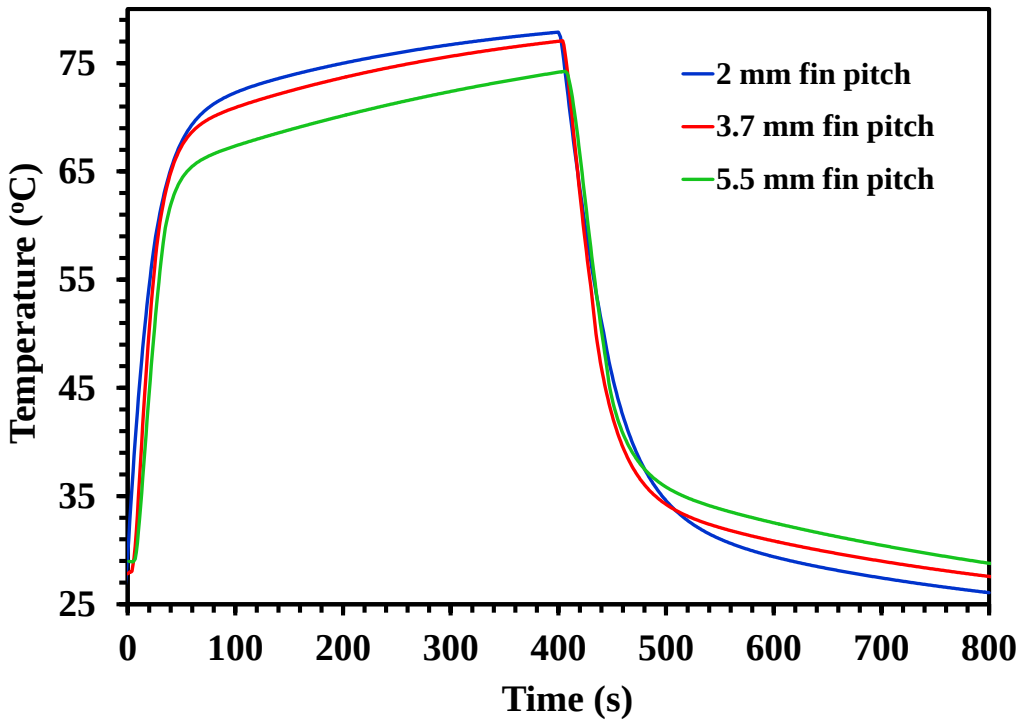

Figure 5.6 Average bed temperature for different fin pitches.

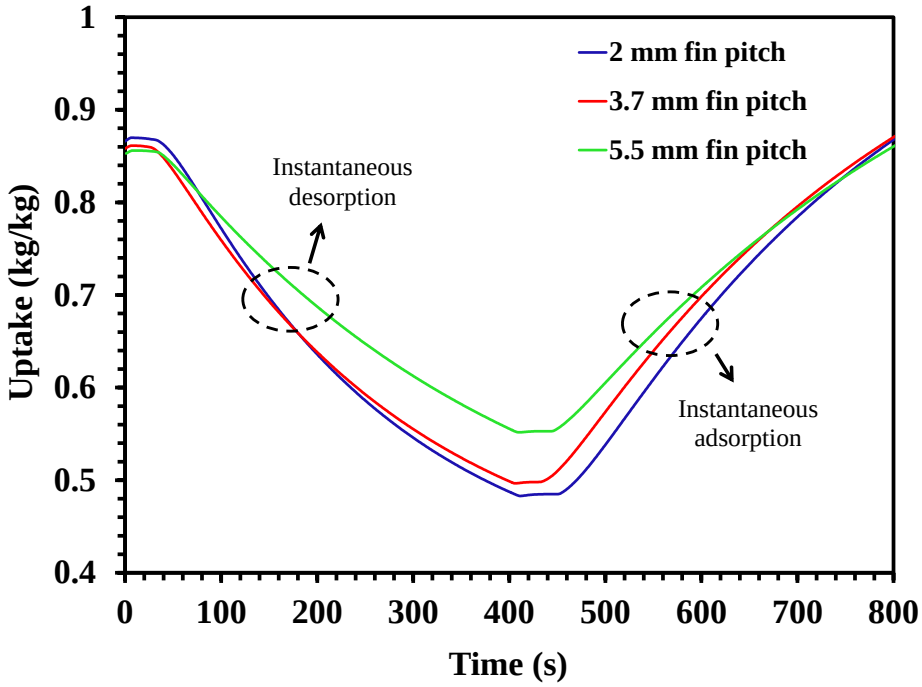

Figure 5.7 Average instantaneous adsorption/desorption for various fin pitches.

5.4.3 Performance study in terms of SCP and COP

Figure 5.8 and 5.9 show the effect of fin height variation on system performance. From the Figure 5.8, it is seen that with the increase of fin height SCP decrease sharply. As the mass diffusion into the adsorbent layer will be lowered with the larger fin height, therefore, it will result in the lower SCP. However, in case of COP, it increases at the beginning with the increase of fin height and then it starts to decrease and gets maximum at 10 mm fin height. This happens due to the reduction of the heat capacity ratio with the increase of fin height. Conversely, due to a large decrease in the SCP at the fin height of 15 mm, the COP was decreased.

The effect of fin pitch variation on COP and SCP is shown in Figure 5.10. As can be seen from the figure, COP increases for larger fin pitch, however, SCP decreases. The increase of the fin pitch results in the decrease of heat capacity ratio. Therefore, the COP will be improved. On the other hand, the heat transfer to the adsorbent will become worse with fin pitch enhancement, therefore, the SCP will decrease. The effect of fin pitch on the VCP is shown in Figure 5.11.

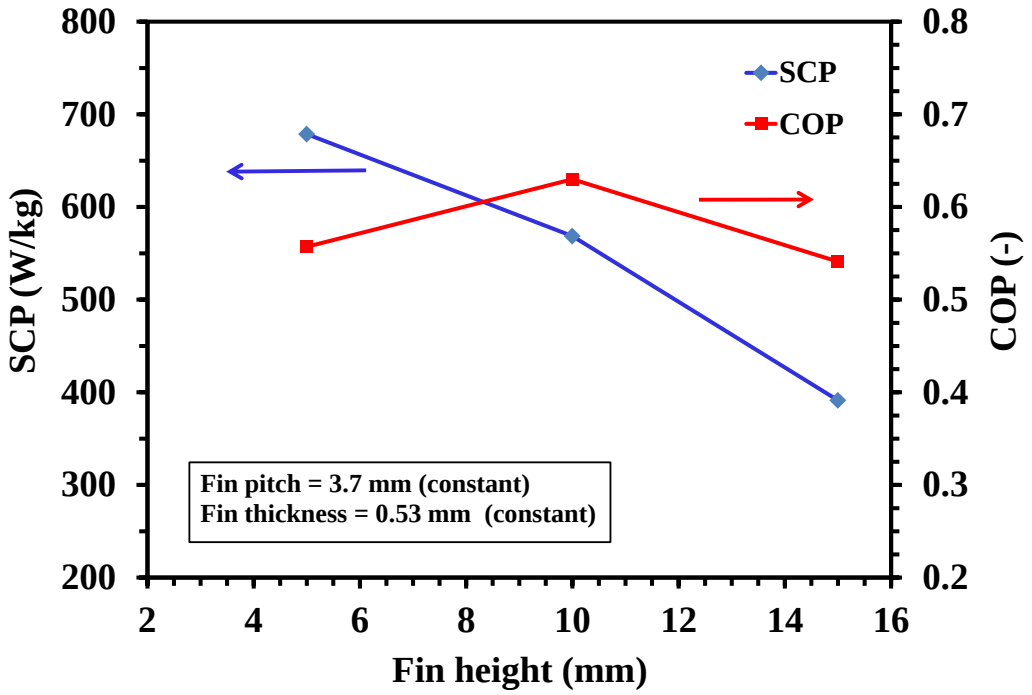

Figure 5.8 Effect of fin height variation on COP and SCP.

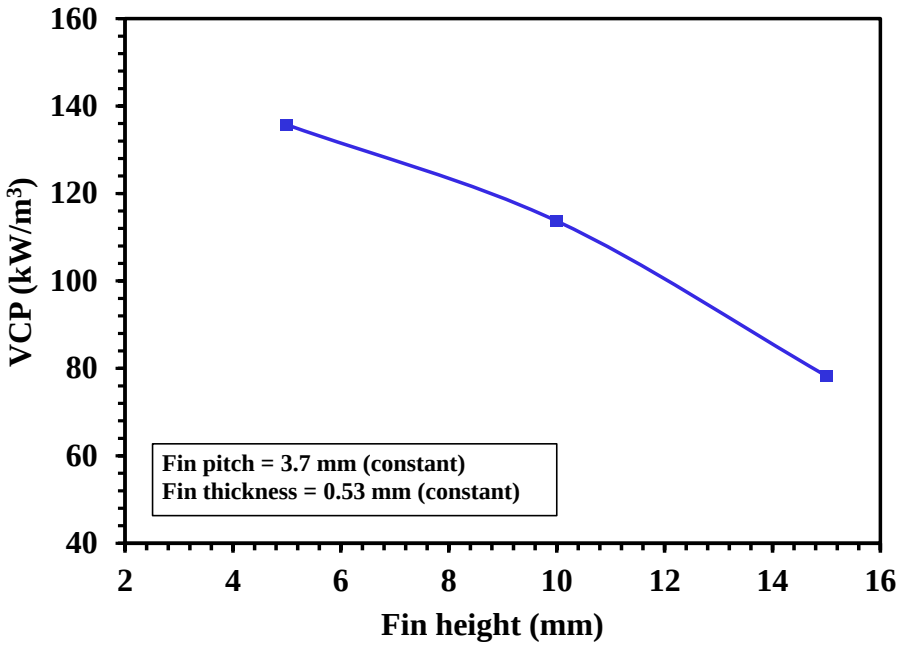

Figure 5.9 Effect of fin height variation on volumetric cooling power (VCP).

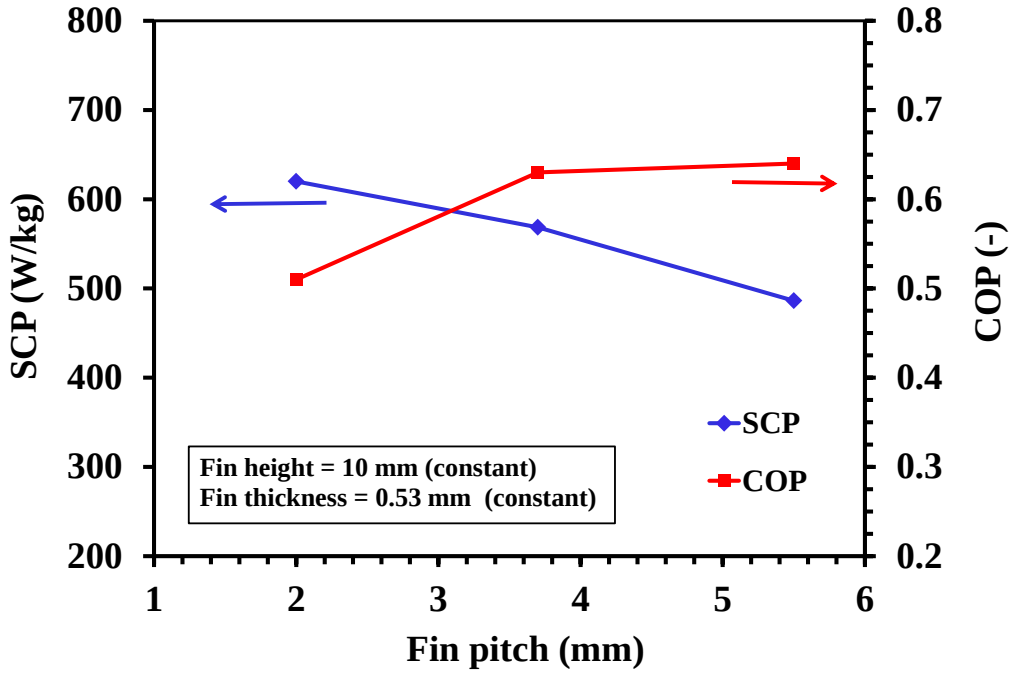

Figure 5.10 Effect of fin pitch variation on COP and SCP.

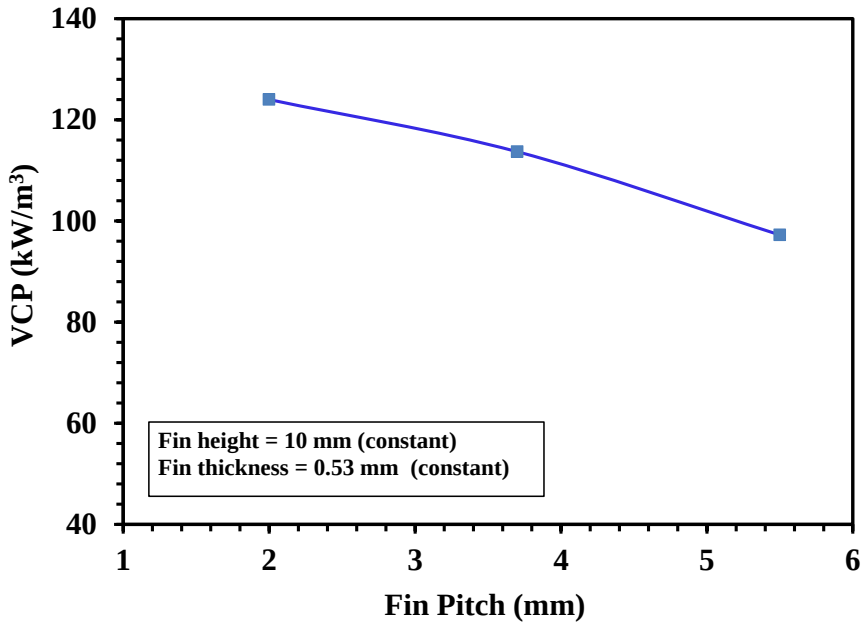

Figure 5.11 Effect of fin pitch variation on volumetric cooling power (VCP).

5.5 Conclusion

The performance investigation for five different domains has been done by dint of CFD simulation. In case-1, fin height was varying 5, 10 and 15 mm considering constant fin pitch 3.7 mm. In case-2, fin height was 10 mm constant but fin pitch was varied 2, 3.7 and 5.5 mm. In both cases, fin thickness was constant 0.53 mm. Simulations were performed for activated carbon and ethanol pair considering 800 s cycle time. Then, the performance of the system was assessed in terms of SCP and COP. The optimum fin specifications are, fin pitch 3.7 mm and fin height 10 mm considering the studied five different domains and the corresponding evaluated SCP and COP were 568 W/kg and 0.63, respectively.

5.6 Nomenclature

A	pre-exponential factor [s^{-1}]
C_p	specific heat capacity at constant pressure [kJ kg^{-1} K^{-1}]
D	diameter [m]
E	energy [kJ]
h_{fg}	heat of evaporation [J kg^{-1}]
k	diffusion time constant [s^{-1}]
n	heterogeneity parameter [−]
$\dot{m}$	mass flow rate [kg s^{-1}]
m	mass [kg]
p	pressure [Pa]
R	gas constant [kJ $kmol^{-1}K^{-1}$]
S_m	mass source term [kg $m^{-3}s^{-1}$]
S_h	heat source term [kW m^{-3}]
q	uptake [kg. kg^{-1}]
Q	thermal energy [J]
Q_{st}	heat of adsorption [kJ kg^{-1}]
t	time [s]
T	temperature [K]
u	velocity at *x* direction [m s^{-1}]
v	velocity at *y* direction [m s^{-1}]

Greek

α	permeability [m^2]
β	inertial loss coefficient [m^{-1}]
ε	porosity [$-$]
v_μ	adsorbent' micropore volume [$cm^3.g^{-1}$]
ρ	density [kg m^{-3}]
μ	dynamic viscosity [Pa. s]
λ	thermal conductivity [W m^{-1} K^{-1}]

Superscripts

$*$	equilibrium

Subscripts

a	apparent, activation
ads	adsorption
$chill$	chill
$cond$	condenser
des	desorption
eff	effective
g	gas phase
p	particle
s	solid, saturated

Acronyms

ACS	adsorption cooling system
CFD	computational fluid dynamics
COP	coefficient of performance
SCP	specific cooling power
NIST	National Institute of Standards and Technology
VCP	volumetric cooling power

5.7 References

Ambrose, D., & Sprake, C. H. S. (1970). Thermodynamic properties of organic oxygen compounds XXV. Vapour pressures and normal boiling temperatures of aliphatic alcohols. The Journal of Chemical Thermodynamics, 2(5), 631–645. https://doi.org/10.1016/0021-9614(70)90038-8

Çağlar, A. (2016). The effect of fin design parameters on the heat transfer enhancement in the adsorbent bed of a thermal wave cycle. Applied Thermal Engineering, 104, 386–393. https://doi.org/10.1016/j.applthermaleng.2016.05.092

El-Sharkawy, I. I., Pal, A., Miyazaki, T., Saha, B. B., & Koyama, S. (2016). A study on consolidated composite adsorbents for cooling application. Applied Thermal Engineering, 98, 1214–1220. https://doi.org/10.1016/j.applthermaleng.2015.12.105

El-Sharkawy, I. I., Uddin, K., Miyazaki, T., Saha, B. B., Koyama, S., Miyawaki, J., & Yoon, S. H. (2014). Adsorption of ethanol onto parent and surface treated activated carbon powders. International Journal of Heat and Mass Transfer, 73, 445–455. https://doi.org/10.1016/j.ijheatmasstransfer.2014.02.046

Jribi, S., Miyazaki, T., Saha, B. B., Koyama, S., Maeda, S., & Maruyama, T. (2016). Corrected adsorption rate model of activated carbon–ethanol pair by means of CFD simulation. International Journal of Refrigeration, 71, 60–68. https://doi.org/10.1016/j.ijrefrig.2016.08.004

Mahdavikhah, M., & Niazmand, H. (2013). Effects of plate finned heat exchanger parameters on the adsorption chiller performance. Applied Thermal Engineering, 50, 939–949. https://doi.org/10.1016/j.applthermaleng.2012.08.033

Mitra, S., Muttakin, M., Thu, K., & Saha, B. B. (2018). Study on the influence of adsorbent particle size and heat exchanger aspect ratio on dynamic adsorption characteristics. Applied Thermal Engineering, 133, 764–773. https://doi.org/10.1016/j.applthermaleng.2018.01.015

Niazmand, H., & Dabzadeh, I. (2012). Numerical simulation of heat and mass transfer in adsorbent beds with annular fins. International Journal of Refrigeration, 35(3), 581–593. https://doi.org/10.1016/j.ijrefrig.2011.05.013

Ramji, H. R., Leo, S. L., & Abdullah, M. O. (2014). Parametric study and simulation of a heat-driven adsorber for air conditioning system employing activated carbon-methanol working pair. Applied Energy, 113, 324–333. https://doi.org/10.1016/j.apenergy.2013.07.017

Saha, B. B., Jribi, S., Koyama, S., & El-Sharkawy, I. I. (2011). Carbon Dioxide Adsorption Isotherms on Activated Carbons. J. Chem. Eng. Data, 56, 1974–1981. https://doi.org/10.1021/je100973t

Uddin, K., Amirul Islam, M., Mitra, S., Lee, J. boong, Thu, K., Saha, B. B., & Koyama, S. (2018). Specific heat capacities of carbon-based adsorbents for adsorption heat pump application. Applied Thermal Engineering, 129, 117–126. https://doi.org/10.1016/j.applthermaleng.2017.09.057

Uddin, K., El-Sharkawy, I. I., Miyazaki, T., Saha, B. B., Koyama, S., Kil, H. S., Yoon, S. H. (2014). Adsorption characteristics of ethanol onto functional activated carbons with controlled oxygen content. Applied Thermal Engineering, 72, 211–218. https://doi.org/10.1016/j.applthermaleng.2014.03.062

Chapter 6

6 Conclusions and Recommendation for Future Work

The main objective of this present work was to investigate the performance of adsorption cooling system with finned tube type adsorber considering different fin specifications. In this regards the following work has been carried out to cope up the objectives.

- The conventional cooling system is responsible for global warming and ozone layer depletion. Besides, it consumes a lot of energy. To consider energy and environmental conservation an alternative cooling system should be developed.
- In this regard, adsorption cooling system can be a feasible alternative as it can be run by low-grade thermal energy, including solar thermal energy, industrial and automobile waste heat in addition with geothermal sources. Besides, it uses natural and environment-friendly refrigerants.
- However, still this system cannot compete with the conventional cooling system. One of the big challenges of adsorption cooling system is the low coefficient of performance and specific cooling power. There are three main ways to improve the system performance such as material's adsorption characteristic's improvement, heat transfer improvement in the adsorber bed and system parameter optimization.

- To improve heat transfer in the bed, there are mainly three ways which can be followed like consolidated or composite adsorbent, heat exchanger design improvement and coated heat exchanger.
- In this present work, performance study of Maxsorb III and newly developed adsorbent spherical activated carbon using ethanol and methanol as a refrigerant has been done.
- Extensive literature review on the heat transfer improvement in the adsorption bed has been made to highlight the importance of heat exchanger design parameters on system performance. Besides, different types of existing heat exchanger design have been reviewed.
- Then a two-dimensional axisymmetric CFD model has been developed for the performance investigation of finned tube type adsorber using activated carbon and ethanol as the working pair and validated with experimental data.
- After that performance investigation has been done for cycle time ranging from 600 to 1400 s to find out the optimum cycle time.
- Finally performance investigation has been carried out for different fin specifications such as variation of fin height and fin pitch.

6.1 General conclusions

General conclusions for this present work can be drawn out as follows:

- Adsorption cooling system can be a feasible alternative to conventional vapor compression system. However, in this case, the performance of this system should be improved which can be done by improving materials adsorption characteristics as well as choosing the suitable heat exchanger design.
- From the performance comparison of SAC-ethanol and SAC-methanol pair, it is found that SAC-ethanol pair is better than SAC-methanol pair over 80℃ of desorption temperature whereas below 80℃ temperature SAC-methanol pair

shows a little better performance than SAC-ethanol pair. On the other hand, SAC-ethanol pair performs comparatively well than Maxsorb-III-ethanol pair for a wide range of desorption temperature 60℃-100℃ , however, for wide scale application of adsorption cooling system Maxsorb III is treated in high regard since the production of SAC is still in a rudimentary stage.

- A review study of existing heat exchanger for adsorption cooling system indicates that finned and tube type adsorber is the commonly used heat exchanger type.
- Then, a two-dimensional axisymmetric CFD model has been developed for the performance investigation of finned tube type adsorber using activated carbon and ethanol as the working pair. The operating conditions of the cooling system were almost 15, 20 and 80^{o}C for evaporation, cooling and heating temperatures, respectively. The developed CFD model showed good agreement between experimental and simulated temperature and pressure profiles.
- Cycle time optimization has been done for finned type adsorber employing activated carbon-ethanol pair with the developed CFD model. The cycle time is considered ranging from 600 to 1400 s. The optimum cycle time was found 800 s and the corresponding evaluated SCP and COP were found to be 488 W/kg and 0.61, respectively.
- Performance investigation has been carried out for different fin specifications through CFD simulation. In this regard, five different domains were considered for activated carbon-ethanol pair for the cycle time of 800 s. In case-1, fin pitch was constant 3.7 mm while fin height was varied 5, 10 and 15 mm. In case-2, fin height was 10 mm constant, but fin pitch was varied and considered 2, 3.7 and 5.5 mm. In both cases, fin thickness was constant 0.53 mm. The optimum fin specifications were found to be 3.7 mm for fin pitch and 10 mm for fin height considering the five domains and the corresponding evaluated SCP and COP were 568 W/kg and 0.63, respectively.

- The findings of this thesis will contribute to the development of the high-performance adsorption cooling system.

6.2 Recommendation for future work

The future research works can be outlined as follows:

- Perform the simulation of finned tube type adsorber for SAC-ethanol pair. Besides, simulation study can be performed for consolidated activated carbon and ethanol pair.
- Investigate the performance of finned tube heat exchanger for different fin thickness as well as base tube thickness.
- Examine the performance for varying fin specifications considering the same metal amount of the heat exchanger for all fin specifications.

Appendix A

Details of User Defined Function Validation

Adsorption rate is an imperative parameter to assess the performance of adsorption cooling system accurately. In this study, 2D axisymmetric simulation has been performed to check the adsorption characteristics and validated with previously measured adsorption isotherm and kinetics at 30^{o} C measured by using the Rubotherm experimental instrument. A good agreement is found between the experiment and simulation results.

A.1 Simulation details

Adsorption kinetics of ethanol onto activated carbon at 30^{o}C temperature has been measured experimentally in our laboratory by Rubotherm magnetic balance (Thermogravimetric adsorption analyzer) (El-Sharkawy et al., 2014). Similar experimental conditions were applied to perform the simulation. Ansys Fluent v. 18.1 is used to perform the simulation. Geometry and meshing were created by using Ansys design modeler and Ansys meshing which was incorporated into Ansys workbench.

A.1.1 Geometry

In thermogravimetric adsorption analyzer, activated carbon was placed inside a cylindrical basket made of stainless steel metal. Figure A.1 represents the schematic of basket & adsorbent and the computational domain part. Figure A.2 shows the geometry used in fluent as well as the boundary conditions to perform the simulation.

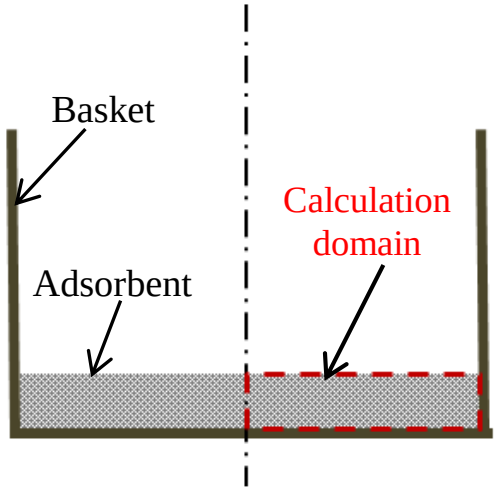

Figure A.1 Schematic of basket & adsorbent and computational domain part.

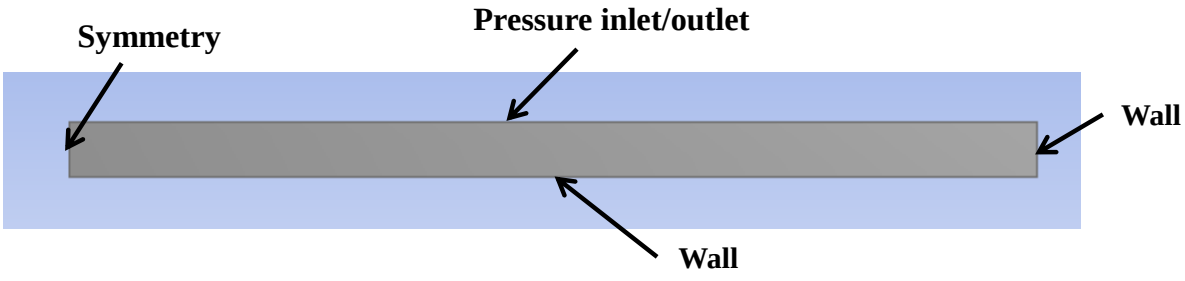

Figure A.2 Geometry used in fluent and boundary conditions.

A.1.2 Boundary conditions

A.1.2.1 Pressure inlet

The adsorbent inside the basket was initially at the equilibrium condition at pressure of 1.713 kPa and the adsorption pressure was set at 2.260 kPa.

A.1.2.2 Wall condition

In the experiment, heat transfer from the basket wall to heat transfer fluid has occurred in a convection process. However, to perform the simulation, constant wall temperature condition has been considered. Therefore, we set the wall temperature 30^{o}C as our adsorption temperature was 30^{o}C.

A.2 Mathematical equations

To perform adsorption simulation, we need to add suitable heat and mass sources with mass, momentum and energy conservation equations.

Heat and mass sources will be different for different adsorbent-adsorbate pairs as it depends on the adsorbent-adsorbate mass transfer characteristics and the value of the heat of adsorption of that pair. In this case, activated carbon-ethanol pair is considered. The adsorption characteristic of this pair is explained as bellows.

A.2.1 Activated carbon-ethanol mass transfer correlation

To predict the adsorption kinetic rate, linear driving force (LDF) equation is used in this modeling which is expressed by:

$$\frac{dq}{dt} = k(q^* - q) \quad \text{(A.1)}$$

Where k and q^* are the diffusion time constant and equilibrium uptake, respectively.

The diffusion time constant is defined by the Arrhenius equation and the Dubinin-Astakhov (D-A) adsorption isotherm equation is used to calculate the equilibrium uptake.

$$k = Aexp\left(-\frac{E_a}{RT}\right) \quad \text{(A.2)}$$

$$q^* = q_s\, exp\left(-\left(\frac{RT}{E} ln\left(\frac{P_s}{P}\right)\right)^n\right) \quad \text{(A.3)}$$

$A = 0.2415\ \text{s}^{-1}$, $E_a = 225\ \text{kJ kg}^{-1}$, $q_s = 1.2\ \text{kg kg}^{-1}$, $E = 139.5\ \text{kJkg}^{-1}$ and $n = 1.8$ denote the pre-exponential factor, activation energy, saturated uptake, characteristic energy and heterogeneity parameter, respectively (El-Sharkawy et al. 2014).

A.3 Adsorption kinetics validation

The simulated fractional uptake is validated with the experimental one as shown in the Figure A.3. The fractional uptake is defined by the following equations. A good agreement is found between experimental and simulated uptake.

$$\text{Fractional uptake} = \frac{q - q_{in}}{q^* - q_{in}} \quad \text{(A.4)}$$

Where,

q^*= equilibrium adsorption uptake (kg/kg)

q = instantaneous adsorption uptake (kg/kg)

q_{in} = initial uptake (kg/kg)

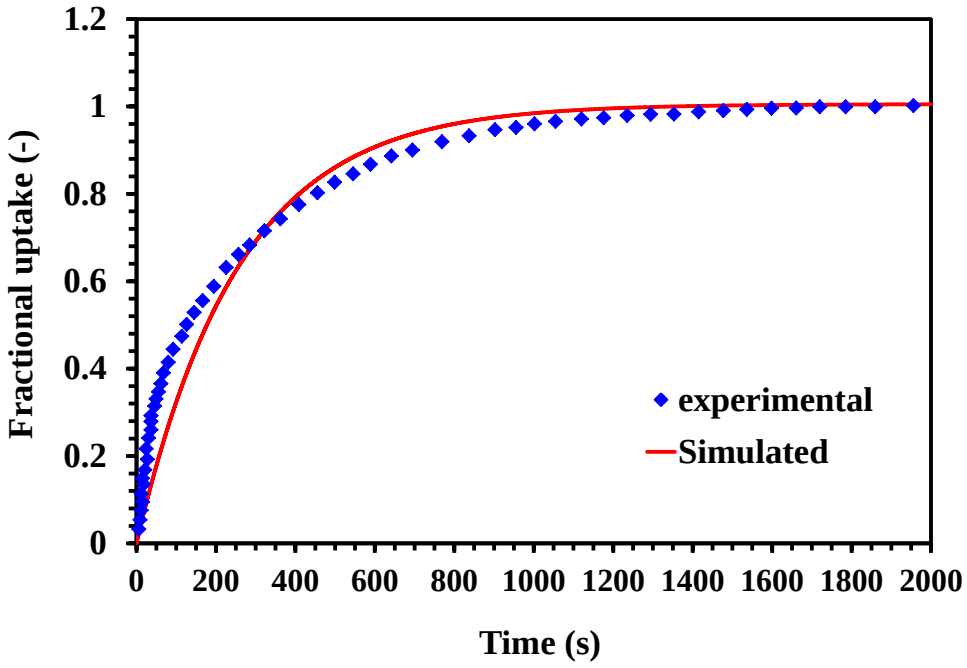

Figure A.3 Validation of simulation and experimental data.

A.4 References

El-Sharkawy, I. I., Uddin, K., Miyazaki, T., Saha, B. B., Koyama, S., Miyawaki, J., & Yoon, S. H. (2014). Adsorption of ethanol onto parent and surface treated activated carbon powders. International Journal of Heat and Mass Transfer, 73, 445–455. https://doi.org/10.1016/j.ijheatmasstransfer.2014.02.

Appendix B

Hydrogen Storage Capacity of Spherical Activated Carbon

The main obstacle for using hydrogen (H_2) for transport applications is safe storage and transportation of H_2. In this case, physisorption of H_2 onto nanoporous materials is one of the technologies for secure storage. In this paper, the results of H_2 adsorption at 1 bar and 77 K onto a newly developed spherical activated carbon (SAC) with large surface area have been discussed. In addition, H_2 adsorption results (wt%) with total pore volume, surface area, and micropore volume have been shown. From results, it has been concluded that this newly developed SAC material can be used for H_2 storage purposes.

B.1 Introduction

In recent years, there is a movement towards the hydrogen-based economy. The use of hydrogen as a fuel is environmentally friendly as well as it will contribute to reduce the dependency on oil. However, one of the biggest problems with H_2 is storage problem which need to solve before using H_2 as a fuel. Currently, hydrogen is stored as a high-pressure gas or liquid in cryogenic reservoirs, and other storage technologies that are under considerations are adsorption on porous materials and complex hydrides etc. Sorption of H_2 on porous materials is considered as a safe and promising storage system for vehicle applications. Studies have been continuing for last few years to establish sorption process for hydrogen storage applications. Commonly used nanoporous materials for this purpose are activated carbon, carbon nanotubes

and metal-organic frameworks. Researchers are showing more interest in carbon materials for hydrogen storage because of their low density, diversity of structural forms, wide-ranging pore structure, good chemical stability, and their structure can be changed by applying extensive carbonization and activation conditions. In this study, hydrogen storage capacity has been checked onto a newly developed Spherical activated carbon (SAC) sample with the large surface area which has shown very promising performance in ethanol adsorption (El-Sharkawy et. al., 2015). In addition, the relation of hydrogen adsorption with total pore volume, surface area and micropore volume of this sample have been presented.

B.2 Hydrogen production and utilization

There are different ways for the production of hydrogen. Few are as follows:

- Coal, oil through gasification
- By pyrolysis of natural gas
- Through photolytic splitting of water or electrolysis of water using solar energy
- Electrolysis of water is used to produce hydrogen from wind, hydro or wave
- Biomass fermentation or gasification or pyrolysis

The application of hydrogen storage is listed as follows:

- Transport applications
- Electricity/heat generation
- Locally stored energy
- Balancing of renewable electricity production
- Portable electronics

B.3 Adsorbent properties

The chemical compositions and pore characteristics of SAC sample are presented in Table B.1. Pore characteristics have been extracted from N_2 adsorption at 77 K. The total surface area of SAC is nearly 3000 m^2/g, which is close to the highest level of commercialized activated carbons.

Table B.1 Characteristics of spherical activated carbon

Sample	**Elemental composition**						**Porosity**			
	C [wt.%]	H [wt.%]	N [wt.%]	$O_{(diff.)}$ [wt.%]	O/C	Ash [wt. %]	Total surface area [m^2/g]	Micro-pore volume [cm^3/g]	Total Pore volume [cm^3/g]	Average pore width [nm]
SAC	95.18	0.22	0.26	4.34	0.034	-	2992	2.29	2.52	1.62

B.4 Experimental method

Adsorption isotherm measurement of hydrogen at 1 bar and 77 K was done by volumetric method. The apparatus used for conducting this experiment is Autosorb-1 which is manufactured by Quantachrome Instruments. Figure B.1 presents the detailed image of the Quantachrome Autosorb-1.

B.5 Results and discussion

Figure B.2 shows the adsorption and desorption isotherms of hydrogen on SAC at 77 K below 1 bar. No hysteresis was observed during the adsorption and desorption. The maximum adsorbed amount of hydrogen onto SAC was found nearly 22 mg/g. In addition, more than 15 mg/g hydrogen was adsorbed even below 0.4 relative pressures. The adsorption isotherm was Freundlich type, suggesting that SAC had the strong adsorption potential of H_2.

Figures B.3, B.4 and B.5 demonstrate the relation of H_2 adsorption with the total pore volume, specific surface area, and micropore volume. In these three figures, SAC had one of the highest performances of H_2 adsorption comparing with other activated carbons (Texier et. al., 2004), although SAC had wider micropore width than others. Those indicated that SAC had the high adsorption potential as well as smooth adsorption in those micropores.

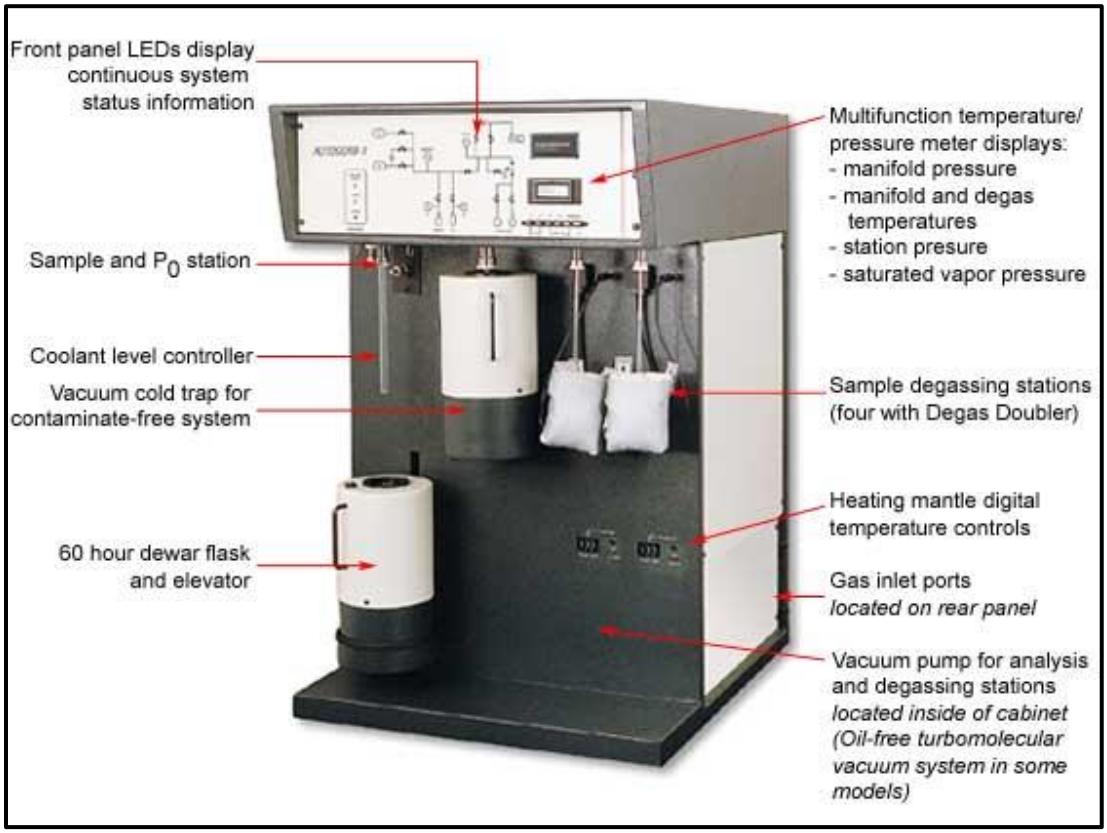

Figure B.1 Apparatus used for conducting the experiment (Autosorb-1).

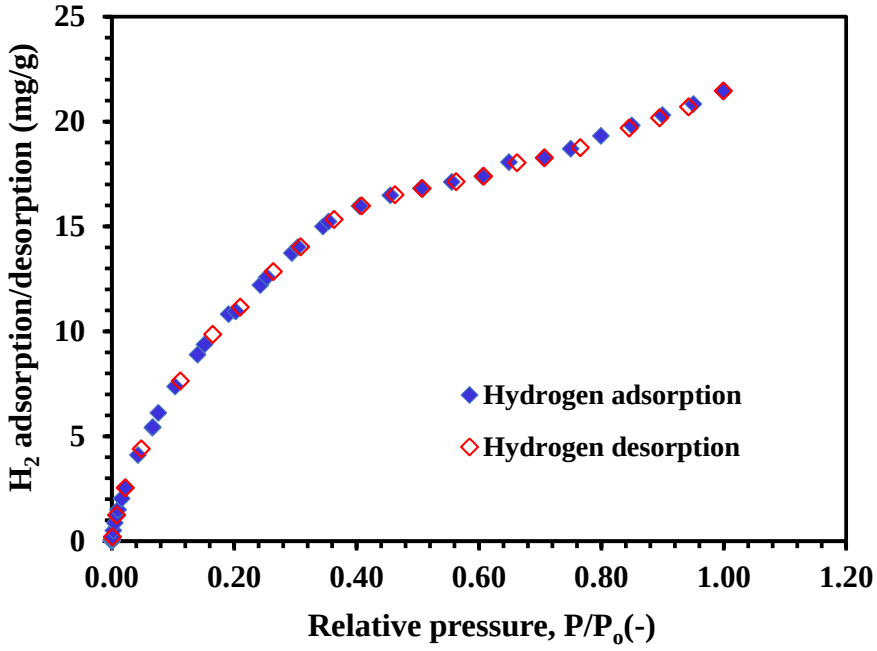

Figure B.2 Isotherms of hydrogen adsorption and desorption onto spherical activated carbon at 77 K.

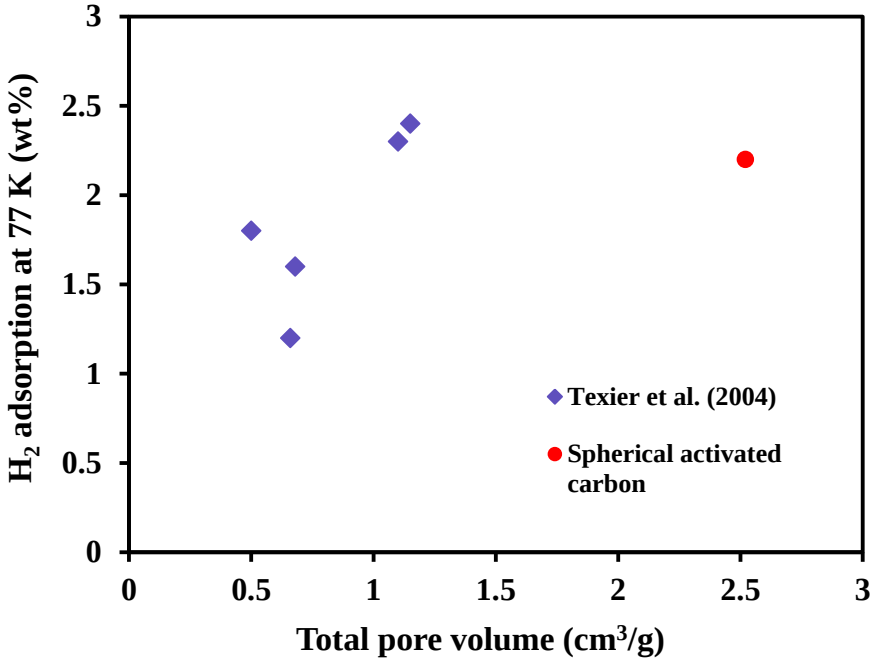

Figure B.3 H_2 adsorption at 1 bar and 77 K with total pore volume.

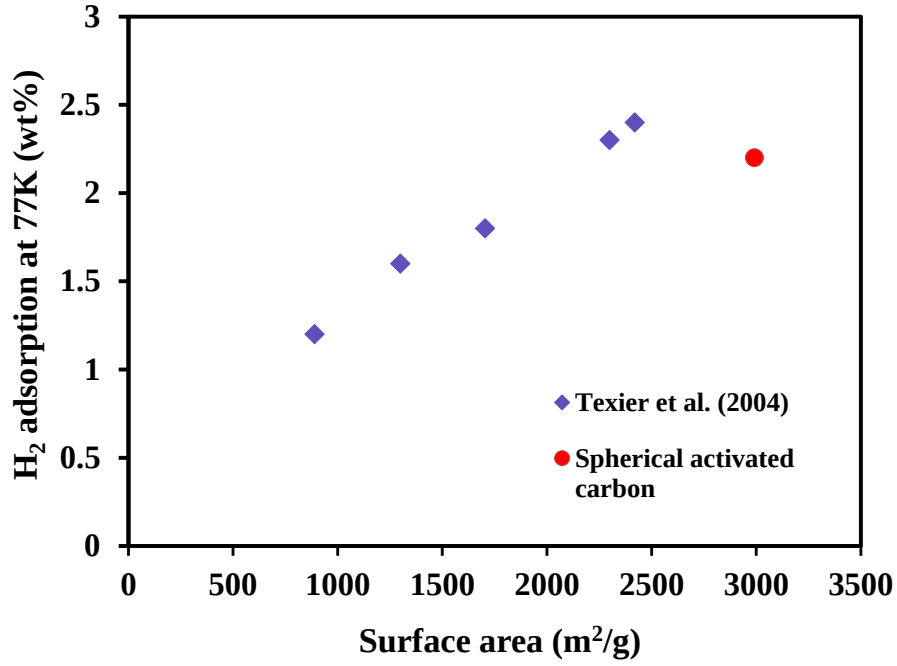

Figure B.4 H_2 adsorption at 1 bar and 77 K with the total surface area.

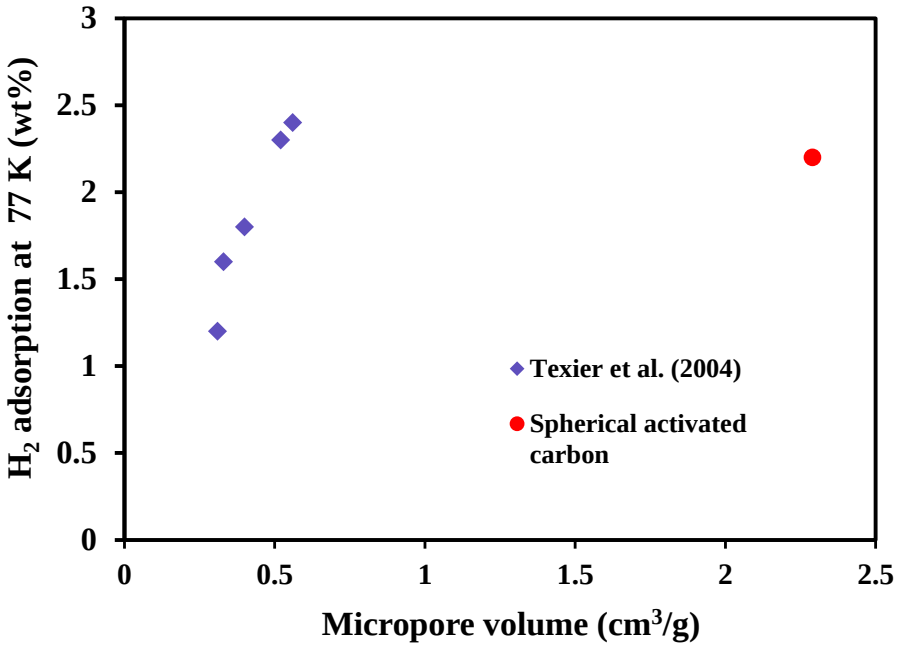

Figure B.5 H_2 adsorption amount with micropore volume at 1 bar and 77 K.

B.6 Conclusions

In this study, H_2 adsorption amount onto SAC at 77 K has been reported, and it is nearly 22 mg/g. Moreover, the relation of H_2 adsorption (wt%) with total pore volume, total surface area, and micropore volume has been shown. Finally, it is concluded that SAC can be used for H_2 storage applications.

B.7 References

El-Sharkawy, I. I., Uddin, K., Miyazaki, T., Baran Saha, B., Koyama, S., Kil, H. S., S.-H. Yoon, J. Miyawaki, J. (2015). Adsorption of ethanol onto phenol resin based adsorbents for developing next generation cooling systems. International Journal of Heat and Mass Transfer, 81, 171–178. https://doi.org/10.1016/j.ijheatmasstransfer.2014.10.012

Texier-Mandoki, N., Dentzer, J., Piquero, T., Saadallah, S., David, P., & Vix-Guterl, C. (2004). Hydrogen storage in activated carbon materials: Role of the nanoporous texture. Carbon, 42(12–13), 2744–2747. https://doi.org/10.1016/j.carbon.2004.05.018